2020

Asset Pricing under Randomized Solvable Diffusions

Hiromichi Kato
kato4650@mylaurier.ca

Asset Pricing under Randomized Solvable Diffusions

By

Hiromichi Kato

BA in Economics and Financial Mathematics, Wilfrid Laurier University, 2019

Thesis

Submitted to the Department of Mathematics

Faculty of Science

in partial fulfilment of the requirements for the

Master of Science in Mathematics

for Science and Finance

Wilfrid Laurier University

2020

Acknowledgement

I would like to appreciate my co-supervisors, Drs. Roman Makarov and Giuseppe Campolieti, for providing me critical feedback on my thesis. They also helped me build my new analytical framework and numerical techniques for the model calibrations. I would not have been able to complete my thesis without both of you.

I would also like to express my gratitude to Drs. Yongzeng Lai and Nick Costanzino for your interesting comments during my thesis defence.

Last but not least, I would like to thank my parents, my sister and a dog for supporting me during the COVID-19 pandemic.

Abstract

By employing a randomization procedure on the geometric Brownian motion (GBM) model, we construct our new pricing models with stochastic volatility exhibiting symmetric smiles in the log-forward moneyness, and admitting simple closed-form analytical expressions for European-style option prices. We assume that there are no infinitesimal correlations between the underlying asset prices and their volatility, and the integrated squared volatility processes are random variables with well-known probability density functions. Under some regularity conditions, closed-form expressions are obtained by taking the expectation of option prices under diffusion models over the integrated squared volatility process, which relate to the Bayesian framework in the GBM model studied by Darsinos and Satchell [12]. Surprisingly, the pricing formulas for the novel models presented in this thesis are even simpler than the classical GBM model as they are expressed as elementary analytical functions. The option prices are also obtained numerically in an efficient manner since they only involve one-dimensional integrals of complementary error functions with respect to the variable of integration. We also calibrate to the market data from Coca Cola to compare the performance on the new models and the SABR model.

Key Words: static randomization, pricing European-style options, Black-Scholes implied volatility, calibration, randomized GBM model, SABR model, CEV model.

Contents

List of Tables

List of Figures

Chapter 1

Introduction and Main Results

1.1 Introduction

Today, investors trade financial assets and contracts in the stock market. They trade because they are willing to take their risks to earn profits with right predictions. In order to hedge their risks associated from trading financial assets, they use options. An option is a contract that gives the owner the right to buy/sell the underlying asset at a predetermined price. Option prices are determined so that no investors can exploit arbitrage opportunities. However, options cannot be priced without a background in mathematics. We thus require mathematical models for pricing options.

Mathematicians have developed stochastic models to value options. The geometric Brownian motion (GBM) model is known as one of the simplest continuous-time models that admits analytical closed-form formulas for pricing various kinds of options [7]. The GBM model is a complete market model which means the risks can be perfectly hedged. The limitation is that there is a discrepancy between anticipated Black Scholes (BS) prices and market traded option prices since the model fails to capture price movements for extreme events [15]. Local volatility diffusion models (also known as state-dependent volatility models) are more flexible continuous-time models known for describing the behavior of implied volatility smile and skew patterns observed in a market place. Local volatility diffusion models are also complete market models like the GBM model. In fact, the (1-dimensional) GBM model is based on a geometric Brownian motion which is simply a local volatility model with constant local volatility. In some cases, nonlinear local volatility models admit closed-form formulas for pricing options. Families of local volatility diffusion models that can be analytically solved in closed form have been developed in several papers, see e.g., Albanese and Campolieti [2] and Campolieti and Makarov [9]. They are obtained by applying the "diffusion canonical transformation" to more basic diffusions such as the Bessel, Cox–Ingersoll–Ross and Ornstein-Uhlenbeck processes. These models have been shown to calibrate quite well to equity and FX options. One drawback of local volatility diffusion models is that they assume a perfect correlation between the underlying asset price and the volatility. In some cases, this contradicts the empirical evidence that they should have an imperfect negative correlation [19].

The stock market is incomplete in many situations as traders cannot use options for hedging all the risks. Stochastic volatility models are incomplete and assume that the volatility is a random process. We can make the movements of the underlying asset price and the volatility to be negatively correlated. One example is the Heston model proposed in 1993 by Heston [14]. Heston successfully applied the Fourier transform method to evaluate European vanilla options with an arbitrary correlation between the asset price and the volatility. He also showed that the distribution of asset returns is asymmetric and found that when the marginal distributions of the asset returns and the volatility are negatively skewed, the BS out-of-the-money (OTM) option prices are negatively biased (i.e., BS OTM option prices are usually smaller compared to market prices) and BS in-the-money (ITM) option prices are positively biased. Another example is the SABR model introduced in 2002 by Hagan et al [13]. The implied volatility curve captured by the SABR model gives consistency with the observed marketplace in dynamics.

In this thesis, we are mainly interested in constructing new pricing models with stochastic volatility exhibiting symmetric smiles in the log-forward moneyness, and admitting simple closed-form analytical expressions for European-style option prices. Classical examples of solvable stochastic volatility models with symmetric smiles include the Heston model and the lognormal SABR model with zero correlation case. These models admit closed-form formulas for European-style option prices which are often expressed as integrals. Closed-form expressions were obtained by taking the expectation of option prices under diffusion models over the integrated squared volatility process, which relate to the Bayesian framework in the GBM model studied by Darsinos and Satchell [12]. We will employ the Bayesian framework to our new models in this thesis. In particular, we will assume that; (1) there are no correlations between the asset prices and their volatility, and (2) the integrated squared volatility processes are random variables with well-known probability density functions.

This thesis is organized as follows. In Section 1.2, we state some of our main results pertaining to static randomization in Part II. In Part I we briefly go through some existing option pricing models that motivated us in studying the new models, namely, the CEV model (Chapter 2) and the SABR model (Chapter 3). In Chapter 2, we formulate two pricing formulas for a European vanilla option under the CEV model. In Chapter 3, we state Hagan et al. implied BS volatility formula (Section 3.1). The closed-form pricing formula assuming zero infinitesimal correlation between asset price and volatility is explained in detail (Section 3.2 and Appendix A). In Part II, we introduce the static randomization in the

GBM framework for the single-asset economy (Chapter 4) and some applications (Chapter 5). Before we state our new main results, we first give motivations on the randomized GBM models by randomizing the volatility parameter in the GBM model (Section 4.1), and also how the randomization can be extended from the GBM model with a time-dependent volatility (Section 4.2). In Sections 4.3 and 4.4, we derive analytical expressions for the transition probability density functions (PDFs) and the cumulative density functions (CDFs) for the randomized processes. In Section 4.5, we obtain our European vanilla call option pricing formulas and compare with the BS formula for the call option prices. In Section 4.6, we find the greeks of European vanilla call options under the randomized GBM models. In Section 4.7, we investigate the shapes of BS implied volatility under randomization. In Section 4.8, we conduct our numerical experiments pertaining to model calibrations to a real world data. In Section 4.9, we test the stability of the parameters in the randomized GBM models. In Chapter 5, we provide an extension to transition PDFs with imposed killing (Section 5.1), first hitting times up to some threshold level (Sections 5.2 and 5.3), novel two-asset economy models (Section 5.4) and randomized CEV models (Section 5.5).

1.2 Main Results

Let $(\Omega, \mathcal{F}, \mathbb{P}, \{\mathcal{F}_t\}_{t\geqslant 0})$ be some fixed filtered probability space where $\{\mathcal{F}_t\}_{t\geqslant 0}$ is the natural filtration generated by the $\mathbb{P}$-BM.[1] Assume we are under the GBM model in a single-asset economy where the asset price (diffusion) process $\{S_t\}_{t\geqslant 0}$ follows a GBM with stochastic differential equation (SDE):

$$\frac{dS_t}{S_t} = r dt + \sqrt{v} d\widetilde{W}_t; \quad S_0 > 0, \tag{1.1}$$

[1]Throughout this thesis, we use $(\Omega, \mathcal{F}, \mathbb{P}, \{\mathcal{F}_t\}_{t\geqslant 0})$ to denote a filtered probability space.

where r is the constant risk-free rate, v is the constant variance[2] and $\{\widetilde{W}_t\}_{t\geqslant 0}$ is a standard $\widetilde{\mathbb{P}}$-BM (i.e., Brownian motion under the risk-neutral measure). The well-known BS formula of a European vanilla call option price struck at K (with current time t and the maturity at calendar time T) can be expressed in terms of the standard normal CDF:[3]

$$\begin{aligned} C_{BS}(\tau, S; K, r, v) =& \mathrm{e}^{-r\tau}\widetilde{\mathbb{E}}_{t,S}[(S_T - K)^+] \equiv \mathrm{e}^{-r\tau}\widetilde{\mathbb{E}}[(S_T - K)^+ | S_t = S] \\ =& S\left[\mathcal{N}\left(\frac{m + \frac{1}{2}v\tau}{\sqrt{v\tau}}\right) - \mathrm{e}^{-m}\mathcal{N}\left(\frac{m - \frac{1}{2}v\tau}{\sqrt{v\tau}}\right)\right], \end{aligned} \tag{1.2}$$

where $\tau = T - t$ is the time to maturity and

$$m = \ln\frac{S}{K} + r\tau \tag{1.3}$$

is the log-forward moneyness.[4] Dividing both sides in (1.2) by S yields:

$$\widehat{C}_{BS}(\tau, m; v) \equiv \frac{C_{BS}(\tau, S; K, r, v)}{S} = \mathcal{N}\left(\frac{m + \frac{1}{2}v\tau}{\sqrt{v\tau}}\right) - \mathrm{e}^{-m}\mathcal{N}\left(\frac{m - \frac{1}{2}v\tau}{\sqrt{v\tau}}\right). \tag{1.4}$$

Note that the RHS in (1.4) depends on (τ, m, v), and hence we write the call option price C_{BS} relative to the spot price S as $\widehat{C}_{BS}(\tau, m; v)$ for convenience. It follows that we have the following symmetry property:[5]

$$\begin{aligned} \widehat{C}_{BS}(\tau, m; v) =& \mathcal{N}\left(\frac{m + \frac{1}{2}v\tau}{\sqrt{v\tau}}\right) - \mathrm{e}^{-m}\mathcal{N}\left(\frac{m - \frac{1}{2}v\tau}{\sqrt{v\tau}}\right) \\ =& \left[1 - \mathcal{N}\left(\frac{-m - \frac{1}{2}v\tau}{\sqrt{v\tau}}\right)\right] - \mathrm{e}^{-m}\left[1 - \mathcal{N}\left(\frac{-m + \frac{1}{2}v\tau}{\sqrt{v\tau}}\right)\right] \\ =& (1 - \mathrm{e}^{-m}) + \mathrm{e}^{-m}\left[\mathcal{N}\left(\frac{-m + \frac{1}{2}v\tau}{\sqrt{v\tau}}\right) - \mathrm{e}^{m}\mathcal{N}\left(\frac{-m - \frac{1}{2}v\tau}{\sqrt{v\tau}}\right)\right] \\ =& (1 - \mathrm{e}^{-m}) + \mathrm{e}^{-m}\widehat{C}_{BS}(\tau, -m; v), \end{aligned} \tag{1.5}$$

which is useful and carries over to the randomized GBM models later. In formulating newly solvable models based on randomization of the variance parameter v, we consider v as a

[2]In the GBM model, $\sigma = \sqrt{v}$ usually denotes the constant volatility parameter.

[3]Throughout this thesis, we will use $\widetilde{\mathbb{E}}$ to denote the risk-neutral expectation with bank account as numéraire.

[4]We denote $m \equiv m(S, K, \tau) = \ln\frac{S}{K} + r\tau$ to avoid clutter.

[5]They are symmetric in a sense that $C_{BS}(\tau, m; v)$ and $C_{BS}(\tau, -m; v)$ are related to one another

random variable equipped with some known PDF. We denote such a random variable by $\mathcal{V}$ to distinguish it from the ordinary variable v. Then, we can formulate the (time-homogeneous) pricing function for a European-style option with payoff function $\Lambda(S)$ by:

$$V_{\mathcal{V}}(\tau, S) = \mathrm{e}^{-r\tau} \int_0^\infty \widetilde{\mathbb{E}}_{t,S}[\Lambda(S_T)] f_{\mathcal{V}}(v) dv \tag{1.6}$$

For example, the price of a European vanilla call option under the BS model, with variance randomized according to the PDF $f_{\mathcal{V}}$, can be expressed as:

$$\begin{aligned} \widehat{C}_{\mathcal{V}}(\tau, m) \equiv \frac{C_{\mathcal{V}}(\tau, S; K, r)}{S} &= \int_0^\infty \frac{C_{BS}(\tau, S; K, r, v)}{S} f_{\mathcal{V}}(v) dv \\ &= \int_0^\infty \mathcal{N}\left(\frac{m + \frac{1}{2}v\tau}{\sqrt{v\tau}}\right) f_{\mathcal{V}}(v) dv - \mathrm{e}^{-m} \int_0^\infty \mathcal{N}\left(\frac{m - \frac{1}{2}v\tau}{\sqrt{v\tau}}\right) f_{\mathcal{V}}(v) dv, \end{aligned} \tag{1.7}$$

which depends on (τ, m) and a set of parameters in $\mathcal{V}$, it is easy to see that under some mild regularity conditions, (1.7) retains the symmetry property after the volatility randomization:

$$\widehat{C}_{\mathcal{V}}(\tau, m) = (1 - \mathrm{e}^{-m}) + \mathrm{e}^{-m} \widehat{C}_{\mathcal{V}}(\tau, -m). \tag{1.8}$$

The interesting and surprising fact about the pricing function in (1.7) is that it can be expressed as an elementary analytical function (perhaps, more trivial than the corresponding BS formula) assuming $\mathcal{V}$ follows either the gamma and the inverse gamma distribution. For example, if $\mathcal{V}$ follows the gamma distribution with shape parameter $\theta = 1$ and scale parameter λ, i.e., $\mathcal{V} \sim G(1, \lambda)$, then the PDF of $\mathcal{V}$ is

$$f_{\mathcal{V}}(v) \equiv f_{G(\theta,\lambda)}(v) = \frac{1}{\lambda^\theta \Gamma(\theta)} v^{\theta-1} \mathrm{e}^{-\frac{v}{\lambda}}. \tag{1.9}$$

By applying (1.7), the price of a European vanilla call option, with variance randomized according to (1.9), can be expressed as the Laplace transform of the standard normal CDFs:[6]

$$
\begin{aligned}
\widehat{C}_{G(1,\lambda)}(\tau,m) \equiv \frac{C_{G(1,\lambda)}\left(\tau,S;K,r\right)}{S} =&\lambda^{-1}\mathcal{L}_v\left\{\mathcal{N}\left(\frac{m+\frac{1}{2}v\tau}{\sqrt{v\tau}}\right)\right\}(\lambda^{-1}) \\
&- \mathrm{e}^{-m}\lambda^{-1}\mathcal{L}_v\left\{\mathcal{N}\left(\frac{m-\frac{1}{2}v\tau}{\sqrt{v\tau}}\right)\right\}(\lambda^{-1}),
\end{aligned}
\tag{1.10}
$$

and (1.10) takes the simple analytical form:

$$
\widehat{C}_{G(1,\lambda)}(\tau,m) = (1-\mathrm{e}^{-m})^{+} + \frac{\sqrt{\lambda\tau}}{\sqrt{8+\lambda\tau}}\exp\left(-\frac{|m|}{2}\frac{\sqrt{8+\lambda\tau}}{\sqrt{\lambda\tau}} - \frac{m}{2}\right), \tag{1.11}
$$

where $x^{+} = \max(x,0)$ and m was defined in (1.3). If $\mathcal{V}$ follows the inverse gamma distribution with shape parameter $\theta = 1$ and scale parameter λ, i.e., $\mathcal{V} \sim IG(1,\lambda)$, then the PDF of $\mathcal{V}$ is

$$
f_{\mathcal{V}}(v) \equiv f_{IG(\theta,\lambda)}(v) = \frac{\lambda^{\theta}}{\Gamma(\theta)}\left(\frac{1}{v}\right)^{\theta+1}\mathrm{e}^{-\frac{\lambda}{v}}. \tag{1.12}
$$

By a change of variable ($v' = \frac{1}{v}$), we have an integral identity:

$$
\int_0^{\infty}\left(\frac{1}{v}\right)^{2}\mathrm{e}^{-\frac{\lambda}{v}}\mathcal{N}\left(\frac{m\pm\frac{1}{2}v\tau}{\sqrt{v\tau}}\right)dv = \int_0^{\infty}\mathrm{e}^{-\lambda v'}\mathcal{N}\left(\frac{m\sqrt{v'}}{\sqrt{\tau}} \pm \frac{\sqrt{\tau}}{2\sqrt{v'}}\right)dv'. \tag{1.13}
$$

Again, by applying (1.7), the price of a European vanilla call option can be expressed as the Laplace transform of the standard normal CDFs:

$$
\begin{aligned}
\widehat{C}_{IG(1,\lambda)}(\tau,m) \equiv \frac{C_{IG(1,\lambda)}\left(\tau,S;K,r\right)}{S} =&\lambda\mathcal{L}_{v'}\left\{\mathcal{N}\left(\frac{m\sqrt{v'}}{\sqrt{\tau}}+\frac{\sqrt{\tau}}{2\sqrt{v'}}\right)\right\}(\lambda) \\
&- \lambda\mathrm{e}^{-m}\mathcal{L}_{v'}\left\{\mathcal{N}\left(\frac{m\sqrt{v'}}{\sqrt{\tau}}-\frac{\sqrt{\tau}}{2\sqrt{v'}}\right)\right\}(\lambda),
\end{aligned}
\tag{1.14}
$$

and (1.14) takes the simple analytical form:

$$
\widehat{C}_{IG(1,\lambda)}(\tau,m) =1-\exp\left(-\frac{1}{2}\left(m+\sqrt{m^2+2\lambda\tau}\right)\right); m \in \mathbb{R}. \tag{1.15}
$$

[6]Recall that a Laplace transform of a function f at s is defined as:

$$
\mathcal{L}_t\{f(t)\}(s) = \int_0^{\infty}\mathrm{e}^{-st}f(t)dt, \quad \Re(s) > c,
$$

where c is the abscissa of convergence.

More generally for any integer-valued shape parameter $\theta = n \in \mathbb{N}$, the pricing function can be expressed in terms of the modified Bessel function of the second kind K. For example, if $\mathcal{V} \sim G(n, \lambda)$, then

$$\begin{aligned}
\widehat{C}_{G(n,\lambda)}(\tau, m) \equiv & \frac{C_{G(n,\lambda)}\left(\tau, S; K, r\right)}{S} \\
= & (1 - \mathrm{e}^{-m})^{+} + \frac{\sqrt{|m|}}{\sqrt{\pi}} \left(\frac{\lambda\tau}{8 + \lambda\tau} \right)^{\frac{1}{4}} \mathrm{e}^{-\frac{m}{2}} \\
& \times \sum_{k=0}^{n-1} \frac{1}{k!} \left(\frac{2|m|}{\sqrt{\lambda\tau}\sqrt{8 + \lambda\tau}} \right)^{k} \mathsf{K}_{k+\frac{1}{2}} \left(\frac{|m|}{2} \frac{\sqrt{8 + \lambda\tau}}{\sqrt{\lambda\tau}} \right).
\end{aligned} \tag{1.16}$$

If $\mathcal{V} \sim IG(n, \lambda)$, then

$$\begin{aligned}
\widehat{C}_{IG(n,\lambda)}(\tau, m) \equiv & \frac{C_{IG(n,\lambda)}\left(\tau, S; K, r\right)}{S} \\
= & 1 - \frac{(m^2 + 2\lambda\tau)^{\frac{1}{4}}}{\sqrt{\pi}} \mathrm{e}^{-\frac{m}{2}} \\
& \times \sum_{k=0}^{n-1} \frac{1}{k!} \left(\frac{\lambda\tau}{2\sqrt{m^2 + 2\lambda\tau}} \right)^{k} \mathsf{K}_{k-\frac{1}{2}} \left(\frac{\sqrt{m^2 + 2\lambda\tau}}{2} \right).
\end{aligned} \tag{1.17}$$

It can be shown that the option prices in (1.16) and (1.17) retain the symmetry property in (1.8), and exhibit symmetric smiles in the BS implied volatility. Thus, these models may be used to calibrate to option price market data

It is also worth noting that the underlying probability distribution of such randomized processes have thicker tails than the GBM. In particular, randomized processes considered in our paper do not have second moments in most cases.

Part I

Literature Review

Chapter 2

CEV Model

2.1 Pricing European Vanilla Options

The stochastic differential equation (SDE) of the driftless CEV process ($\{F_t\}_{t\geqslant 0}$) with deterministic time-dependent squared volatility $v(t) > 0$ for any $t \geqslant 0$ is

$$\frac{dF_t}{F_t} = \sqrt{v(t)} F_t^{\beta} dW_t; \quad F_0 > 0, \tag{2.1}$$

where F_t is the forward price at time t, β is the skew parameter and $\{W_t\}_{t\geqslant 0}$ is a standard $\mathbb{P}$-BM. Our objective here is to convert the driftless CEV into a squared Bessel (SQB) process for $\beta \neq 0$. In our first step, we define the monotonic mapping:

$$\mathfrak{X} : F \longrightarrow \frac{F^{-2\beta}}{\beta^2} \tag{2.2}$$

to construct a new process:

$$X_t = \mathfrak{X}(F_t) = \frac{F_t^{-2\beta}}{\beta^2} = 4\nu^2 F_t^{-\frac{1}{\nu}}, \tag{2.3}$$

where $\nu = \frac{1}{2\beta}$. By Ito's formula, the process satisfies the SDE:

$$
\begin{aligned}
dX_t =& \frac{1}{2}\left(4(\nu+1)F_t^{-2-\frac{1}{\nu}}\right)(dF_t)^2 - \left(4\nu F_t^{-1-\frac{1}{\nu}}\right)dF_t \\
=& \left(2(\nu+1)F_t^{-2-\frac{1}{\nu}}\right)v(t)F_t^{2+\frac{1}{\nu}}dt - \left(4\nu F_t^{-1-\frac{1}{\nu}}\right)\sqrt{v(t)}F_t^{1+\frac{1}{2\nu}}dW_t \\
=& 2(\nu+1)v(t)dt + 2\sqrt{v(t)}\left(2|\nu|F_t^{-\frac{1}{2\nu}}\right)dW_t \\
=& 2(\nu+1)v(t)dt + 2\sqrt{v(t)}\sqrt{X_t}dW_t.
\end{aligned} \tag{2.4}
$$

We define a deterministic time change[1] as:

$$
\Upsilon(s,t) = \int_s^t v(u)du, \quad s < t, \tag{2.5}
$$

where we denote $\Upsilon(t) \equiv \Upsilon(0,t)$. Then $X_{\Upsilon(t)}$ is a SQB process with the SDE:

$$
dX_{\Upsilon(t)} = 2(\nu+1)d\Upsilon(t) + 2\sqrt{X_{\Upsilon(t)}}dW_{\Upsilon(t)}; \qquad dW_{\Upsilon(t)} = \sqrt{v(t)}dW_t. \tag{2.6}
$$

The transition probability density function (PDF) of the SQB process is[2]

$$
\begin{aligned}
p^{\mathrm{SQB}}(\tau;x,y) =& \frac{\mathbb{P}(X_T \in dy | X_t = x)}{dy} = \frac{1}{2\tau}\left(\frac{y}{x}\right)^{\frac{\nu}{2}} \mathrm{e}^{-\frac{x+y}{2\tau}} I_{\widetilde{\nu}}\left(\frac{\sqrt{xy}}{\tau}\right) \\
=& \frac{1}{\tau} f_{\chi^2}\left(\frac{x}{\tau}; 2+2\widetilde{\nu}, \frac{y}{\tau}\right); \quad \tau = T-t > 0, \quad x, y > 0,
\end{aligned} \tag{2.7}
$$

where $I_{\widetilde{\nu}}$ is the modified Bessel function of the first kind of order $\widetilde{\nu}$, and where

$$
\widetilde{\nu} = \begin{cases} \nu & \text{if } \nu \geqslant 0 \text{ or } \nu \in (-1,0) \text{ with 0 specified as a reflecting boundary,} \\ |\nu| & \text{if } \nu \leqslant -1 \text{ or } \nu \in (-1,0) \text{ with 0 specified as a killing boundary.} \end{cases} \tag{2.8}
$$

f_{χ^2} is the PDF of the noncentral chi-square distribution

$$
f_{\chi^2}(x;k,\lambda) = \frac{1}{2}\left(\frac{x}{\lambda}\right)^{\frac{k-2}{4}} I_{\frac{k-2}{2}}(\sqrt{\lambda x}) \exp\left(-\frac{\lambda+x}{2}\right), \tag{2.9}
$$

where $k > 0$ is the degree of freedom and $\lambda \geqslant 0$ is the noncentrality parameter. For $\beta < 0$ with killing boundary at 0, the transition PDF for the driftless CEV process $\{F_t\}_{t \geqslant 0}$ can be

[1] We may call it a "stochastic time-changed process", denoted by $\Upsilon_{s,t}$ if $v(t) \equiv \sigma_t^2$ is a stochastic process.

[2] Note that $\mathbb{P}_x(X_\tau \in dy) = p(\tau;x,y)dy$. That is, the density is w.r.t. the Lebesgue measure.

obtained from the change of variables:

$$
\begin{aligned}
p_{\text{cev}}(t,T;F,y) =& p^{\text{SQB}}(\Upsilon(t,T);\mathfrak{X}(F),\mathfrak{X}(y))\cdot\mathfrak{X}'(y)\\
=& \frac{y^{-2\beta-\frac{3}{2}}F^{\frac{1}{2}}}{|\beta|\Upsilon(t,T)}\exp\left(-\frac{y^{-2\beta}+F^{-2\beta}}{2\beta^2\Upsilon(t,T)}\right)I_{\frac{1}{2|\beta|}}\left(\frac{y^{-\beta}F^{-\beta}}{\beta^2\Upsilon(t,T)}\right).
\end{aligned}
\tag{2.10}
$$

Let us extend it to the CEV process with a constant drift r satisfiying the SDE:

$$
\frac{dS_t}{S_t} = rdt + \sqrt{v(t)}S_t^{\beta}d\widetilde{W}_t; \qquad S_0 > 0, \tag{2.11}
$$

where r is the constant risk-free interest rate. One can easily show that it can be transformed into (2.6) using the following scaling transformation and deterministic time change:[3]

$$
\mathfrak{X}: S \longrightarrow \frac{S^{-2\beta}}{\beta^2}, \quad \Upsilon:(s,t)\longrightarrow \int_s^t \mathrm{e}^{2\beta r(u-s)}v(u)du. \tag{2.12}
$$

For $\beta < 0$ with killing boundary at 0, the (risk-neutral) transition PDF for the drifted CEV process $\{S_t\}_{t\geqslant 0}$ can be obtained from the change of variables:[4]

$$
\begin{aligned}
&\widetilde{p}_{\text{cev}}(t,T;S,y) = \mathrm{e}^{-r\tau}p^{\text{SQB}}(\Upsilon(t,T);\mathfrak{X}(S),\mathfrak{X}(\mathrm{e}^{-r\tau}y))\cdot\mathfrak{X}'(\mathrm{e}^{-r\tau}y)\\
&= \mathrm{e}^{-r\tau}\frac{(\mathrm{e}^{-r\tau}y)^{-2\beta-\frac{3}{2}}S^{\frac{1}{2}}}{|\beta|\Upsilon(t,T)}\exp\left(-\frac{(\mathrm{e}^{-r\tau}y)^{-2\beta}+S^{-2\beta}}{2\beta^2\Upsilon(t,T)}\right)I_{\frac{1}{2|\beta|}}\left(\frac{(\mathrm{e}^{-rt}y)^{-\beta}S^{-\beta}}{\beta^2\Upsilon(t,T)}\right).
\end{aligned}
\tag{2.13}
$$

Note that the discounted asset price process $\{\mathrm{e}^{-rt}S_t\}_{t\geqslant 0}$, with $\beta < 0$ and killing boundary at 0, is a $\widetilde{\mathbb{P}}$-martingale. The pricing formula for a European vanilla call option at time t (with current price $S_t = S$, maturity time T and strike price K) is as follows:[5]

$$
\begin{aligned}
C_{\text{cev}}(t,T,S;K,r) =& \mathrm{e}^{-r\tau}\int_K^{\infty}(y-K)^+\widetilde{p}_{\text{cev}}(t,T;S,y)dy\\
=& S_0Q\left(m;2+\frac{1}{|\beta|},y_0\right) - e^{-r\tau}K\left(1-Q\left(y_0;\frac{1}{|\beta|},m\right)\right),
\end{aligned}
\tag{2.14}
$$

where

$$
\tau = T-t, \quad m = \frac{(\mathrm{e}^{-r\tau}K)^{-2\beta}}{\beta^2\Upsilon(t,T)}, \quad y_0 = \frac{S^{-2\beta}}{\beta^2\Upsilon(t,T)}, \quad \Upsilon(t,T) = \int_t^T \mathrm{e}^{2\beta r(u-t)}v(u)du, \tag{2.15}
$$

[3]We defined the time change in a way that it retains time-homogeneity (i.e. $\Upsilon(s,t)$ depends solely on the time difference $t-s$) for the time-independent CEV model (i.e., constant variance $v(t)\equiv v$).

[4]See (16.21) in Campolieti and Makarov [10].

[5]See (16.28) in Campolieti and Makarov [10]

and Q is the complementary distribution function for the noncentral chi-square distribution

$$Q(x; k.\lambda) = \int_x^\infty f_{\chi^2}(y; k, \lambda) dy. \tag{2.16}$$

The option price in (2.14) can be easily obtained numerically using quadrature rules. Alternatively, since the complementary noncentral chi-square distribution function can be computed using the double series:

$$Q(x, k, \lambda) = 1 - \sum_{n=1}^{\infty} \left(g(n + \frac{k}{2}, \frac{x}{2}) \sum_{j=1}^{n} g(j, \frac{\lambda}{2}) \right), \tag{2.17}$$

where g is the gamma PDF

$$g(m, x) = \frac{\mathrm{e}^{-x} x^{m-1}}{\Gamma(m)}. \tag{2.18}$$

In the next section, we will present an alternative approach for computing European vanilla call option prices from Antonov et al. and state its advantages and disadvantages.

2.2 An Integral Representation of the Pricing Formula

For general time-homogeneous diffusion models, we assume that the forward price process $\{F_t\}_{t \geqslant 0}$ is a $\mathbb{P}$-martingale obeying the following SDE:

$$\frac{dF_t}{F_t} = \sigma(F_t) dW_t, \tag{2.19}$$

where $\sigma(\cdot)$ is the time-independent local volatility function. (Here, the local volatility function depends only on the spot forward price.) The price of a European vanilla call option on the forward price struck at K, with spot $F_t = F$, can be decomposed into its intrinsic and time value in the following sense:[6]

$$C(\tau, F; K) = \overbrace{(F - K)^+}^{\text{intrinsic value}} + \overbrace{\frac{\sigma^2(K) K^2}{2} \int_0^\tau p(t; F, K) dt}^{\text{time value}}, \tag{2.20}$$

[6]See (26) in Carr and Jarrow [11].

where p is the transition PDF for the diffusion process. The decomposition can also be used for the driftless CEV process with time-dependent variance $v(t)$. In this case, the local volatility function is time-dependent, i.e.,

$$\sigma^2(t,F) = v(t)F^{2\beta}, \tag{2.21}$$

and the transition PDF for $\{F_t\}_{t\geqslant 0}$ is given in (2.10). So that the price of a European vanilla call option (with $r=0$) for the driftless CEV process can be expressed as

$$\begin{aligned} C_{\text{cev}}(t,T,F;K) =&(F-K)^+ + \frac{K^{2(1+\beta)}}{2}\int_t^T p_{\text{cev}}(t,u;F,K)du. \\ =&(F-K)^+ + \frac{\sqrt{KF}}{2|\beta|}\int_t^T \frac{\exp\left(-\frac{q_K^2+q_0^2}{2\Upsilon(t,u)}\right)}{\Upsilon(t,u)} I_{\frac{1}{2|\beta|}}\left(\frac{q_K q_0}{\Upsilon(t,u)}\right)dt, \end{aligned} \tag{2.22}$$

where $\tau = T-t$ and

$$q_K = \sqrt{\mathfrak{X}(K)} = \frac{K^{-\beta}}{-\beta}, \quad q_0 = \sqrt{\mathfrak{X}(F)} = \frac{F^{-\beta}}{-\beta}, \quad \Upsilon(t,T) = \int_t^T v(u)du. \tag{2.23}$$

And the integral representation of the modified Bessel function of the first kind is:

$$I_\nu(s) = \frac{1}{2\pi i}\int_{C_w} \mathrm{e}^{\cosh w - \nu w}dw \tag{2.24}$$

where C_w is the three-legged contour bounded by $(-\pi i+\infty, -\pi i], [-\pi i, \pi i], [\pi i, \pi i+\infty)$. Applying the change of variable $s = \frac{q_k q_0}{\tau}$ and integration by parts in w yields:[7]

$$\begin{aligned} C_{\text{cev}}(t,T,F;K) =&(F-K)^+ + \frac{\sqrt{KF}}{4|\beta|\pi i}\int_{C_w} \mathrm{e}^{-\frac{w}{2|\beta|}}\int_{\frac{q_k q_0}{\Upsilon(t,T)}}^\infty \frac{\mathrm{e}^{-s(b-\cosh w)}}{s}dsdw \\ =&(F-K)^+ + \frac{\sqrt{KF}}{4|\beta|\pi i}\int_{C_w} \mathrm{e}^{-\frac{w}{2|\beta|}}\sinh w\int_{\frac{q_k q_0}{\Upsilon(t,T)}}^\infty \mathrm{e}^{-s(b-\cosh w)}dsdw \\ =&(F-K)^+ + \frac{\sqrt{KF}}{2\pi i}\int_{C_w} \frac{\mathrm{e}^{-\frac{w}{2|\beta|}}\sinh w}{b-\cosh w}\mathrm{e}^{-\frac{q_K q_0(b-\cosh w)}{\Upsilon(t,T)}}dw \\ =&(F-K)^+ + \frac{\sqrt{KF}}{\pi}\left(\int_0^\pi \frac{\sin(\frac{\theta}{2|\beta|})\sin\theta}{b-\cos\theta}\mathrm{e}^{\frac{-q_k q_0(b-\cos\theta)}{\Upsilon(t,T)}}d\theta\right. \\ &\left.+\sin\left(\frac{\pi}{2|\beta|}\right)\int_0^\infty \frac{\mathrm{e}^{-\frac{x}{2|\beta|}}\sinh x}{b+\cosh x}\mathrm{e}^{-\frac{q_k q_0(b+\cosh x)}{\Upsilon(t,T)}}dx\right), \end{aligned} \tag{2.25}$$

[7] See (2.3) in Antonov et al [4]

where $\tau = T - t$ and

$$q_0 = \frac{F^{-\beta}}{-\beta}, \quad q_k = \frac{K^{-\beta}}{-\beta}, \quad b = \frac{q_k^2 + q_0^2}{2q_k q_0}, \quad \Upsilon(t,T) = \int_t^T v(u)du. \tag{2.26}$$

From (2.25), we obtain an alternative pricing formula for the call option by sending $F \to S$ and $K \to \mathrm{e}^{-r\tau}K$

$$\begin{aligned} C_{\text{cev}}(t,T,S;K,r) =& (S - \mathrm{e}^{-r\tau}K)^+ + \frac{\sqrt{\mathrm{e}^{-r\tau}KS}}{\pi}\left(\int_0^\pi \frac{\sin(\frac{\theta}{2|\beta|})\sin\theta}{b-\cos\theta}\mathrm{e}^{\frac{-q_k q_0(b-\cos\theta)}{\Upsilon(t,T)}}d\theta\right. \\ &\left. + \sin\left(\frac{\pi}{2|\beta|}\right)\int_0^\infty \frac{\mathrm{e}^{-\frac{x}{2|\beta|}}\sinh x}{b+\cosh x}\mathrm{e}^{-\frac{q_k q_0(b+\cosh x)}{\Upsilon(t,T)}}dx\right), \end{aligned} \tag{2.27}$$

where

$$q_0 = \frac{S^{-\beta}}{-\beta}, \quad q_k = \frac{(\mathrm{e}^{-r\tau}K)^{-\beta}}{-\beta}, \quad b = \frac{q_k^2 + q_0^2}{2q_k q_0}, \quad \Upsilon(t,T) = \int_t^T \mathrm{e}^{2\beta r(u-t)}v(u)du. \tag{2.28}$$

However, the integrands in (2.25) and (2.27) are oscillatory functions and we require evaluating the integrals using quadrature rules. Despite the issues in evaluating integrals of oscillatory functions numerically, the integral representations in (2.25) and (2.27) can be extended to the SABR model for the zero correlation case. We will illustrate this in more detail in Chapter 3.

Chapter 3

SABR Model

3.1 The Hagan et al. Implied Volatility Formula

The classical stochastic-alpha-beta-rho (SABR) model is a two-factor model governed by two SDEs:[1]

$$\begin{cases} \dfrac{dF_t}{F_t} = \sigma_t F_t^{\beta} dW_t^{(1)}, \quad & F_0 > 0, \\ \dfrac{d\sigma_t}{\sigma_t} = \alpha dW_t^{(2)}, \quad & \sigma_0 > 0, \\ dW_t^{(1)} dW_t^{(2)} = \rho\, dt, \end{cases} \tag{3.1}$$

where $\{\sigma_t\}_{t\geqslant 0}$ is the volatility process, α is the volatility of the volatility, β is the skew parameter, ρ is a correlation parameter, and $\{\mathbf{W}_t\}_{t\geqslant 0} \equiv \{(W_t^{(1)}, W_t^{(2)})\}_{t\geqslant 0}$ is a two-dimensional $\mathbb{P}$-BM, with $\{W_t^{(i)}\}_{t\geqslant 0}, i = 1, 2,$ as standard $\mathbb{P}$-BMs. Note that $\{(F_t, \sigma_t)\}_{t\geqslant 0}$ is time-homogeneous jointly Markovian[2] so we can obtain the joint density function in terms of the time to maturity ($\tau = T - t$):

$$p_{\text{sabr}}(\tau; F, \sigma, x, y) \equiv p_{\text{sabr}}(t, T; F, \sigma, x, y) = \frac{\mathbb{P}_{t,F,\sigma}\left(F_T \in dx, \sigma_T \in dy\right)}{dxdy}, \tag{3.2}$$

[1]The reader must be careful with the notations as Hagan et al used α to denote the volatility process (or the initial volatility) and v to denote the volatility of the volatilty.

[2]For example, see Section 2.1 in Wu [22].

and path-independent option prices with payoff function $\Lambda(F)$ can be expressed as double integrals:

$$V_{\text{sabr}}(\tau, F, \sigma) = \int_0^\infty \int_0^\infty \Lambda(x) p_{\text{sabr}}(\tau; F, \sigma, x, y) dx dy. \tag{3.3}$$

Based on the singular perturbation method, the Hagan et al. approximate formula for the implied BS volatility given strike K, spot forward price $F_t = F$ and volatility at spot time $\sigma_t = \sigma$ with maturity time τ is:[3]

$$\begin{aligned}\sigma_{\text{hagan}} &\equiv \sigma_{\text{hagan}}(\tau, F, \sigma; K)\\ &= \frac{\left(1 + \left(\frac{\beta^2\sigma^2}{24}(KF)^{\beta} + \frac{\alpha\beta\rho\sigma}{4}(KF)^{\frac{\beta}{2}} + \frac{\alpha^2(2-3\rho^2)}{24}\right)\tau\right)\sigma(KF)^{\frac{\beta}{2}}}{\left[1 + \frac{\beta^2}{24}\left(\ln\frac{F}{K}\right)^2 + \frac{\beta^4}{1920}\left(\ln\frac{F}{K}\right)^4\right]} \frac{z}{\chi(z)},\end{aligned} \tag{3.4}$$

where

$$\begin{aligned} z =& \frac{\alpha}{\sigma}(KF)^{-\frac{\beta}{2}} \ln\frac{F}{K},\\ \chi(z) =& \ln\left(\frac{\sqrt{1-2\rho z + z^2} + z - \rho}{1-\rho}\right). \end{aligned} \tag{3.5}$$

After taking a careful limit in (3.4) as $K \to F$, we obtain the at-the-money (ATM) BS implied volatility

$$\sigma_{\text{atm}} \equiv \sigma_{\text{atm}}(\tau, F, \sigma; F) = \left(1 + \left(\frac{\beta^2\sigma^2}{24}F^{2\beta} + \frac{\alpha\beta\rho\sigma}{4}F^{\beta} + \frac{\alpha^2(2-3\rho^2)}{24}\right)\tau\right)\sigma F^{\beta} \tag{3.6}$$

So the price of a European vanilla call option can be approximated by plugging $\sigma = \sigma_{\text{hagan}}$ for the volatility in the BS formula:

$$C_{\text{sabr}}(\tau, F, \sigma; K) = F\mathcal{N}\left(d_+(\frac{F}{K}, \tau)\right) - K\mathcal{N}\left(d_-(\frac{F}{K}, \tau)\right) \tag{3.7}$$

where

$$d_+(x, \tau) = \frac{\ln x + \frac{1}{2}\sigma_{\text{hagan}}^2\tau}{\sigma_{\text{hagan}}\sqrt{\tau}}; \quad d_-(x, \tau) = d_+(x, \tau) - \sigma_{\text{hagan}}\sqrt{\tau}. \tag{3.8}$$

We plotted the implied volatility in Figure 3.2. We can see that the Hagan et al. formula works well for shorter maturity times, but exhibits substantial errors for longer maturity

[3] See Hagan et al. [13] or (13) in West [20].

times. In Section 3.2, we will state the Antonov et al. formula which works well for both short and long maturity times.

3.2 Pricing European Vanilla Options with Zero Correlation

European vanilla option prices can be expressed in integral forms assuming there is no infinitesimal correlation between an asset price and its volatility. The zero correlation SABR option prices (given τ, $S_t = S$, $\sigma_t = \sigma$) can be written as the expectation of the CEV price (with a constant volatility) over the cumulative variance, i.e.,

$$\begin{aligned} V_{\text{sabr}}(\tau, S, \sigma) =& \mathbb{E}[V_{\text{cev}}(\tau, S, \sigma)] = \int_0^\infty V_{\text{cev}}(\tau, S)\mathbb{P}_{t,\sigma}\left(\Upsilon_{t,T} \in d\gamma\right) \\ =& \int_0^\infty V_{\text{cev}}(\tau, S; K)\mathbb{P}_{\sigma}\left(\Upsilon_{\tau} \in d\gamma\right). \end{aligned} \tag{3.9}$$

where the asset price process S_t conditional on σ_t follows the drifted CEV process. Note that the PDF of an integrated squared GBM given $\sigma_t = \sigma$:

$$\Upsilon_\tau(\sigma) \equiv \int_0^\tau \mathrm{e}^{2\beta r u}\sigma_{t+u}^2 du, \tag{3.10}$$

can be expressed as a series representation.[4] Recall from (2.27) that European vanilla call option prices under the CEV process, with a constant volatility σ and a time to maturity τ, can be expressed as:

$$\begin{aligned} C_{\text{cev}}(\tau, S; K, r) =& (S - \mathrm{e}^{-r\tau}K)^+ + \frac{\sqrt{\mathrm{e}^{-r\tau}KS}}{\pi}\left(\int_0^\pi \frac{\sin(\frac{\theta}{2|\beta|})\sin\theta}{b-\cos\theta}\mathrm{e}^{\frac{-q_k q_0(b-\cos\theta)}{\Upsilon(\tau)}}d\theta\right. \\ & \left. + \sin\left(\frac{\pi}{2|\beta|}\right)\int_0^\infty \frac{\mathrm{e}^{-\frac{x}{2|\beta|}}\sinh x}{b+\cosh x}\mathrm{e}^{-\frac{q_k q_0(b+\cosh x)}{\Upsilon(\tau)}}dx\right), \end{aligned} \tag{3.11}$$

where

$$q_0 = \frac{S^{-\beta}}{-\beta}, \quad q_k = \frac{(\mathrm{e}^{-r\tau}K)^{-\beta}}{-\beta}, \quad b = \frac{q_k^2 + q_0^2}{2q_k q_0}, \quad \Upsilon(\tau) = \int_0^\tau \mathrm{e}^{2\beta r u}\sigma^2 du. \tag{3.12}$$

[4]See 1.9.4 in Borodin et al [8].

From (3.11) and (3.9), we can write out the pricing formula for a European vanilla call option given strike K, spot price $S_t = S$ and volatility at spot time $\sigma_t = \sigma$ as:[5]

$$
\begin{aligned}
C_{\text{sabr}}(\tau, S, \sigma; K, r) =& (S - \mathrm{e}^{-r\tau} K)^{+} \\
&+ \frac{\sqrt{\mathrm{e}^{-r\tau} K S}}{\pi} \left(\int_0^{\pi} \frac{\sin(\frac{\theta}{2|\beta|}) \sin\theta}{b - \cos\theta} \mathbb{E}\left[\mathrm{e}^{\frac{-q_k q_0 (b - \cos\theta)}{\Upsilon_\tau(\sigma)}} \right] d\theta \right. \\
&\left. + \sin\left(\frac{\pi}{2|\beta|}\right) \int_0^{\infty} \frac{\mathrm{e}^{-\frac{x}{2|\beta|}} \sinh x}{b + \cosh x} \mathbb{E}\left[\mathrm{e}^{-\frac{q_k q_0 (b + \cosh x)}{\Upsilon_\tau(\sigma)}} \right] dx \right),
\end{aligned} \tag{3.13}
$$

where q_0, q_k, b, $\Upsilon_\tau(\sigma)$ were defined in (3.12) and (3.10). To obtain the option price analytically, we require the moment generating function of $\Upsilon_\tau^{-1}(\sigma)$ in (3.13) to be analytically tractable. Note that the MGF of an integrated GBM can be expressed in analytically closed form. The expression for the MGF of $\Upsilon_\tau^{-1}(\sigma)$ is:[6]

$$
\mathbb{E}\left[\exp\left(-\frac{\lambda}{\Upsilon_\tau(\sigma)} \right) \right] = \frac{G(\tau, s)}{\cosh s}, \tag{3.14}
$$

where

$$
\begin{aligned}
G(\tau, s) =& \frac{2e^{-\frac{\mu^2 \alpha^2 \tau}{2}}}{\mu^2 \sqrt{2\pi \alpha^2 \tau}} \left(1 + \frac{2\alpha^2 \lambda}{\sigma^2} \right)^{\frac{1+\mu}{2}} \\
& \times \int_s^{\infty} \frac{u}{\alpha^2 \tau} \exp\left(-\frac{u^2}{2\alpha^2 \tau} \right) \sinh\left[|\mu| \cosh^{-1}\left(\frac{\cosh u}{\cosh s} \right) \right] du, \\
\mu =& \frac{\beta r}{\alpha^2} - \frac{1}{2}, \\
s =& \cosh^{-1}\left(\sqrt{1 + \frac{2\alpha^2 \lambda}{\sigma^2}} \right) = \sinh^{-1}\left(\sqrt{\frac{2\alpha^2 \lambda}{\sigma^2}} \right).
\end{aligned} \tag{3.15}
$$

Thus, we arrive at

$$
\begin{aligned}
C_{\text{sabr}}(\tau, S, \sigma; K, r) =& (S - \mathrm{e}^{-r\tau} K)^{+} + \frac{\sqrt{\mathrm{e}^{-r\tau} K S}}{\pi} \left(\int_0^{\pi} \frac{\sin(\frac{\theta}{2|\beta|}) \sin\theta}{b - \cos\theta} \frac{G(\tau, s(\theta))}{\cosh s(\theta)} d\theta \right. \\
&\left. + \sin\left(\frac{\pi}{2|\beta|}\right) \int_0^{\infty} \frac{\mathrm{e}^{-\frac{x}{2|\beta|}} \sinh x}{b + \cosh x} \frac{G(\tau, s(x))}{\cosh s(x)} dx \right)
\end{aligned} \tag{3.16}
$$

[5]See (3.3) in Antonov et al [4].

[6]The detailed proof can be found in Appendix A

where

$$
\begin{aligned}
s(\theta) &= \sinh^{-1}\left(\frac{\sqrt{2\alpha^2 q_k q_0(b-\cos\theta)}}{\sigma}\right),\\
s(x) &= \sinh^{-1}\left(\frac{\sqrt{2\alpha^2 q_k q_0(b+\cosh x)}}{\sigma}\right).
\end{aligned}
\tag{3.17}
$$

By change of variables,

$$
\begin{aligned}
\theta(s) = 2\tan^{-1}\left(\sqrt{\frac{\sinh^2 s - \sinh^2 s_-}{\sinh^2 s_+ - \sinh^2 s}}\right), &\quad x(s) = 2\tanh^{-1}\left(\sqrt{\frac{\sinh^2 s - \sinh^2 s_+}{\sinh^2 s - \sinh^2 s_-}}\right),\\
s_- = \sinh^{-1}\left(\frac{\alpha|q_k - q_0|}{\sigma}\right), &\quad s_+ = \sinh^{-1}\left(\frac{\alpha(q_k + q_0)}{\sigma}\right),
\end{aligned}
\tag{3.18}
$$

we can express (3.16) as an integral over $s \in (s_-, s_+)$ and $s \in (s_+, \infty)$:

$$
\begin{aligned}
C(\tau, S; K) = &(S - \mathrm{e}^{-r\tau}K)^+ + \frac{2\sqrt{\mathrm{e}^{-r\tau}KS}}{\pi}\left(\int_{s_-}^{s_+} \frac{\sin(\frac{\theta(s)}{2|\beta|})}{\sinh s} G(\tau, s)ds\right.\\
&\left. + \sin\left(\frac{\pi}{2|\beta|}\right)\int_{s_+}^{\infty} \frac{\mathrm{e}^{-\frac{x(s)}{2|\beta|}}}{\sinh s} G(\tau, s)ds\right).
\end{aligned}
\tag{3.19}
$$

We can compute the two-dimensional integrals numerically to value the option under the drifted SABR model for the zero correlation case. Unfortunately, it is difficult to integrate such functions as they are often oscillatory. We will not consider evaluating integrals numerically here since it is not the main objective of this thesis.

We will compare the integral formula in (3.19) with a plain Monte Carlo SABR prices where the set of parameter values are listed in Table 3.1. Figure 3.1 shows the plot the Plain Monte Carlo (MC) using the Euler-Maruyama method. We can observe that both curves exhibit the same patterns and the error between the two is small (with 95% confidence interval).

The exact pricing formula for the zero correlation case allows us to obtain more precise BS implied volatility in the general correlation case, even for longer time to maturity τ. Antonov et al. considered mapping the parameter space in the general correlation to the zero correlation one via small-time asymptotic expansions. We will not give the approximate implied BS volatility formula here explicitly since it is unnecessarily long. The reader may refer to Antonov et al. [6], [3], and [5] for more details.

Variable Name	Description	Value
S	spot price	$1, 10$
τ	time to maturity (in years)	$1, 10$
β	skew parameter	-0.4
r	constant risk-free interest rate (%)	3
σ	spot volatility (%)	30
α	volatility of volatility (%)	30
ρ	correlation parameter (%)	0
h	Step size	0.01
M	Sample size	$100, 000$

Table 3.1: Set of parameters used for the numerical experiment.

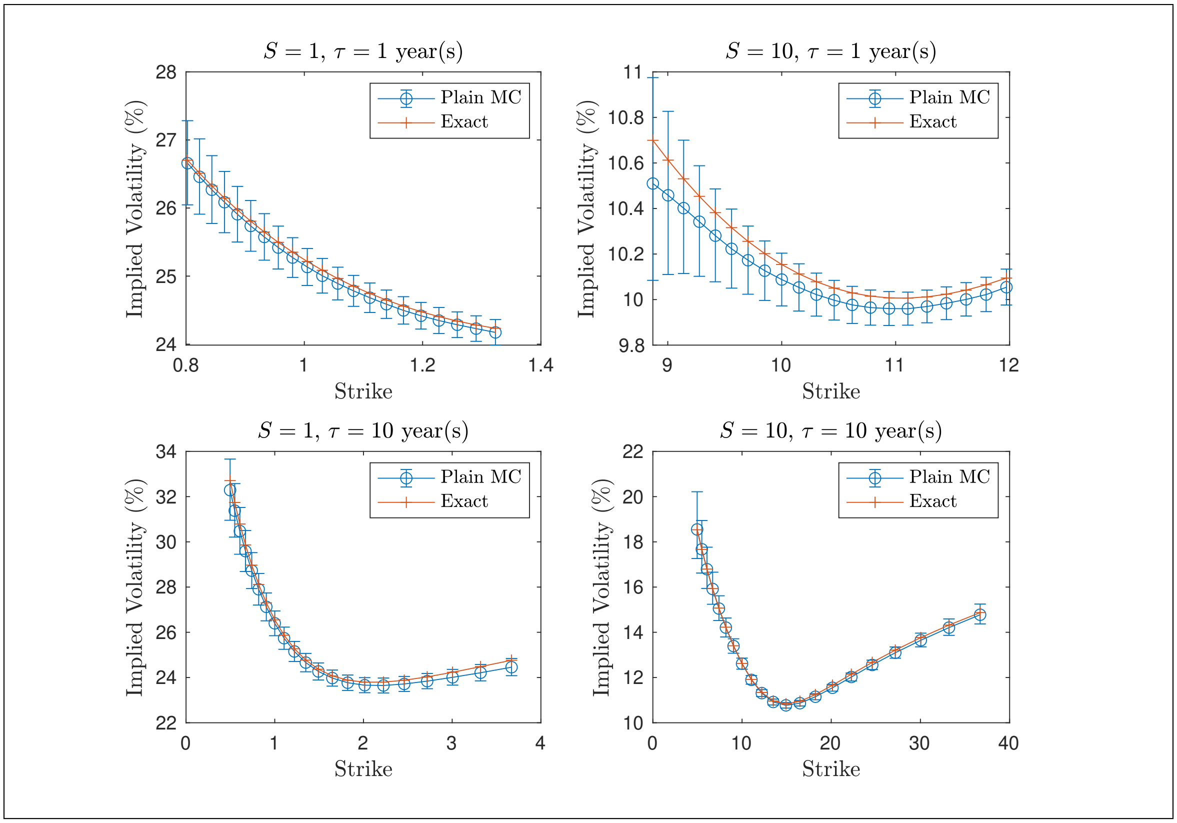

Figure 3.1: Plots of implied volatility under the drifted SABR model. We used 95% confidence interval for the plain MC.

3.3 Numerical Example

In this section, we sketch plots of BS implied volatility using the following methods:

- The MC method with the zero correlation SABR model as a control variate **(MC)**.
- The Hagan et al. formula **(Hagan)**.
- The Antonov et al. formula: Map to the zero correlation SABR model **(ZC Map)** .

The set of parameter values can be found in Table 3.2. We can observe from Figure 3.2 that all three BS implied volatility are almost the same for small maturity times (i.e., $\tau = 1$), but accuracy of the Hagan et al. formula worsens as time to maturity increases (i.e., $\tau = 10$) and the Antonov et al. formula remains accurate for long times to maturity.

Variable Name	Description	Value
$S = F$	spot price	$1, 10$
τ	time to maturity (in years)	$1, 10$
β	skew parameter	-0.4
r	constant risk-free interest rate (%)	0
σ	spot volatility (%)	30
α	volatility of volatility (%)	30
ρ	correlation parameter (%)	-20
h	Step size	0.01
M	Sample size	$100,000$

Table 3.2: Set of parameters used for the numerical experiment.

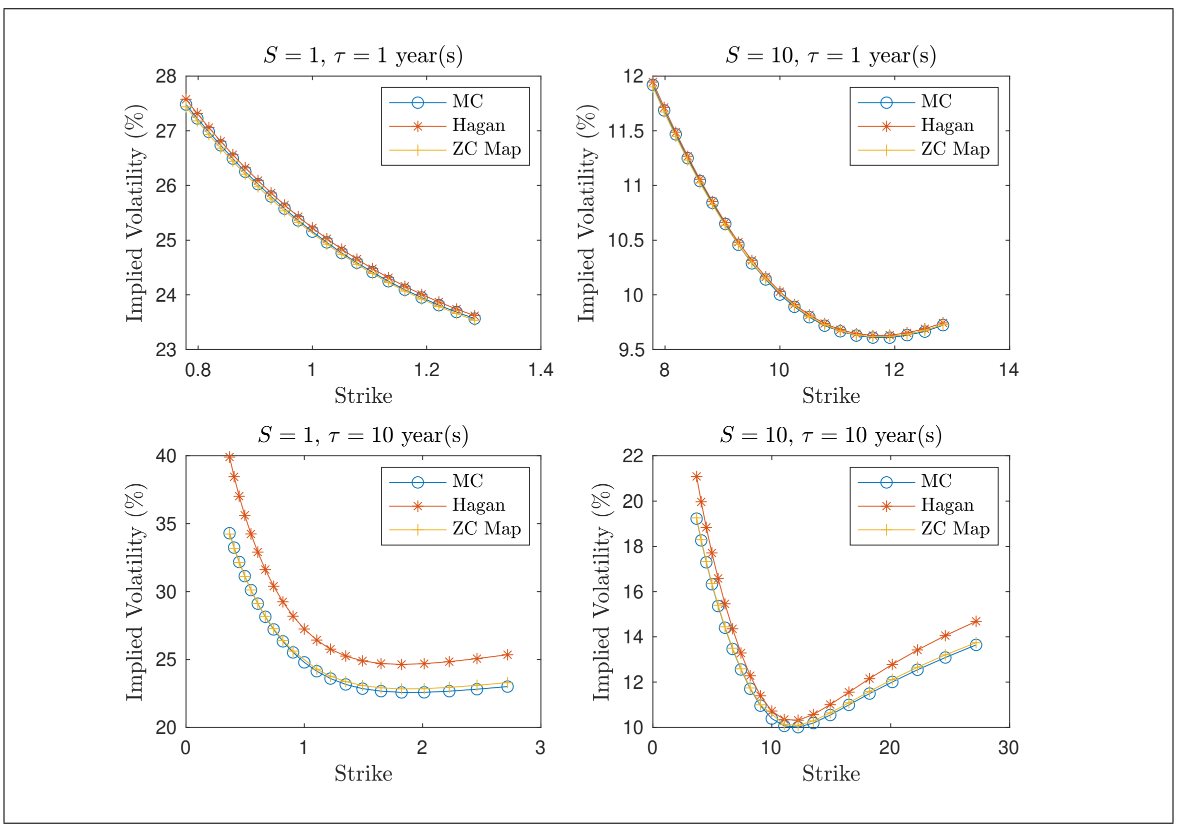

Figure 3.2: Plots of implied volatility under the classical SABR model.

Part II

Parameter/Static Randomization

Chapter 4

Risk-Neutral Pricing in the Single-Asset Economy

4.1 Motivation: Randomizing the Asset Price Volatility

Assume we are under a general diffusion model in the single-asset economy where the asset price (diffusion) process $\{S_t\}_{t\geqslant 0}$ obeys the SDE:

$$\frac{dS_t}{S_t} = r dt + \sigma(S_t) d\widetilde{W}_t; \quad S_0 > 0, \tag{4.1}$$

where r is the constant risk-free interest rate, $\sigma(S_t)$ is the time-independent local volatility function, and $\{\widetilde{W}_t\}_{t\geqslant 0}$ is a standard $\widetilde{\mathbb{P}}$-BM. We will write the local volatility function $\sigma(S)$ in the following way:

$$\sigma^2(S) = v f(S) \tag{4.2}$$

where v is the constant variance (i.e., $v = \sigma^2$ with σ as volatility parameter) and f is a non-negative function in $C^2(0, \infty)$. We randomize the parameter v as a random variable equipped with some known PDF. We will denote such a random variable by $\mathcal{V}$ to distinguish it from the parameter v. Then we can formulate the pricing function for a European-style option with payoff function $\Lambda(S)$ by:

$$V_{\mathcal{V}}(\tau, S) = \mathrm{e}^{-r\tau} \int_0^\infty \widetilde{\mathbb{E}}_{t,S}[\Lambda(S_T)] f_{\mathcal{V}}(v) dv, \quad \tau = T - t. \tag{4.3}$$

Note that $V_{\mathcal{V}}$ denotes the pricing function for a given choice of r.v. $\mathcal{V}$. Our methodology for computing option prices using (4.3) is closely related to the Bayesian framework in the GBM model studied by Darsinos and Satchell [12]. They considered randomizing the volatility where the variance follows the inverse gamma distribution. They were successful in deriving analytically closed-form expressions for the joint PDF of the asset price and the volatility, as well as the marginal PDF of the asset price. However, they were unable to determine the call pricing formulas analytically, and the option prices could only be obtained numerically.

We will specify the unconditional distribution of $\mathcal{V}$ in two separate ways: as a gamma and as an inverse gamma random variable in the GBM framework. We will refer to Prudnikov's book [17] which provides many integration identities that are helpful in our analysis.

4.2 Motivation: Extending to the Time-inhomogeneous Case

Assume we are under a general diffusion model in the single-asset economy where the asset price (diffusion) process $\{S_t\}_{t\geqslant 0}$ obeys the SDE:

$$\frac{dS_t}{S_t} = rdt + \sigma(t, S_t) d\widetilde{W}_t; \quad S_0 > 0, \tag{4.4}$$

where r is the constant risk-free interest rate, $\sigma(t, S)$ is the time-dependent local volatility function, and $\{\widetilde{W}_t\}_{t\geqslant 0}$ is a standard $\widetilde{\mathbb{P}}$-BM. Let us suppose that $\sigma(t, S)$ is separable, i.e.,

$$\sigma^2(t, S) = v(t) f(S) \tag{4.5}$$

where $v(t)$ is the deterministic time-dependent variance function and f is a non-negative function in $C^2(0, \infty)$. We consider cases where the discounted process $\{F_t\}_{t\geqslant 0} = \{\mathrm{e}^{-rt} S_t\}_{t\geqslant 0}$

is a $\widetilde{\mathbb{P}}$-martingale. By Itô's formula,

$$\frac{dF_t}{F_t} = \sqrt{v(t) f(\mathrm{e}^{rt} F_t)} d\widetilde{W}_t. \tag{4.6}$$

We will further assume that f is separable in the following sense,

$$f(\mathrm{e}^{rt} F) = g(t) h(F). \tag{4.7}$$

This assumption is met for a family of local volatility functions taking the form of a power function:

$$h(F) = AF^B, \tag{4.8}$$

where $A, B, \in \mathbb{R}$.[1] For example, in the GBM model with time-dependent variance function $v(t)$, we have the trivial case: $f(S) = g(t) = h(F) = 1$. Another example is the CEV model with time-dependent variance function $v(t)$ where

$$f(S) = S^{2\beta}, \quad g(t) = \mathrm{e}^{2\beta rt}, \quad h(F) = F^{2\beta}. \tag{4.9}$$

We can construct a deterministic time change by defining:

$$\Upsilon(s,t) \equiv \int_s^t g(u-s) v(u) du, \quad s < t. \tag{4.10}$$

We can notice that if $g(t) \equiv 1$ (which is true for the GBM model and the driftless CEV model), then (4.10) is just the cumulative variance. The construction above allows us to construct a time-changed forward price process $\{F_{\Upsilon(t)}\}_{t \geqslant 0}$ which obeys a SDE with time-independent local volatility function:

$$\frac{dF_{\Upsilon(t)}}{F_{\Upsilon(t)}} = \sqrt{f(F_{\Upsilon(t)})} d\widetilde{W}_{\Upsilon(t)}, \quad d\widetilde{W}_{\Upsilon(t)} = \sqrt{g(t) v(t)} d\widetilde{W}_t. \tag{4.11}$$

In particular, for the GBM model with a constant variance v, recall that the (risk-neutral) transition PDF for $\{S_t\}_{t \geqslant 0}$ is:

$$\widetilde{p}(t,T;S,y) = \frac{1}{y\sqrt{2\pi v \tau}} \exp\left(-\frac{[\ln \frac{y}{S} - (r - \frac{1}{2}v)\tau]^2}{2v\tau} \right); \quad S, y > 0, \tau > 0 \tag{4.12}$$

[1] See Section 6.1 in Campolieti and Makarov [9]

where S is the spot price at time t, T is the maturity at calendar time, and $\tau = T - t$ is the time to maturity. Since the time-changed GBM process $\{F_{\Upsilon(t)}\}_{t\geqslant 0}$ is Markovian, we can obtain the transition PDF of the GBM process with time-dependent volatility by mapping $v \mapsto 1$ and $\tau \mapsto \Upsilon(t,T)$ (or simply, $v \mapsto \frac{\Upsilon(t,T)}{\tau}$):

$$\widetilde{p}(t,T;S,y) = \frac{1}{y\sqrt{2\pi\Upsilon(t,T)}} \exp\left(-\frac{[\ln\frac{y}{S} - r\tau + \frac{1}{2}\Upsilon(t,T)]^2}{2\Upsilon(t,T)}\right); \qquad S,y>0, \tau>0, \quad (4.13)$$

and we can obtain the price of a path-independent European-style option under the GBM model with time-dependent variance by a mapping $v \mapsto \frac{\Upsilon(t,T)}{\tau}$.

Now, we consider extending the notion from the deterministic time-dependent variance to the stochastic variance process $\{v_t\}_{t\geqslant 0}$. We define a stochastic time change process:

$$\Upsilon_{t,T} = \int_t^T g(u-t)v_u du \quad (4.14)$$

We can formulate the pricing function for a European-style option for the zero correlation case with payoff function $\Lambda(S)$ by:

$$V_{\mathcal{V}}(t,T,S) = \mathrm{e}^{-r\tau}\int_0^\infty \widetilde{\mathbb{E}}_{t,S}[\Lambda(S_T)]\mathbb{P}_{t,v}\left(\Upsilon_{t,T}\in d\gamma\right), \quad \tau = T-t. \quad (4.15)$$

For example, we saw in Section 3.2 that the zero correlation (drifted) SABR option prices are computed by randomizing volatility in the (drifted) CEV model prices where the stochastic time-change given $\sigma_t = \sigma$:

$$\Upsilon_\tau(\sigma) \equiv \int_0^\tau \mathrm{e}^{\beta r u}\sigma^2_{t+u}du, \quad (4.16)$$

follows an integrated squared GBM process (recall that σ_t is a driftless GBM process). In this chapter, we take a different approach by assuming that $\Upsilon_{t,T}$ is a random variable. In particular, for the randomized GBM model, we take the cumulative variance as a parameter to be randomized. Thus, the idea of randomizing the parameter v is equivalent to randomizing time-averaged variance for the GBM model with time-dependent variance in some sense. However, this notion cannot be applied to pricing path-dependent options.

4.3 Transition Probability Density Functions

Assume the underlying asset price (diffusion) process $\{S_t\}_{t\geqslant 0}$ follows a GBM with SDE:

$$\frac{dS_t}{S_t} = rdt + \sqrt{v}d\widetilde{W}_t; \quad S_0, v > 0, r \geqslant 0. \tag{4.17}$$

Let $X_t = \ln \frac{S_t}{S_0} - rt$. Then, $\{X_t\}_{t\geqslant 0}$ is a drifted Brownian motion:

$$X_t = -\frac{1}{2}vt + \sqrt{v}\widetilde{W}_t; \quad X_0 = 0. \tag{4.18}$$

The transition PDF of this process started at 0 is[2]

$$\widetilde{p}(\tau; x) = \frac{1}{\sqrt{2\pi v\tau}} \exp\left(-\frac{[x + \frac{1}{2}v\tau]^2}{2v\tau}\right); \quad x \in \mathbb{R}, \tau > 0 \tag{4.19}$$

Let us consider a static randomization of the parameter v. We assume $\mathcal{V}$ is a random variable equipped with a Borel measurable PDF $f_\mathcal{V}$. Then we can easily show that the joint PDF $\widetilde{p}f_\mathcal{V}$ is (Lebesgue) integrable (i.e., $\widetilde{p}f_\mathcal{V} \in L^1(\mathbb{R}^2, \mathcal{B}(\mathbb{R}^2), \mu)$, where μ is the Lebesgue measure):

$$\begin{aligned} \int_0^\infty \int_0^\infty \widetilde{p}(\tau; S, y) f_\mathcal{V}(v) dv dy &= \int_0^\infty \left(\int_0^\infty \widetilde{p}(\tau; S, y) dy\right) f_\mathcal{V}(v) dv \\ &= \int_0^\infty f_\mathcal{V}(v) dv = 1. \end{aligned} \tag{4.20}$$

By applying the Fubini's theorem, the (marginal) transition PDF $\widetilde{p}_\mathcal{V}$ for the asset price process with a randomized volatility **(the randomized GBM process)**, denoted by $\{S_t^\mathcal{V}\}_{t\geqslant 0}$,[3] is well-defined for fixed $\tau, S > 0$:[4]

$$\widetilde{p}_\mathcal{V}(\tau; S, y) := \int_0^\infty f_\mathcal{V}(v)\widetilde{p}(\tau; S, y) dv < \infty; \quad y > 0 \text{ almost everywhere.}^5 \tag{4.21}$$

Since $\widetilde{p}$ is bounded, i.e, for every $y > 0$, there exists 2 positive constants $C(y), q(y) > 0$ and a non-negative constant $p(y) \geqslant 0$ such that

$$\widetilde{p}(\tau; S, y) = \frac{C(y)}{\sqrt{v}} \mathrm{e}^{-p(y)v - \frac{q(y)}{v}} < \infty. \tag{4.22}$$

[2]A drifted Brownian motion is both time- and space-homogeneous. Thus, the transition PDF depends on the time difference τ and the spatial distance $x - 0$.

[3]We use $\{S_t\}_{t\geqslant 0}$ to denote the asset price (diffusion) process with constant volatility and $\{S_t^\mathcal{V}\}_{t\geqslant 0}$ to denote the asset price (non-diffusion) process under a probability distribution.

[4]Note that $\widetilde{\mathbb{P}}_{t,S}\left(S_T^\mathcal{V} \in dy\right) = \widetilde{p}_\mathcal{V}(\tau; S, y)dy, \quad \tau = T - t$.

[5]$\mu(\{y \in \mathbb{R}^+ : \widetilde{p}_\mathcal{V}(\tau; S, y) \text{ is undefined}\}) = 0$.

Note that $p(y) = 0$ occurs with Lebesgue measure zero, so we can alternatively say that for $y > 0$ almost everywhere, there exists 3 positive constants $C(y), p(y), q(y) > 0$ such that

$$\widetilde{p}(\tau; S, y) = \frac{C(y)}{\sqrt{v}} \mathrm{e}^{-p(y)v - \frac{q(y)}{v}} < \infty. \tag{4.23}$$

By employing the boundedness property in (4.23), we can write an equivalent statement of the transition PDF $\widetilde{p}_{\mathcal{V}}$ in (4.21):

$$\int_0^\infty f_{\mathcal{V}}(v) \frac{1}{\sqrt{v}} \mathrm{e}^{-pv - \frac{q}{v}} dv < \infty \tag{4.24}$$

for all $p, q > 0$.[6] In particular, the gamma and the inverse gamma PDFs give analytical expressions for (4.24), which is why we consider the gamma and the inverse gamma randomization.

In this section, we derive the transition PDFs of the asset price process with static randomization of the parameter under the gamma and the inverse gamma randomization. Firstly, we look at the transition PDF for the randomized asset price process under the gamma randomization **(the randomized G process)**, denoted by $\{S_t^{G(\theta,\lambda)}\}_{t \geqslant 0}$, where $\mathcal{V}$ follows the gamma distribution with shape parameter θ and scale parameter λ (i.e., $\mathcal{V} \sim G(\theta, \lambda)$).[7] The PDF of $\mathcal{V}$ is

$$f_{G(\theta,\lambda)}(v) = \frac{1}{\lambda^\theta \Gamma(\theta)} v^{\theta - 1} \mathrm{e}^{-\frac{v}{\lambda}}; \qquad \theta, \lambda > 0 \tag{4.25}$$

where $\Gamma(\theta) = \int_0^\infty t^{\theta-1} \mathrm{e}^{-t} dt$ is the gamma function. The transition PDF for the drifted BM $\{X_t\}_{t \geqslant 0}$ under the gamma randomization, denoted by $\{X_t^{G(\theta,\lambda)}\}_{t \geqslant 0}$, started at 0 is:

$$\begin{aligned} \widetilde{p}_{G(\theta,\lambda)}(\tau; x) &= \int_0^\infty f_{G(\theta,\lambda)}(v) \widetilde{p}(\tau; x) dv \\ &= \int_0^\infty f_{G(\theta,\lambda)}(v) \left(\frac{A}{\sqrt{v}} \right) \exp\left(-\frac{C}{v} - D - Ev \right) dv, \end{aligned} \tag{4.26}$$

[6] Similarly, the transition PDF for $\{X_t^{\mathcal{V}}\}_{t \geqslant 0}$ is well-defined almost everywhere if (4.24) holds for all $p, q > 0$.

[7] In general, θ, λ are time-dependent (e.g., $\theta = \theta(t, T)$).

where

$$A = \frac{1}{\sqrt{2\pi\tau}}, \qquad C = \frac{x^2}{2\tau}, \qquad D = \frac{x}{2}, \qquad E = \frac{\tau}{8}. \tag{4.27}$$

We state a useful integral formula:[8]

$$\int_0^\infty v^{r-1} \mathrm{e}^{-pv-\frac{q}{v}} dv = 2\left(\frac{q}{p}\right)^{\frac{r}{2}} \mathsf{K}_r\left(2\sqrt{pq}\right); \qquad r \in \mathbb{R}, \quad p, q > 0, \tag{4.28}$$

where $\mathsf{K}_\nu(\cdot)$ is the modified Bessel function of the second kind of order ν. Using this within (4.26) gives[9]

$$\begin{aligned} \widetilde{p}_{G(\theta,\lambda)}(\tau; x) =& \frac{2A}{\lambda^\theta \Gamma(\theta)} \left(\frac{C}{E+\frac{1}{\lambda}}\right)^{\frac{1}{2}(\theta-\frac{1}{2})} \mathsf{K}_{\theta-\frac{1}{2}}\left(2\sqrt{C\left(E+\frac{1}{\lambda}\right)}\right) \\ =& \frac{\mathrm{e}^{-\frac{x}{2}}}{\sqrt{\pi}\Gamma(\theta)} \left(\frac{2}{\lambda\tau}\right)^\theta \left(\frac{\lambda\tau x^2}{8+\lambda\tau}\right)^{\frac{\theta}{2}-\frac{1}{4}} \mathsf{K}_{\theta-\frac{1}{2}}\left(\sqrt{\frac{(8+\lambda\tau)\,x^2}{4\lambda\tau}}\right). \end{aligned} \tag{4.29}$$

By a change of variable: $x(y) = \ln\frac{y}{S} - r\tau$, we have the transition PDF for the randomized G process $\{S_t^{G(\theta,\lambda)}\}_{t\geqslant 0}$:

$$\begin{aligned} \widetilde{p}_{G(\theta,\lambda)}(\tau; S, y) =& x'(y) \cdot \widetilde{p}_{G(\theta,\lambda)}(\tau; x(y)) \\ =& \frac{\mathrm{e}^{-\frac{x(y)}{2}}}{y\sqrt{\pi}\Gamma(\theta)} \left(\frac{2}{\lambda\tau}\right)^\theta \left(\frac{\lambda\tau x(y)^2}{8+\lambda\tau}\right)^{\frac{\theta}{2}-\frac{1}{4}} \mathsf{K}_{\theta-\frac{1}{2}}\left(\sqrt{\frac{x(y)^2\,(8+\lambda\tau)}{4\lambda\tau}}\right). \end{aligned} \tag{4.30}$$

Note that we have the following expressions:[10]

$$\begin{cases} \mathsf{K}_{\frac{1}{2}}(z) = \sqrt{\frac{\pi}{2z}}\mathrm{e}^{-z}, \\ \mathsf{K}_{\frac{3}{2}}(z) = \sqrt{\frac{\pi}{2z}}\mathrm{e}^{-z}\left(1+\frac{1}{z}\right), \\ \mathsf{K}_{\frac{5}{2}}(z) = \sqrt{\frac{\pi}{2z}}\mathrm{e}^{-z}\left(1+\frac{3}{z}+\frac{3}{z^2}\right), \end{cases} \tag{4.31}$$

and higher order terms can also be expressed as elementary functions using the recurrence relation for $n = 0, \pm 1, \pm 2, \ldots$:[11]

$$K_{n+\frac{3}{2}}(z) = \left(\frac{2n+1}{z}\right) K_{n+\frac{1}{2}}(z) + K_{n-\frac{1}{2}}(z). \tag{4.32}$$

[8] See 2.3.16.1 in Prudnikov et al, [17]

[9] The transition PDF with $\theta \leqslant \frac{1}{2}$ is undefined at $x = 0$.

[10] E.g. See 10.2.17 in Abramowitz and Stegun [1].

[11] E.g. See 10.2.18 in Abramowitz and Stegun [1].

This implies that for $\theta = n \in \mathbb{N}$, the transition PDF can be represented by elementary functions. In particular, when $\theta = 1, 2$, the transition PDF in (4.30) simplify to the respective expressions (where $x = \ln \frac{y}{S} - r\tau$):[12]

$$\begin{aligned}\widetilde{p}_{G(1,\lambda)}(\tau; S, y) =& \frac{2}{y\sqrt{\lambda\tau}\sqrt{8+\lambda\tau}} \exp\left(-\frac{|x|}{2}\frac{\sqrt{8+\lambda\tau}}{\sqrt{\lambda\tau}} - \frac{x}{2}\right), \\ \widetilde{p}_{G(2,\lambda)}(\tau; S, y) =& \frac{4}{y\lambda\tau(8+\lambda\tau)} \exp\left(-\frac{|x|}{2}\frac{\sqrt{8+\lambda\tau}}{\sqrt{\lambda\tau}} - \frac{x}{2}\right)\left(1 + \frac{2\sqrt{\lambda\tau}}{|x|\sqrt{8+\lambda\tau}}\right),\end{aligned} \tag{4.33}$$

Another interesting fact is if $\theta = \lambda\tau = 1$, then we see that the PDF is distributed uniformly for $y \leqslant S\mathrm{e}^{r\tau}$:

$$\widetilde{p}_{G(1,\lambda)}(\tau; S, y) = \frac{2}{\sqrt{3}S}\mathrm{e}^{-r\tau}; \quad y \leqslant S\mathrm{e}^{r\tau}. \tag{4.34}$$

We plotted the PDFs in (4.33) in Figure 4.1. Note that the asymptotic behavior of $\mathsf{K}_\nu(x)$ as $x \to \infty$ is:

$$\mathsf{K}_\nu(x) \sim \frac{\sqrt{\pi}\mathrm{e}^{-x}}{\sqrt{2x}}. \tag{4.35}$$

As a result, the asymptotic behaviours at the endpoints are:

$$\begin{aligned}\widetilde{p}_{G(\theta,\lambda)}(\tau; S, y) &\sim y^{-\frac{3}{2}+\sqrt{\frac{1}{4}+\frac{2}{\lambda\tau}}}\left(\ln\frac{1}{y}\right)^{\theta-1} \qquad \text{as} \quad y \to 0, \\ \widetilde{p}_{G(\theta,\lambda)}(\tau; S, y) &\sim y^{-\frac{3}{2}-\sqrt{\frac{1}{4}+\frac{2}{\lambda\tau}}}(\ln y)^{\theta-1} \quad \text{as} \quad y \to \infty.\end{aligned} \tag{4.36}$$

Based on the asymptotic behaviours of the transition PDF, we can say that the α-moment ($\alpha > 0$) of the randomized G process:

$$\widetilde{\mathbb{E}}_{t,S}\left[\left(S_T^{G(\theta,\lambda)}\right)^\alpha\right] \equiv \widetilde{\mathbb{E}}\left[\left(S_T^{G(\theta,\lambda)}\right)^\alpha | S_t^{G(\theta,\lambda)} = S\right] = \int_0^\infty y^\alpha \widetilde{p}_{G(\theta,\lambda)}(\tau; S, y)dy \tag{4.37}$$

is finite iff $\alpha < \frac{1}{2} + \sqrt{\frac{1}{4} + \frac{2}{\lambda\tau}}$. This implies the first moment exists, but the second moment exists iff $\lambda\tau < 1$.

Let us now consider the transition PDF for the asset price process under the inverse gamma randomization **(the randomized IG process)**, denoted by $\{S_t^{IG(\theta,\lambda)}\}_{t\geqslant 0}$. Assume that $\mathcal{V}$ now follows the inverse gamma distribution with shape parameter θ and scale

[12]We denote $x = x(y, S, \tau) = \ln \frac{y}{S} - r\tau$ to avoid clutter.

parameter λ (i.e., $\mathcal{V} \sim IG(\theta, \lambda)$). The PDF of $\mathcal{V}$ is

$$f_{IG(\theta,\lambda)}(v) = \frac{\lambda^\theta}{\Gamma(\theta)} \left(\frac{1}{v}\right)^{\theta+1} \mathrm{e}^{-\frac{\lambda}{v}}; \theta, \lambda > 0. \tag{4.38}$$

By using the integral identity in (4.28) we obtain the transition PDF for the drifted BM $\{X_t\}_{t \geqslant 0}$ under the inverse gamma randomization, denoted by $\{X_t^{IG(\theta,\lambda)}\}_{t \geqslant 0}$:

$$\widetilde{p}_{IG(\theta,\lambda)}(\tau; x) = \frac{\mathrm{e}^{-\frac{x}{2}}}{\sqrt{\pi}\Gamma(\theta)} \left(\frac{\lambda\tau}{2}\right)^\theta \left(x^2 + 2\lambda\tau\right)^{-\frac{\theta}{2}-\frac{1}{4}} \mathsf{K}_{\theta+\frac{1}{2}}\left(\sqrt{\frac{x^2+2\lambda\tau}{4}}\right). \tag{4.39}$$

By a change of variable: $x(y) = \ln \frac{y}{S} - r\tau$, we have the transition PDF for the randomized IG process $\{S_t^{IG(\theta,\lambda)}\}_{t \geqslant 0}$:

$$\widetilde{p}_{IG(\theta,\lambda)}(\tau; S, y) = \frac{\mathrm{e}^{-\frac{x(y)}{2}}}{y\sqrt{\pi}\Gamma(\theta)} \left(\frac{\lambda\tau}{2}\right)^\theta \left(x(y)^2 + 2\lambda\tau\right)^{-\frac{\theta}{2}-\frac{1}{4}} \mathsf{K}_{\theta+\frac{1}{2}}\left(\sqrt{\frac{x(y)^2+2\lambda\tau}{4}}\right). \tag{4.40}$$

In particular, if $\mathcal{V} \sim IG(1, \lambda)$ the transition PDF in (4.40) simplifies to

$$\widetilde{p}_{IG(1,\lambda)}(\tau; S, y) = \frac{\lambda\tau(\sqrt{x^2+2\lambda\tau}+2)}{2y(x^2+2\lambda\tau)^{\frac{3}{2}}} \exp\left(-\frac{|x|}{2}\frac{\sqrt{8+\lambda\tau}}{\sqrt{\lambda\tau}} - \frac{x}{2}\right). \tag{4.41}$$

The plots of the PDFs in (4.41) can be found in Figure 4.1. The asymptotic behaviours of the transition PDF is as follows:

$$\begin{aligned} \widetilde{p}_{IG(\theta,\lambda)}(\tau; S, y) &\sim y^{-1}\left(\ln\frac{1}{y}\right)^{-\theta-1} \quad \text{as} \quad y \to 0, \\ \widetilde{p}_{IG(\theta,\lambda)}(\tau; S, y) &\sim y^{-2}(\ln y)^{-\theta-1} \quad \text{as} \quad y \to \infty. \end{aligned} \tag{4.42}$$

From the asymptotic behaviours, we can observe that

$$\int_0^\infty y^\alpha \widetilde{p}_{IG(\theta,\lambda)}(\tau; S, y) dy \tag{4.43}$$

is finite iff $\alpha \leqslant 1$.

We can see from Figure 4.1 that the GBM has the thinnest tail among the three models for $\theta = 1, 2$. The plot in the top-left shows that for $\theta = 1$, the randomized G process has thinner tail than the randomized IG process for $\theta = 1$. The randomized G process appears to have the thickest tail among the three for $\theta = 2$, but eventually the randomized G process tails off faster than the randomized IG process as shown in the bottom-right corner plot. It is interesting to see that the PDF of the randomized G process is uniform for $y \leqslant S\mathrm{e}^{r\tau}$ at the bottom-left corner plot. We can also observe that the PDF of the randomized G process is not differentiable at $y = S\mathrm{e}^{r\tau}$ since $\mathsf{K}_\nu(z)$ is not differentiable at $z = 0$.

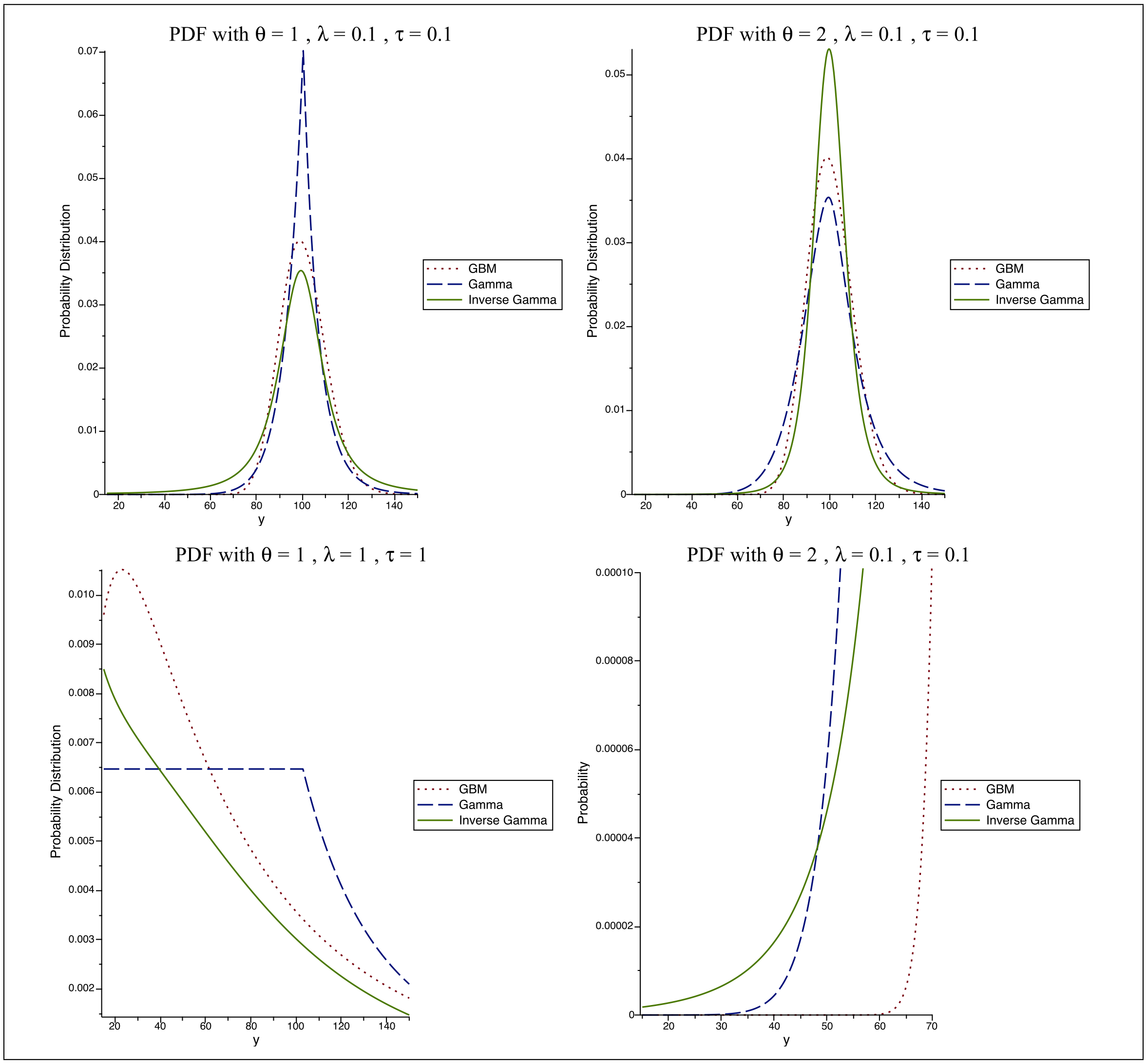

Figure 4.1: Plots of the transition PDFs for the process S_t, $S_t^{G(\theta,\lambda)}$ and $S_t^{IG(\theta,\lambda)}$, where $S = 100$, $r = 0.03$ and $v = 0.1$ is the variance parameter in the GBM model.

4.4 Risk-neutral Probabilities and Expectations

Let $\{V_t\}_{t\geqslant 0} \equiv \{f(t,S_t)\}_{t\geqslant 0}$ with a Borel function $f:\mathbb{R}_+\to\mathbb{R}_+$ be an $\mathcal{F}_t$-adapted[13] bounded stochastic process. The risk-neutral expectation of $V_T^{\mathcal{V}} = f(T,S_T^{\mathcal{V}})$ is

$$V_{\mathcal{V}}(t,S) = \mathrm{e}^{-r\tau}\widetilde{\mathbb{E}}_{t,S}\left[V_T^{\mathcal{V}}\right] = \mathrm{e}^{-r\tau}\widetilde{\mathbb{E}}\left[V_T^{\mathcal{V}}|S_t^{\mathcal{V}}=S\right] = \mathrm{e}^{-r\tau}\int_0^\infty f_{\mathcal{V}}(v)\widetilde{\mathbb{E}}_{t,S}\left[V_T\right]dv, \tag{4.44}$$

where T is the expiry time at a calendar time and $\tau = T-t$ is the time to maturity. We know that $\{\mathrm{e}^{-rt}S_t\}_{t\geqslant 0}$ is a $\widetilde{\mathbb{P}}$-martingale process, i.e., for the GBM process:

$$\widetilde{\mathbb{E}}_{t,S}\left[\mathrm{e}^{-rT}S_T\right] = \mathrm{e}^{-rt}S. \tag{4.45}$$

We can easily show that the randomized process $\{\mathrm{e}^{-rt}S_t^{\mathcal{V}}\}_{t\geqslant 0}$ is a $\widetilde{\mathbb{P}}$-martingale process:

$$\begin{aligned}
\widetilde{\mathbb{E}}_{t,S}\left[\mathrm{e}^{-rT}S_T^{\mathcal{V}}\right] =& \mathrm{e}^{-rT}\int_0^\infty y\widetilde{p}_{\mathcal{V}}(\tau;S,y)dy = \mathrm{e}^{-rT}\int_0^\infty y\left(\int_0^\infty f_{\mathcal{V}}(v)\widetilde{p}(\tau;S,y)dvdy\right)\\
=& \mathrm{e}^{-rt}\int_0^\infty f_{\mathcal{V}}(v)\left(\int_0^\infty \mathrm{e}^{-r\tau}y\widetilde{p}(\tau;S,y)dy\right)dv\\
=& \mathrm{e}^{-rt}S\int_0^\infty f_{\mathcal{V}}(v)dv = \mathrm{e}^{-rt}S.
\end{aligned} \tag{4.46}$$

By taking $V_t = \mathbb{1}_{\{S_t>K\}}$ with $K>0$, where $\mathbb{1}_A$ is the indicator function of some event A., we can obtain the following risk-neutral probability that the asset price is above the strike K at time T:

$$\begin{aligned}
\widetilde{\mathbb{P}}_{t,S}(S_T^{\mathcal{V}}>K) =& \widetilde{\mathbb{E}}_{t,S}\left[\mathbb{1}_{\{S_T^{\mathcal{V}}>K\}}\right] = \int_K^\infty \widetilde{p}_{\mathcal{V}}(\tau;S,y)dy\\
=& \int_{-m}^\infty \widetilde{p}_{\mathcal{V}}(\tau;x)dx = \widetilde{\mathbb{P}}_t(X_T^{\mathcal{V}}>-m).
\end{aligned} \tag{4.47}$$

where $m = \ln\frac{S}{K}+r\tau$. In particular for $\theta=1$, the risk-neutral probability can be obtained easily by making use of (4.33), (4.41) and (4.47):

$$\begin{aligned}
\widetilde{\mathbb{P}}_{t,S}\left(S_T^{G(1,\lambda)}>K\right) = \widetilde{\mathbb{P}}_t(X_T^{G(1,\lambda)}>-m) =& \mathbb{1}_{\{m\geqslant 0\}} - \frac{1}{2}\left(\mathrm{sgn}(m)+\frac{\sqrt{\lambda\tau}}{\sqrt{8+\lambda\tau}}\right)\\
&\times\exp\left(-\frac{|m|}{2}\frac{\sqrt{8+\lambda\tau}}{\sqrt{\lambda\tau}}+\frac{m}{2}\right),
\end{aligned} \tag{4.48}$$

[13] Note that V_t is $\mathcal{F}_t$-adapted w.r.t. its natural filtration $\mathcal{F}_t = \{\sigma(\widetilde{W}_s): 0\leqslant s\leqslant t\})$ where σ here is the σ-algebra generated by the $\widetilde{\mathbb{P}}$-BM.

where $\mathrm{sgn}(\cdot)$ is the sign function with $\mathrm{sgn}(0) \equiv 1$, and:

$$\widetilde{\mathbb{P}}_{t,S}\left(S_T^{IG(1,\lambda)} > K\right) = \frac{\lambda\tau \mathrm{e}^{-\frac{1}{2}(-m+\sqrt{m^2+2\lambda\tau})}}{\sqrt{m^2+2\lambda\tau}(-m+\sqrt{m^2+2\lambda\tau})}. \tag{4.49}$$

Recall that under the GBM model, the risk-neutral probability that the asset price is above the strike K at time T is:

$$\widetilde{\mathbb{P}}_{t,S}(S_T > K) = \int_K^\infty \widetilde{p}(\tau; S, y)dy = \mathcal{N}\left(\frac{m - \frac{1}{2}\upsilon\tau}{\sqrt{\upsilon\tau}}\right). \tag{4.50}$$

Sometimes, it may be more convenient to express (4.47) in the following way:

$$\widetilde{\mathbb{P}}_{t,S}(S_T^{\mathcal{V}} > K) = \int_0^\infty f_{\mathcal{V}}(v)\mathcal{N}\left(\frac{m - \frac{1}{2}\upsilon\tau}{\sqrt{\upsilon\tau}}\right) dv = \frac{1}{2}\int_0^\infty f_{\mathcal{V}}(v)\,\mathrm{erfc}\left(-\frac{m - \frac{1}{2}\upsilon\tau}{\sqrt{2\upsilon\tau}}\right) dv, \tag{4.51}$$

where $\mathrm{erfc}(\cdot)$ is the complementary error function. We state another integral formula:[14]

$$\begin{aligned}\int_0^\infty x^n \mathrm{e}^{-px}\mathrm{erfc}\left(c\sqrt{x} + \frac{b}{\sqrt{x}}\right) dx = \frac{2(n!)\sqrt{b}(c^2+p)^{\frac{1}{4}}}{\sqrt{\pi}p^{n+1}}\mathrm{e}^{-2bc}\sum_{k=0}^{n}\frac{p^k}{k!}\left(\frac{b^2}{c^2+p}\right)^{\frac{k}{2}} \\ \times\left[\mathsf{K}_{k-\frac{1}{2}}(2b\sqrt{c^2+p}) - \frac{c}{\sqrt{c^2+p}}\mathsf{K}_{k+\frac{1}{2}}(2b\sqrt{c^2+p})\right].\end{aligned} \tag{4.52}$$

In particular for $n = 0$, the integral formula in (4.52) reduces to the Laplace transform of the complementary error function:

$$\int_0^\infty \mathrm{e}^{-px}\mathrm{erfc}\left(c\sqrt{x} + \frac{b}{\sqrt{x}}\right) dx = \frac{1}{p}\left(1 - \frac{c}{\sqrt{c^2+p}}\right)\mathrm{e}^{-2b(c+\sqrt{c^2+p})}. \tag{4.53}$$

We can use (4.52) to obtain analytical formulas for the randomized processes in the case with integer-valued $\theta = n \in \mathbb{N}$. For the randomized G process, we have two cases. For $m < 0$ we have

$$\begin{aligned}\widetilde{\mathbb{P}}_{t,S}(S_T^{G(n,\lambda)} > K) =& \frac{1}{2}\int_0^\infty \frac{1}{\lambda^n(n-1)!}\upsilon^{n-1}\mathrm{e}^{-\frac{\upsilon}{\lambda}}\mathrm{erfc}\left(\frac{-m}{\sqrt{2\upsilon\tau}} + \frac{\sqrt{\upsilon\tau}}{2\sqrt{2}}\right) d\upsilon \\ =& \frac{1}{2\lambda^n(n-1)!}\int_0^\infty \upsilon^{n-1}\mathrm{e}^{-\frac{\upsilon}{\lambda}}\mathrm{erfc}\left(\frac{|m|}{\sqrt{2\upsilon\tau}} + \frac{\sqrt{\upsilon\tau}}{2\sqrt{2}}\right) d\upsilon \\ =& \frac{\sqrt{|m|}}{2\sqrt{\pi}}\left(\frac{8+\lambda\tau}{\lambda\tau}\right)^{\frac{1}{4}}\mathrm{e}^{\frac{m}{2}}\sum_{k=0}^{n-1}\frac{1}{k!}\left(\frac{2|m|}{\sqrt{\lambda\tau}\sqrt{8+\lambda\tau}}\right)^k \\ &\times\left[\mathsf{K}_{k-\frac{1}{2}}\left(\frac{|m|}{2}\frac{\sqrt{8+\lambda\tau}}{\sqrt{\lambda\tau}}\right) - \frac{\sqrt{\lambda\tau}}{\sqrt{8+\lambda\tau}}\mathsf{K}_{k+\frac{1}{2}}\left(\frac{|m|}{2}\frac{\sqrt{8+\lambda\tau}}{\sqrt{\lambda\tau}}\right)\right].\end{aligned} \tag{4.54}$$

[14] See 2.8.9.7 in Prudnikov et al [17]. The integral formula is valid for $b > 0, \Re(c^2 + p) > 0$.

For $m \geqslant 0$, we use the identity

$$\operatorname{erfc}(a) = 2 - \operatorname{erfc}(-a); \qquad a \in \mathbb{R}, \tag{4.55}$$

to obtain

$$\begin{aligned}
\widetilde{\mathbb{P}}_{t,S}(S_T^{G(n,\lambda)} > K) =& \frac{1}{2}\int_0^\infty \frac{1}{\lambda^n (n-1)!} v^{n-1} \mathrm{e}^{-\frac{v}{\lambda}} \operatorname{erfc}\left(\frac{-m}{\sqrt{2v\tau}} + \frac{\sqrt{v\tau}}{2\sqrt{2}}\right) dv \\
=& \int_0^\infty \frac{1}{\lambda^n (n-1)!} v^{n-1} \mathrm{e}^{-\frac{v}{\lambda}} dv \\
&- \frac{1}{2\lambda^n (n-1)!} \int_0^\infty v^{n-1} \mathrm{e}^{-\frac{v}{\lambda}} \operatorname{erfc}\left(\frac{|m|}{\sqrt{2v\tau}} - \frac{\sqrt{v\tau}}{2\sqrt{2}}\right) dv \\
=& 1 - \frac{\sqrt{|m|}}{2\sqrt{\pi}} \left(\frac{8+\lambda\tau}{\lambda\tau}\right)^{\frac{1}{4}} \mathrm{e}^{\frac{m}{2}} \sum_{k=0}^{n-1} \frac{1}{k!} \left(\frac{2|m|}{\sqrt{\lambda\tau}\sqrt{8+\lambda\tau}}\right)^k \\
&\times \left[\mathsf{K}_{k-\frac{1}{2}}\left(\frac{|m|}{2}\frac{\sqrt{8+\lambda\tau}}{\sqrt{\lambda\tau}}\right) + \frac{\sqrt{\lambda\tau}}{\sqrt{8+\lambda\tau}} \mathsf{K}_{k+\frac{1}{2}}\left(\frac{|m|}{2}\frac{\sqrt{8+\lambda\tau}}{\sqrt{\lambda\tau}}\right)\right].
\end{aligned} \tag{4.56}$$

By combining (4.54) and (4.56), we have for $m \in \mathbb{R}$:

$$\begin{aligned}
&\widetilde{\mathbb{P}}_{t,S}(S_T^{G(n,\lambda)} > K) \\
=& \mathbb{1}_{\{m \geqslant 0\}} - \frac{\operatorname{sgn}(m)\sqrt{|m|}}{2\sqrt{\pi}} \left(\frac{8+\lambda\tau}{\lambda\tau}\right)^{\frac{1}{4}} \mathrm{e}^{\frac{m}{2}} \sum_{k=0}^{n-1} \frac{1}{k!} \left(\frac{2|m|}{\sqrt{\lambda\tau}\sqrt{8+\lambda\tau}}\right)^k \\
&\times \left[\mathsf{K}_{k-\frac{1}{2}}\left(\frac{|m|}{2}\frac{\sqrt{8+\lambda\tau}}{\sqrt{\lambda\tau}}\right) + \frac{\operatorname{sgn}(m)\sqrt{\lambda\tau}}{\sqrt{8+\lambda\tau}} \mathsf{K}_{k+\frac{1}{2}}\left(\frac{|m|}{2}\frac{\sqrt{8+\lambda\tau}}{\sqrt{\lambda\tau}}\right)\right].
\end{aligned} \tag{4.57}$$

For the randomized IG process, by using the change of integration variable ($w = \frac{1}{v}$), we have

$$\begin{aligned}
&\widetilde{\mathbb{P}}_{t,S}(S_T^{IG(n,\lambda)} > K) \\
=& \frac{1}{2}\int_0^\infty \frac{\lambda^n}{(n-1)!} \left(\frac{1}{v}\right)^{n+1} \mathrm{e}^{-\frac{\lambda}{v}} \operatorname{erfc}\left(\frac{-m}{\sqrt{2v\tau}} + \frac{\sqrt{v\tau}}{2\sqrt{2}}\right) dv \\
=& \frac{1}{2}\frac{\lambda^n}{(n-1)!} \int_0^\infty w^{n-1} \mathrm{e}^{-\lambda w} \operatorname{erfc}\left(\frac{-m\sqrt{w}}{\sqrt{2\tau}} + \frac{\sqrt{\tau}}{2\sqrt{2w}}\right) dw \\
=& \frac{(m^2+2\lambda\tau)^{\frac{1}{4}}}{2\sqrt{\pi}} \mathrm{e}^{\frac{m}{2}} \sum_{k=0}^{n-1} \frac{1}{k!} \left(\frac{\lambda\tau}{2\sqrt{m^2+2\lambda\tau}}\right)^k \\
&\times \left[K_{k-\frac{1}{2}}\left(\frac{\sqrt{m^2+2\lambda\tau}}{2}\right) + \frac{m}{\sqrt{m^2+2\lambda\tau}} K_{k+\frac{1}{2}}\left(\frac{\sqrt{m^2+2\lambda\tau}}{2}\right)\right].
\end{aligned} \tag{4.58}$$

Asymptotic behaviours are:[15]

$$
\begin{aligned}
&\widetilde{\mathbb{P}}_{t,S}(S_T^{G(n,\lambda)} \leqslant K) \sim K^{\frac{1}{2}\left(\frac{\sqrt{8+\lambda\tau}}{\sqrt{\lambda\tau}}-1\right)} \left(\ln\frac{1}{K}\right)^{n-1} \quad \text{as } K\to 0,\\
&\widetilde{\mathbb{P}}_{t,S}(S_T^{G(n,\lambda)} > K) \sim K^{-\frac{1}{2}\left(\frac{\sqrt{8+\lambda\tau}}{\sqrt{\lambda\tau}}+1\right)} (\ln K)^{n-1} \quad \text{as } K\to \infty,\\
&\widetilde{\mathbb{P}}_{t,S}(S_T^{IG(n,\lambda)} \leqslant K) \sim \left(\ln\frac{1}{K}\right)^{-n} \quad \text{as } K\to 0,\\
&\widetilde{\mathbb{P}}_{t,S}(S_T^{IG(n,\lambda)} > K) \sim K^{-1} (\ln K)^{-n-1} \quad \text{as } K\to \infty.
\end{aligned}
\tag{4.59}
$$

Note that the asymptotic behavior of the complementary error function as $x \to \infty$ is:

$$
\operatorname{erfc}(x) \sim \frac{\mathrm{e}^{-x^2}}{\sqrt{\pi}x} \tag{4.60}
$$

For the GBM case (with constant variance parameter v), asymptotic behaviours are :

$$
\begin{aligned}
\widetilde{\mathbb{P}}_{t,S}(S_T > K) &\sim \frac{1}{\ln\frac{1}{K}} \exp\left(-\frac{\left(\ln\frac{1}{K}\right)^2}{2v\tau}\right) \quad \text{as } K\to 0,\\
\widetilde{\mathbb{P}}_{t,S}(S_T > K) &\sim \frac{1}{\ln K} \exp\left(-\frac{(\ln K)^2}{2v\tau}\right) \quad \text{as } K\to \infty,
\end{aligned}
\tag{4.61}
$$

We can see from the analytical expressions that the CDF of the GBM model has the thinnest tail , whereas the randomized IG process has the thickest tail among the three models for any given $\theta, \lambda > 0$. We can also observe from the visual plots in Figure 4.2 that the GBM has the thinnest tail among the three models for $\theta = 1, 2$. The randomized G process has thinner tails than the randomized IG process for $\theta = 1$, whereas the randomized G process appears to have the thickest tails among the three for $\theta = 2$ (the opposite is true for deep in (and out-of) -the-money options).

Now, we consider the risk-neutral conditional probability $\widehat{\mathbb{P}} \equiv \widetilde{\mathbb{P}}^{(S)}$ under an equivalent martingale measure with the original asset price process $\{S_t\}_{t\geqslant 0}$ as the numéraire, where

$$
\begin{aligned}
\widehat{\mathbb{P}}_{t,S}(S_T^{\mathcal{V}} > K) &= \int_0^\infty f_{\mathcal{V}}(v)\widehat{\mathbb{E}}_{t,S}\left[\mathbb{1}_{\{S_T>K\}}\right] dv = \int_0^\infty f_{\mathcal{V}}(v)\left(\frac{\widetilde{\mathbb{E}}_{t,S}\left[S_T\mathbb{1}_{\{S_T>K\}}\right]}{S\mathrm{e}^{r\tau}}\right) dv\\
&= \frac{1}{S\mathrm{e}^{r\tau}}\int_0^\infty f_{\mathcal{V}}(v)\left(\int_K^\infty y\widetilde{p}(\tau;S,y)dy\right) dv = \frac{1}{S\mathrm{e}^{r\tau}}\int_K^\infty y\widetilde{p}_{\mathcal{V}}(\tau;S,y)dy,
\end{aligned}
\tag{4.62}
$$

[15] Asymptotic behaviours w.r.t. S can be obtained by a change of variable $K \to \frac{1}{S}$.

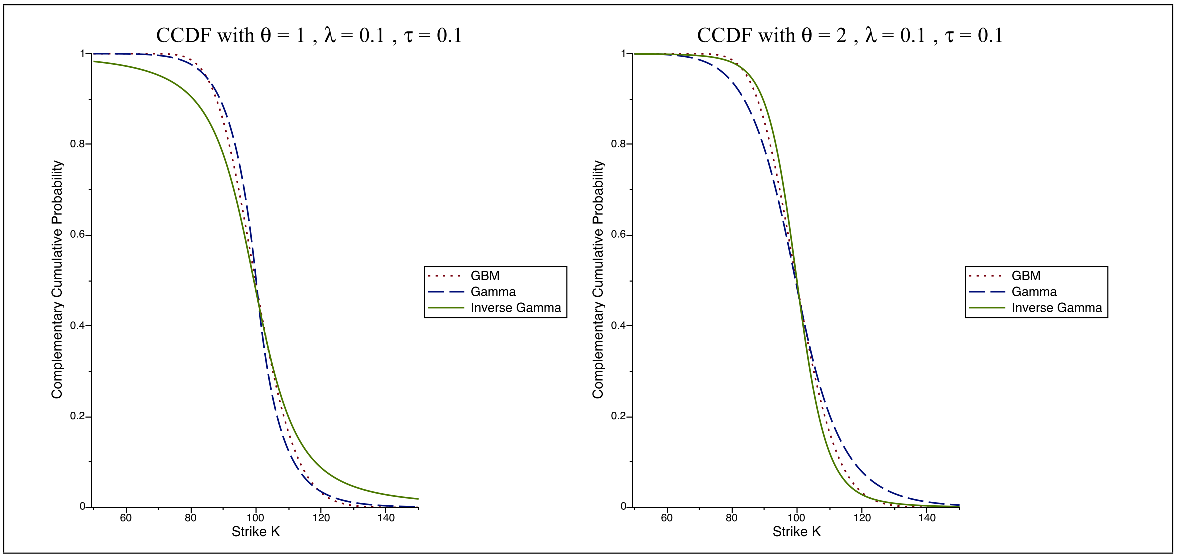

Figure 4.2: Plots of the transition complementary CDFs for the process S_t, $S_t^{G(\theta,\lambda)}$ and $S_t^{IG(\theta,\lambda)}$, where $S = 100$, $r = 0.03$ and $v = 0.1$ is the variane parameter in the GBM model.

or equivalently,

$$\widehat{\mathbb{P}}_{t,S}(S_T^{\mathcal{V}} > K) = \frac{\widetilde{\mathbb{E}}_{t,S}\left[S_T^{\mathcal{V}} \mathbb{1}_{\{S_T^{\mathcal{V}} > K\}}\right]}{S\mathrm{e}^{r\tau}}. \tag{4.63}$$

The above identity follows from the Radon-Nikodym derivative:

$$\widehat{\mathbb{E}}_{t,S}[V_T] = \frac{1}{S}\widehat{\mathbb{E}}_{t,S}\left[\frac{S_t}{S_T} S_T V_T\right] = \frac{1}{S}\widetilde{\mathbb{E}}_{t,S}^{(B)}\left[\frac{B_t}{B_T} S_T V_T\right] = \frac{B_t}{S}\widetilde{\mathbb{E}}_{t,S}^{(B)}\left[\frac{S_T V_T}{B_T}\right] \tag{4.64}$$

where $B_t = \mathrm{e}^{\int_0^t r_s ds}$ is the bank account value at time t. Assuming that $r_t = r$, we have $B_t = \mathrm{e}^{rt}$ and $\frac{B_t}{B_T} = \mathrm{e}^{-r\tau}$. The PDF defined in (4.19) has the following useful symmetry identity

$$\widetilde{p}(\tau; -x) = \mathrm{e}^{x}\widetilde{p}(\tau; x). \tag{4.65}$$

We can use (4.65) to obtain the following probability:

$$\begin{aligned}\widehat{\mathbb{P}}_{t,S}\left(S_T^{\mathcal{V}} > K\right) =& \frac{1}{S\mathrm{e}^{r\tau}}\int_K^{\infty} y\widetilde{p}_{\mathcal{V}}(\tau; S, y)dy = \frac{1}{S\mathrm{e}^{r\tau}}\int_{-m}^{\infty} S\mathrm{e}^{x+r\tau}\widetilde{p}_{\mathcal{V}}(\tau; x)dx \\ \overset{(4.65)}{=}& \int_{-m}^{\infty}\widetilde{p}_{\mathcal{V}}(\tau; -x)dx = \int_{-\infty}^{m}\widetilde{p}_{\mathcal{V}}(\tau; x)dx \\ =& \widetilde{\mathbb{P}}_t\left(X_T^{\mathcal{V}} \leqslant m\right),\end{aligned} \tag{4.66}$$

In particular for $\theta = 1$, by using (4.66) and (4.48) we obtain the following risk-neutral probability explicitly for the randomized G process:

$$\begin{aligned}&\widehat{\mathbb{P}}_{t,S}\left(S_T^{G(1,\lambda)} > K\right)\\ =&\mathbb{1}_{\{m\geqslant 0\}} - \frac{1}{2}\left(\operatorname{sgn}(m) - \frac{\sqrt{\lambda\tau}}{\sqrt{8+\lambda\tau}}\right)\exp\left(-\frac{|m|}{2}\frac{\sqrt{8+\lambda\tau}}{\sqrt{\lambda\tau}} - \frac{m}{2}\right).\end{aligned} \tag{4.67}$$

Similarly for the randomized IG process, we can obtain it by using (4.66) and (4.49):

$$\widehat{\mathbb{P}}_{t,S}(S_T^{IG(1,\lambda)} > K) = 1 - \frac{\lambda\tau \mathrm{e}^{-\frac{1}{2}(m+\sqrt{m^2+2\lambda\tau})}}{\sqrt{m^2+2\lambda\tau}(m+\sqrt{m^2+2\lambda\tau})}. \tag{4.68}$$

For the randomized G process $\{S_t^{G(n,\lambda)}\}_{t\geqslant 0}, n \in \mathbb{N}$, by using (4.66) and (4.57) we have

$$\begin{aligned}&\widehat{\mathbb{P}}_{t,S}(S_T^{G(n,\lambda)} > K)\\ =&\mathbb{1}_{\{m\geqslant 0\}} - \frac{\operatorname{sgn}(m)\sqrt{|m|}}{2\sqrt{\pi}}\left(\frac{8+\lambda\tau}{\lambda\tau}\right)^{\frac{1}{4}}\mathrm{e}^{-\frac{m}{2}}\sum_{k=0}^{n-1}\frac{1}{k!}\left(\frac{2|m|}{\sqrt{\lambda\tau}\sqrt{8+\lambda\tau}}\right)^k\\ &\times\left[\mathsf{K}_{k-\frac{1}{2}}\left(\frac{|m|}{2}\frac{\sqrt{8+\lambda\tau}}{\sqrt{\lambda\tau}}\right) - \frac{\operatorname{sgn}(m)\sqrt{\lambda\tau}}{\sqrt{8+\lambda\tau}}\mathsf{K}_{k+\frac{1}{2}}\left(\frac{|m|}{2}\frac{\sqrt{8+\lambda\tau}}{\sqrt{\lambda\tau}}\right)\right].\end{aligned} \tag{4.69}$$

For the randomized IG process $\{S_t^{IG(n,\lambda)}\}_{t\geqslant 0}, n \in \mathbb{N}$, by using (4.66) and (4.58) we have

$$\begin{aligned}&\widehat{\mathbb{P}}_{t,S}(S_T^{IG(n,\lambda)} > K)\\ =&1 - \frac{(m^2+2\lambda\tau)^{\frac{1}{4}}}{2\sqrt{\pi}}\mathrm{e}^{-\frac{m}{2}}\sum_{k=0}^{n-1}\frac{1}{k!}\left(\frac{\lambda\tau}{2\sqrt{m^2+2\lambda\tau}}\right)^k\\ &\times\left[\mathsf{K}_{k-\frac{1}{2}}\left(\frac{\sqrt{m^2+2\lambda\tau}}{2}\right) - \frac{m}{\sqrt{m^2+2\lambda\tau}}\mathsf{K}_{k+\frac{1}{2}}\left(\frac{\sqrt{m^2+2\lambda\tau}}{2}\right)\right].\end{aligned} \tag{4.70}$$

The main feature of this section is that the risk-neutral probability that the randomized asset price process is above strike K at time T can be written as elementary analytical functions for $\theta = n \in \mathbb{N}$. This will help us obtain analytical pricing formulas for European vanilla options. We will illustrate it in the next section.

4.5 Pricing European Options

The price of a European vanilla call option can be written in terms of $\widehat{\mathbb{P}}_{t,S}$ and $\widetilde{\mathbb{P}}_{t,S}$, i.e.,

$$\begin{aligned}\widehat{C}_{\mathcal{V}}(\tau, m) \equiv \frac{C_{\mathcal{V}}(\tau, S; K, r)}{S} =& \widehat{\mathbb{P}}_{t,S}(S_T^{\mathcal{V}} > K) - \frac{K\mathrm{e}^{-r\tau}}{S}\widetilde{\mathbb{P}}_{t,S}(S_T^{\mathcal{V}} > K) \\ =& \widetilde{\mathbb{P}}_t(X_T^{\mathcal{V}} \leqslant m) - \mathrm{e}^{-m}\widetilde{\mathbb{P}}_t(X_T^{\mathcal{V}} > -m).\end{aligned} \tag{4.71}$$

For the randomized G process with $\theta = 1$, by substituting (4.48) and (4.67) into (4.71), we have

$$\widehat{C}_{G(1,\lambda)}(\tau, m) = (1 - \mathrm{e}^{-m})^+ + \frac{\sqrt{\lambda\tau}}{\sqrt{8+\lambda\tau}} \exp\left(-\frac{|m|}{2}\frac{\sqrt{8+\lambda\tau}}{\sqrt{\lambda\tau}} - \frac{m}{2}\right). \tag{4.72}$$

For the randomized IG process with $\theta = 1$, by substituting (4.49) and (4.68) into (4.71), we have

$$\widehat{C}_{IG(1,\lambda)}(\tau, m) = 1 - \exp\left(-\frac{1}{2}\left(m + \sqrt{m^2 + 2\lambda\tau}\right)\right), \tag{4.73}$$

For the randomized G process with $\theta = n \in \mathbb{N}$, by substituting (4.57) and (4.69) into (4.71), we have

$$\begin{aligned}\widehat{C}_{G(n,\lambda)}(\tau, m) =& (1 - \mathrm{e}^{-m})^+ + \frac{\sqrt{|m|}}{\sqrt{\pi}}\left(\frac{\lambda\tau}{8+\lambda\tau}\right)^{\frac{1}{4}} \mathrm{e}^{-\frac{m}{2}} \\ & \sum_{k=0}^{n-1}\frac{1}{k!}\left(\frac{2|m|}{\sqrt{\lambda\tau}\sqrt{8+\lambda\tau}}\right)^k \mathsf{K}_{k+\frac{1}{2}}\left(\frac{|m|}{2}\frac{\sqrt{8+\lambda\tau}}{\sqrt{\lambda\tau}}\right).\end{aligned} \tag{4.74}$$

For the randomized IG process with $\theta = n \in \mathbb{N}$, by substituting (4.58) and (4.70) into (4.71), we have

$$\begin{aligned}\widehat{C}_{IG(n,\lambda)}(\tau, m) =& 1 - \frac{(m^2 + 2\lambda\tau)^{\frac{1}{4}}}{\sqrt{\pi}}\mathrm{e}^{-\frac{m}{2}} \\ & \sum_{k=0}^{n-1}\frac{1}{k!}\left(\frac{\lambda\tau}{2\sqrt{m^2+2\lambda\tau}}\right)^k \mathsf{K}_{k-\frac{1}{2}}\left(\frac{\sqrt{m^2+2\lambda\tau}}{2}\right).\end{aligned} \tag{4.75}$$

We can see from Figure 4.3 that when $\theta = 1$, for a given time to maturity, the option price under the inverse gamma randomization has the highest value, and the gap increases as the time to maturity increases. When $\theta = 2$, for a given time to maturity, the option price under the gamma randomization has the highest value. From Figure 4.4, we can see that the model prices differ from the other for near in- or out-the-money options, and the gap shrinks for deep in- or out-the-money options. For $\theta \notin \mathbb{N}$, we can derive the at-the-money forward (ATMF) option prices in closed-form in terms of the hypergeometric functions. In particular, for the randomized G process, we have

$$\widehat{C}_{G(\theta,\lambda)}(\tau,0) = 1 - \frac{\Gamma(\theta+\frac{1}{2})}{\sqrt{\pi}\Gamma(\theta+1)} \left(\frac{8}{\lambda\tau}\right)^{\theta} {}_2F_1\left(\theta, \theta+\frac{1}{2}; \theta+1, -\frac{8}{\lambda\tau}\right). \tag{4.76}$$

For the randomized IG process, we have

$$\begin{aligned}\widehat{C}_{IG(\theta,\lambda)}(\tau,0) =& \frac{\sqrt{\lambda\tau}}{2\sqrt{2\pi}\left(\theta-\frac{1}{2}\right)\Gamma(\theta+1)}\left[2\theta\Gamma\left(\theta+\frac{1}{2}\right) {}_1F_2\left(\frac{1}{2}; \frac{3}{2}, \frac{3}{2}-\theta; \frac{\lambda\tau}{8}\right)\right. \\ & \left. - \left(\frac{\lambda\tau}{8}\right)^{\theta-\frac{1}{2}} \Gamma\left(\frac{3}{2}-\theta\right) {}_1F_2\left(\theta; \theta+1, \theta+\frac{1}{2}; \frac{\lambda\tau}{8}\right)\right]\end{aligned} \tag{4.77}$$

We will derive (4.76) and (4.77) rigorously in Appendix B.

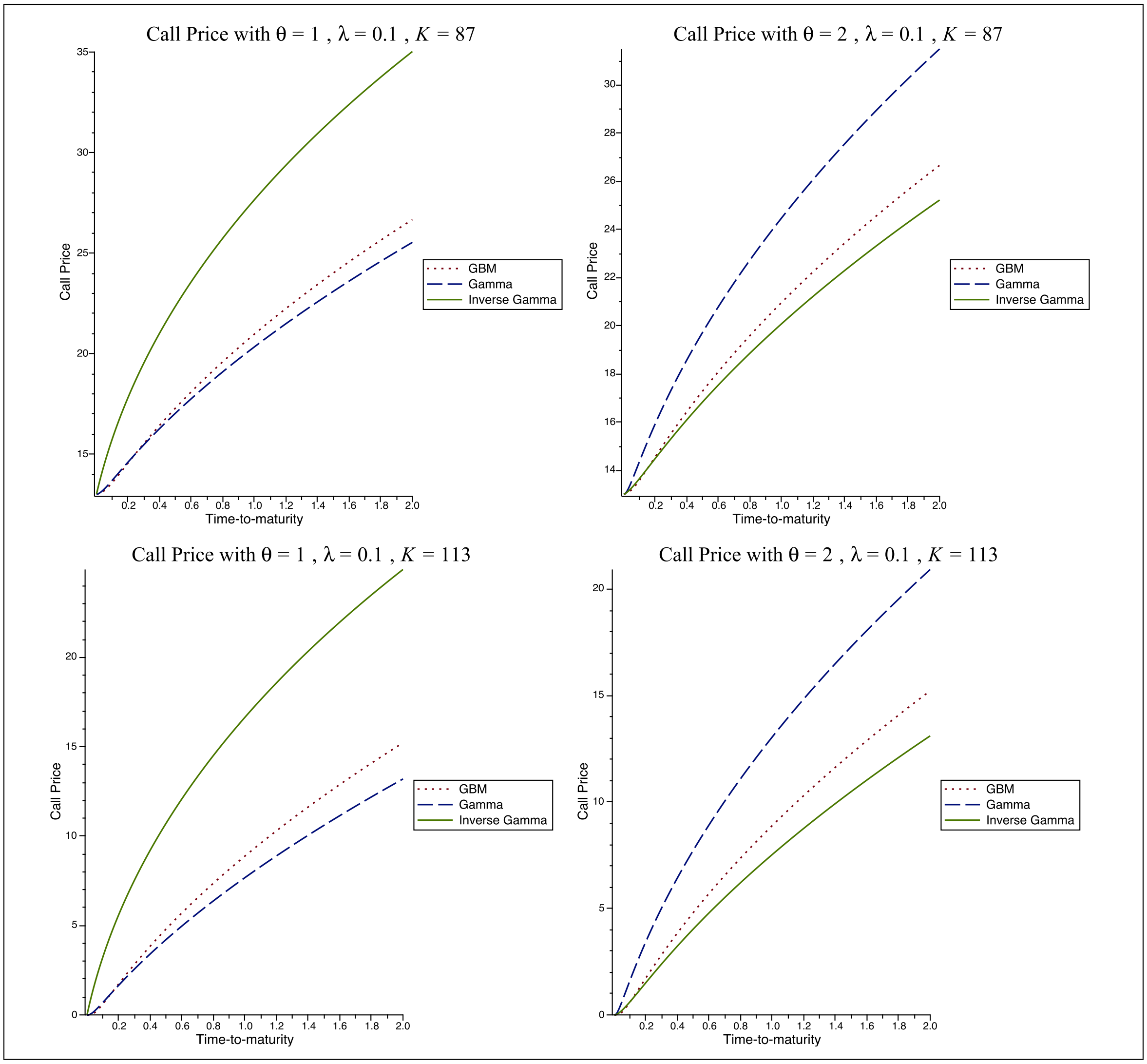

Figure 4.3: Plots of the in-the-money call option prices (top row) and out-of-the-money call option prices (bottom row), where $S = 100$, $r = 0.03$ and $v = 0.1$ is the variane parameter in the GBM model.

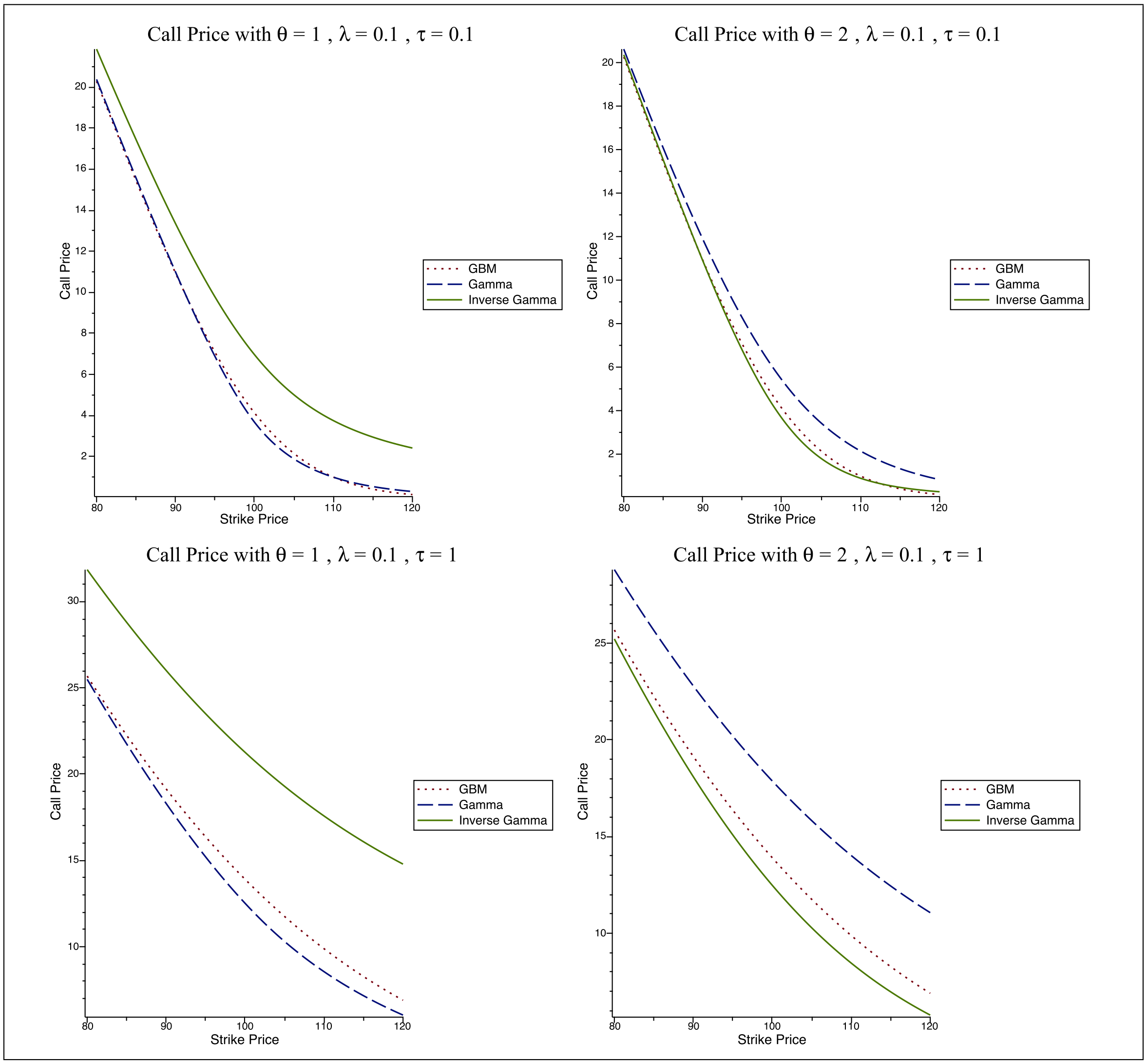

Figure 4.4: Plots of the call option prices for short time-to-maturity (top row) and for long time-to-maturity (bottom row), where $S = 100$, $r = 0.03$ and $v = 0.1$ is the variance parameter in the GBM model.

4.6 Greeks

In this section, we derive general formulas for the main Greeks of a European vanilla call option under the randomized GBM model.The Delta of a European vanilla call option is

$$\begin{aligned}
\Delta_{\mathcal{V}} = \frac{\partial C_{\mathcal{V}}}{\partial S} =& \frac{\partial}{\partial S}\left(S\widehat{\mathbb{P}}_{t,S}(S_T^{\mathcal{V}} > K)\right) - K\mathrm{e}^{-r\tau}\frac{\partial}{\partial S}\left(\widetilde{\mathbb{P}}_{t,S}(S_T^{\mathcal{V}} > K)\right) \\
=& \widehat{\mathbb{P}}_{t,S}(S_T^{\mathcal{V}} > K) + S\frac{\partial}{\partial S}\left(\widehat{\mathbb{P}}_{t,S}(S_T^{\mathcal{V}} > K)\right) - K\mathrm{e}^{-r\tau}\frac{\partial}{\partial S}\left(\widetilde{\mathbb{P}}_{t,S}(S_T^{\mathcal{V}} > K)\right) \\
=& \widehat{\mathbb{P}}_{t,S}(S_T^{\mathcal{V}} > K) + S\frac{\partial m}{\partial S}\cdot\frac{\partial}{\partial m}\left(\widehat{\mathbb{P}}_{t}(X_T^{\mathcal{V}} \leqslant m)\right) \\
& - K\mathrm{e}^{-r\tau}\frac{\partial(-m)}{\partial S}\cdot\frac{\partial}{\partial(-m)}\left(\widetilde{\mathbb{P}}_{t}(X_T^{\mathcal{V}} > -m)\right) \\
=& \widehat{\mathbb{P}}_{t,S}(S_T^{\mathcal{V}} > K) + \frac{\partial}{\partial m}\left(\widetilde{\mathbb{P}}_{t}(X_T^{\mathcal{V}} \leqslant m)\right) \\
& + \frac{K\mathrm{e}^{-r\tau}}{S}\frac{\partial}{\partial(-m)}\left(1 - \widetilde{\mathbb{P}}_{t}(X_T^{\mathcal{V}} \leqslant -m)\right) \\
=& \widehat{\mathbb{P}}_{t,S}(S_T^{\mathcal{V}} > K) + \widetilde{p}_{\mathcal{V}}(\tau; m) - \mathrm{e}^{-m}\widetilde{p}_{\mathcal{V}}(\tau; -m) \\
=& \widehat{\mathbb{P}}_{t,S}(S_T^{\mathcal{V}} > K) = \widetilde{\mathbb{P}}_{t}(X_T^{\mathcal{V}} \leqslant m) = \widetilde{\mathbb{P}}_{t,S}\left(S_T^{\mathcal{V}} \leqslant \frac{S^2\mathrm{e}^{2r\tau}}{K}\right).
\end{aligned} \tag{4.78}$$

The Gamma of a European vanilla call option is

$$\begin{aligned}
\Gamma_{\mathcal{V}} = \frac{\partial^2 C_{\mathcal{V}}}{\partial S^2} =& \frac{\partial}{\partial S}\left(\widehat{\mathbb{P}}_{t,S}(S_T^{\mathcal{V}} > K)\right) = \frac{\partial m}{\partial S}\cdot\frac{\partial}{\partial m}\left(\widetilde{\mathbb{P}}_{t}(X_T^{\mathcal{V}} \leqslant m)\right) \\
=& \frac{1}{S}\widetilde{p}_{\mathcal{V}}(\tau; m) = \frac{S}{K}\mathrm{e}^{2r\tau}\widetilde{p}_{\mathcal{V}}\left(\tau; S, \frac{S^2\mathrm{e}^{2r\tau}}{K}\right).
\end{aligned} \tag{4.79}$$

The Rho of a European vanilla call option is

$$\begin{aligned}
\rho_{\mathcal{V}} = \frac{\partial C_{\mathcal{V}}}{\partial r} =& S\frac{\partial}{\partial r}\left(\widehat{\mathbb{P}}_{t,S}(S_T^{\mathcal{V}} > K)\right) - K\frac{\partial}{\partial r}\left(\mathrm{e}^{-r\tau}\widetilde{\mathbb{P}}_{t,S}(S_T^{\mathcal{V}} > K)\right) \\
=& S\frac{\partial m}{\partial r}\cdot\frac{\partial}{\partial m}\left(\widetilde{\mathbb{P}}_{t,S}(X_T^{\mathcal{V}} \leqslant m)\right) \\
& - K\left[-\tau\mathrm{e}^{-r\tau}\widetilde{\mathbb{P}}_{t,S}(S_T^{\mathcal{V}} > K) + \mathrm{e}^{-r\tau}\frac{\partial}{\partial r}\left(\widetilde{\mathbb{P}}_{t,S}(S_T^{\mathcal{V}} > K)\right)\right] \\
=& S\frac{\partial m}{\partial r}\cdot\frac{\partial}{\partial m}\left(\widetilde{\mathbb{P}}_{t}(X_T^{\mathcal{V}} \leqslant m)\right) K\tau\mathrm{e}^{-r\tau}\widetilde{\mathbb{P}}_{t,S}(S_T^{\mathcal{V}} > K) \\
& - K\mathrm{e}^{-r\tau}\frac{\partial(-m)}{\partial r}\cdot\frac{\partial}{\partial(-m)}\left(1 - \widetilde{\mathbb{P}}_{t}(X_T^{\mathcal{V}} \leqslant -m)\right) \\
=& \tau S\widetilde{p}_{\mathcal{V}}(\tau; m) + K\tau\mathrm{e}^{-r\tau}\widetilde{\mathbb{P}}_{t,S}(S_T^{\mathcal{V}} > K) - K\tau\mathrm{e}^{-r\tau}\widetilde{p}_{\mathcal{V}}(\tau; -m) \\
=& K\tau\mathrm{e}^{-r\tau}\widetilde{\mathbb{P}}_{t,S}(S_T^{\mathcal{V}} > K).
\end{aligned} \tag{4.80}$$

Recall that the price of a European vanilla call option under the GBM model satisfies the BS partial differential equation (PDE) in the time to maturity τ:

$$\frac{\partial C_{BS}}{\partial \tau} = \frac{1}{2} v S^2 \frac{\partial^2 C_{BS}}{\partial S^2} + rS\frac{\partial C_{BS}}{\partial S} - rC_{BS}. \tag{4.81}$$

By multiplying $f(v)$ on both sides and then integrating w.r.t v from 0 to infinity, we have the formula for theta:

$$\begin{aligned}\Theta_{\mathcal{V}} = -\frac{\partial C_{\mathcal{V}}}{\partial \tau} &= -\frac{1}{2}S^2\frac{\partial^2}{\partial S^2}\left(\int_0^\infty vf(v)C_{BS}dv\right) - rS\frac{\partial C_{\mathcal{V}}}{\partial S} + rC_{\mathcal{V}}\\ &= -\frac{1}{2}S^2\frac{\partial^2}{\partial S^2}\left(\int_0^\infty vf(v)C_{BS}dv\right) - rS\widehat{\mathbb{P}}_{t,S}(S_T^{\mathcal{V}} > K)\\ &\quad + r\left[S\widehat{\mathbb{P}}_{t,S}(S_T^{\mathcal{V}} > K) - K\mathrm{e}^{-r\tau}\widetilde{\mathbb{P}}_{t,S}(S_T^{\mathcal{V}} > K)\right]\\ &= -\frac{1}{2}S^2\frac{\partial^2}{\partial S^2}\left(\int_0^\infty vf(v)C_{BS}dv\right) - rK\mathrm{e}^{-r\tau}\widetilde{\mathbb{P}}_{t,S}(S_T^{\mathcal{V}} > K)\\ &= -\frac{1}{2}S\int_0^\infty vf(v)\widetilde{p}(\tau;m)dv - rK\mathrm{e}^{-r\tau}\widetilde{\mathbb{P}}_{t,S}(S_T^{\mathcal{V}} > K).\end{aligned} \tag{4.82}$$

The first integral in (4.82) can be expressed analytically for the gamma and inverse gamma. For the randomized G process, by substituting (4.29) into (4.82), we have

$$\begin{aligned}&-\frac{1}{2}S\int_0^\infty vf_{G(\theta,\lambda)}(v)\widetilde{p}(\tau;m)dv = -\frac{1}{2}S\int_0^\infty v\left(\frac{1}{\lambda^\theta\Gamma(\theta)}v^{\theta-1}\mathrm{e}^{-\frac{v}{\lambda}}\right)\widetilde{p}(\tau;m)dv\\ &= -\frac{1}{2}S\int_0^\infty \frac{\lambda\Gamma(\theta+1)}{\Gamma(\theta)}\left(\frac{1}{\lambda^{\theta+1}\Gamma(\theta+1)}v^{(\theta+1)-1}\mathrm{e}^{-\frac{v}{\lambda}}\right)\widetilde{p}(\tau;m)dv\\ &= -\frac{S\lambda}{2}\frac{\Gamma(\theta+1)}{\Gamma(\theta)}\widetilde{p}_{G(\theta+1,\lambda)}(\tau;m)\\ &= -\frac{S\mathrm{e}^{-\frac{m}{2}}}{\tau\sqrt{\pi}\Gamma(\theta)}\left(\frac{2}{\lambda\tau}\right)^\theta\left(\frac{\lambda\tau m^2}{8+\lambda\tau}\right)^{\frac{\theta}{2}+\frac{1}{4}}\mathsf{K}_{\theta+\frac{1}{2}}\left(\sqrt{\frac{m^2(8+\lambda\tau)}{4\lambda\tau}}\right).\end{aligned} \tag{4.83}$$

For the randomized IG process, by substituting (4.39) into (4.82), we obtain

$$\begin{aligned}&-\frac{1}{2}S\int_0^\infty vf_{IG(\theta,\lambda)}(v)\widetilde{p}(\tau;m)dv = -\frac{1}{2}S\int_0^\infty v\left(\frac{\lambda^\theta}{\Gamma(\theta)}\left(\frac{1}{v}\right)^{\theta+1}\mathrm{e}^{-\frac{\lambda}{v}}\right)\widetilde{p}(\tau;m)dv\\ &= -\frac{1}{2}S\int_0^\infty \frac{\lambda\Gamma(\theta-1)}{\Gamma(\theta)}\left(\frac{\lambda^{\theta-1}}{\Gamma(\theta-1)}\left(\frac{1}{v}\right)^{(\theta+1)-1}\mathrm{e}^{-\frac{\lambda}{v}}\right)\widetilde{p}(\tau;m)dv\\ &= -\frac{S\lambda}{2}\frac{\Gamma(\theta-1)}{\Gamma(\theta)}\widetilde{p}_{IG(\theta-1,\lambda)}(\tau;m)\\ &= -\frac{S\mathrm{e}^{-\frac{m}{2}}}{\tau\sqrt{\pi}\Gamma(\theta)}\left(\frac{\lambda\tau}{2}\right)^\theta(m^2+2\lambda\tau)^{-\frac{\theta}{2}+\frac{1}{4}}\mathsf{K}_{\theta-\frac{1}{2}}\left(\frac{\sqrt{m^2+2\lambda\tau}}{2}\right).\end{aligned} \tag{4.84}$$

4.7 Implied BS Volatility

In this section, we study the implied BS volatility under the randomized GBM model where the variance process follows the gamma and the inverse gamma randomization. Theoretical results of implied volatility under the GBM model with stochastic volatility are given in the Renualt and Touzi's paper [18]. They have shown that an implied volatility surface is an even function of the log-forward moneyness and necessarily produces a smile effect under the randomized GBM models with zero correlation. Recall that the ratio of a European vanilla call option price relative to a spot price under the GBM model can be expressed in terms of (τ, m, v):

$$\widehat{C}_{BS}(\tau, m; v) \equiv \frac{C_{BS}(\tau, S; K, r, v)}{S}. \tag{4.85}$$

Recall the symmetry property from (1.5):

$$\widehat{C}_{BS}(\tau, m; v) = (1 - \mathrm{e}^{-m}) + \mathrm{e}^{-m}\widehat{C}_{BS}(\tau, -m; v). \tag{4.86}$$

By multiplying both sides by $f_{\mathcal{V}}$ and integrating w.r.t v on the real positive line yields:

$$\widehat{C}_{\mathcal{V}}(\tau, m) = (1 - \mathrm{e}^{-m}) + \mathrm{e}^{-m}\widehat{C}_{\mathcal{V}}(\tau, -m). \tag{4.87}$$

where

$$\widehat{C}_{\mathcal{V}}(\tau, m) := \int_0^\infty \widehat{C}_{BS}(\tau, m; v) f_{\mathcal{V}}(v) dv. \tag{4.88}$$

was defined in (1.7).

In particular, we can easily show that the symmetry property holds true for the call option pricing functions under the gamma randomization in (4.74):

$$\begin{aligned}\widehat{C}_{G(n,\lambda)}(\tau,m) =&(1-\mathrm{e}^{-m})^{+}+\frac{\sqrt{|m|}}{\sqrt{\pi}}\left(\frac{\lambda\tau}{8+\lambda\tau}\right)^{\frac{1}{4}}\mathrm{e}^{-\frac{m}{2}}\\ &\sum_{k=0}^{n-1}\frac{1}{k!}\left(\frac{2|m|}{\sqrt{\lambda\tau}\sqrt{8+\lambda\tau}}\right)^{k}K_{k+\frac{1}{2}}\left(\frac{|m|}{2}\frac{\sqrt{8+\lambda\tau}}{\sqrt{\lambda\tau}}\right)\\ =&1-\mathrm{e}^{-m}+\mathrm{e}^{-m}\Bigg[(1-\mathrm{e}^{m})^{+}+\frac{\sqrt{|m|}}{\sqrt{\pi}}\left(\frac{\lambda\tau}{8+\lambda\tau}\right)^{\frac{1}{4}}\mathrm{e}^{\frac{m}{2}}\\ &\sum_{k=0}^{n-1}\frac{1}{k!}\left(\frac{2|m|}{\sqrt{\lambda\tau}\sqrt{8+\lambda\tau}}\right)^{k}K_{k+\frac{1}{2}}\left(\frac{|m|}{2}\frac{\sqrt{8+\lambda\tau}}{\sqrt{\lambda\tau}}\right)\Bigg]\\ &1-\mathrm{e}^{-m}+\mathrm{e}^{-m}\widehat{C}_{G(n,\lambda)}(\tau,-m),\end{aligned} \tag{4.89}$$

where we used the identity:

$$(1-\mathrm{e}^{-m})^{+}=(1-\mathrm{e}^{-m})+(\mathrm{e}^{-m}-1)^{+}. \tag{4.90}$$

We can also show that that the symmetry property holds true for the call option pricing functions under the inverse gamma randomization in (4.75):

$$\begin{aligned}\widehat{C}_{IG(n,\lambda)}(\tau,m) =&1-\frac{(m^2+2\lambda\tau)^{\frac{1}{4}}}{\sqrt{\pi}}\mathrm{e}^{-\frac{m}{2}}\\ &\sum_{k=0}^{n-1}\frac{1}{k!}\left(\frac{\lambda\tau}{2\sqrt{m^2+2\lambda\tau}}\right)^{k}K_{k-\frac{1}{2}}\left(\frac{\sqrt{m^2+2\lambda\tau}}{2}\right)\\ =&1-\mathrm{e}^{-m}+\mathrm{e}^{-m}\Bigg[1-\frac{(m^2+2\lambda\tau)^{\frac{1}{4}}}{\sqrt{\pi}}\mathrm{e}^{\frac{m}{2}}\\ &\sum_{k=0}^{n-1}\frac{1}{k!}\left(\frac{\lambda\tau}{2\sqrt{m^2+2\lambda\tau}}\right)^{k}K_{k-\frac{1}{2}}\left(\frac{\sqrt{m^2+2\lambda\tau}}{2}\right)\Bigg]\\ =&1-\mathrm{e}^{-m}+\mathrm{e}^{-m}\widehat{C}_{IG(n,\lambda)}(\tau,-m).\end{aligned} \tag{4.91}$$

Let us define the BS implied volatility $\sigma_{\mathcal{V}}$ here as a function depending on m (i.e., $\sigma_{\mathcal{V}}\equiv\sigma_{\mathcal{V}}(m)$). Then we can see that $\sigma_{\mathcal{V}}$ is a unique solution of:

$$\widehat{C}_{BS}(\tau,m;\sigma_{\mathcal{V}}^2(m))\equiv\widehat{C}_{\mathcal{V}}(\tau,m). \tag{4.92}$$

Since the call option pricing functions under the classical GBM and the randomized GBM models have the symmetry property in (4.86), (4.89) and (4.91) respectively, we can use

(4.86) and (4.87) to show that $\sigma_{\mathcal{V}}$ is an even function of m:[16]

$$\widehat{C}_{BS}(\tau, m; \sigma_{\mathcal{V}}^2(m)) \equiv \widehat{C}_{\mathcal{V}}(\tau, m) = (1 - \mathrm{e}^{-m}) + \mathrm{e}^{-m}\widehat{C}_{\mathcal{V}}(\tau, -m)$$
$$= (1 - \mathrm{e}^{-m}) + \mathrm{e}^{-m}\widehat{C}_{BS}(\tau, -m, \sigma_{\mathcal{V}}^2(-m)) \tag{4.93}$$
$$= \widehat{C}_{BS}(\tau, m; \sigma_{\mathcal{V}}^2(-m)).$$

Note that $\sigma_{\mathcal{V}}^2(m)$ and $\sigma_{\mathcal{V}}^2(-m)$ yield the same price, and hence we can conclude that $\sigma_{\mathcal{V}}(m) = \sigma_{\mathcal{V}}(-m)$ for arbitrary $m \in \mathbb{R}$.

In Figure 4.5, we can see that for given $\lambda > 0$, $\tau > 0$ and log-forward moneyness m, the BS implied volatility is increasing in θ, and deep in- (and out-) of-the-money option (i.e., large value of m in absolute term) prices are more sensitive to the parameter θ than near in- (and out-) of-the-money option (i.e., small vale of m in absolute term) prices. In Figure 4.6, we can see that for given $\lambda > 0$, $\tau > 0$ and log-forward moneyness m, the BS implied volatility is decreasing in θ, and deep in- (and out-) of-the-money option prices are less sensitive to the parameter θ than near in- (and out-) of-the-money options. Both figures show symmetric smile effects.

We can also see that the BS implied volatility under the gamma randomization exhibits the V-shaped (i.e., concave) smile, whereas the BS implied volatility under the inverse gamma randomization exhibits the U-shaped (i.e., convex) smile. We will present in the next section that the inverse gamma randomization model calibrates well to some U-shaped market volatility, and hence it may be useful for practitioners to employ the model. However, the gamma randomization model does not fit well as we rarely see market volatility with concave smiles in practice.

[16]See Proposition 3.1 from Renault and Touzi [18].

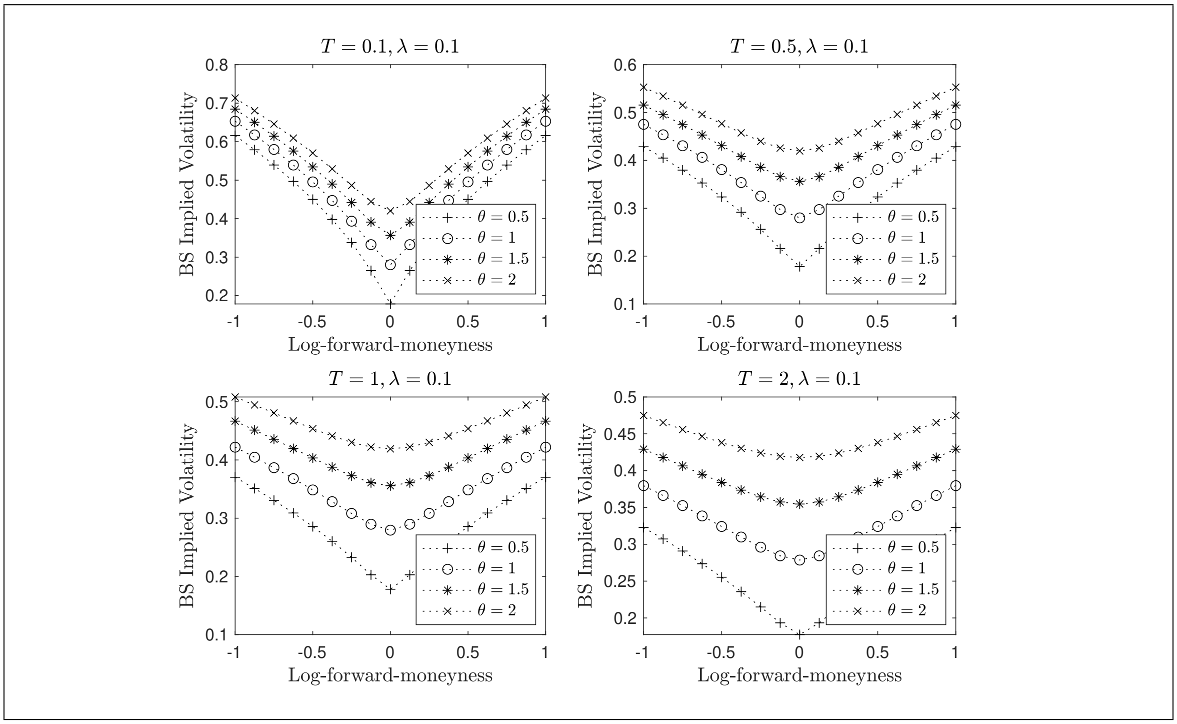

Figure 4.5: BS implied volatility of a European vanilla call option under the gamma randomization.

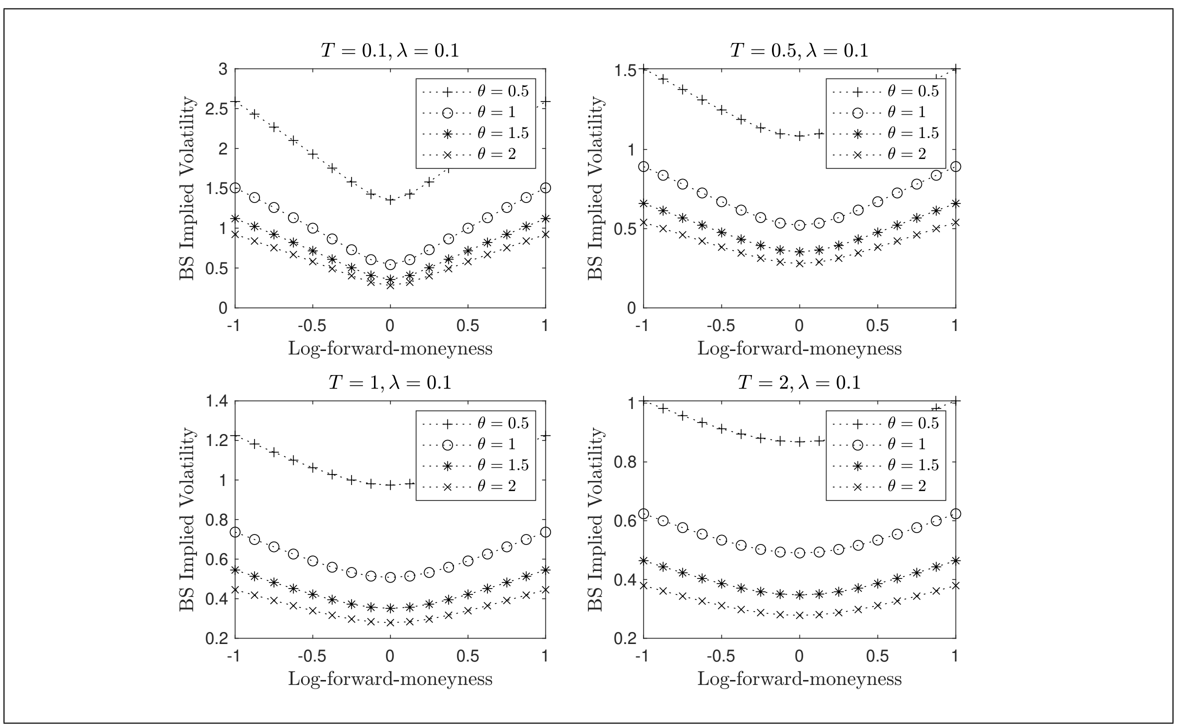

Figure 4.6: BS implied volatility of a European vanilla call option under the inverse gamma randomization.

4.8 Numerical Example

In this section, we calibrate our models to some market option data. We extract the market data for the Coca Cola European call options with spot time on April 2, 2019. The market data contains 354 sample data points with 15 distinct values of the maturity time. The market volatility in the data set exhibits pronounced smiles across different strikes fro small times to maturity, and skewed smiles for long times to maturity. We consider the following two scenarios:

- The **time-invariant case** where we calibrate the models to the market data across all maturity times. The reader may refer to Tables 4.1, 4.2, 4.3 and Figure 4.7 (more plots can be found in Figures D.1, D.2, D.3, D.4, D.5, D.6).
- The **time-variant case** where we calibrate the models to the market data among classes consisting of all observations with same maturity times. The reader may refer to Tables 4.4, 4.5, 4.6 and Figures 4.8, 4.9.

Firstly, we consider the time-invariant case. Suppose that V_i^*, Σ_i^* are the observed market option price and market volatility respectively for $i = 1, \dots, N$ where N is the number of sample points, and τ_i, K_i are the corresponding maturity time and strike price. Here, we use the root mean squared error (RMSE) as a loss function $L(\theta, \lambda)$ for the model calibration under the gamma and the inverse gamma randomization whose weights depend on the maturity times, i.e.,

$$L(\theta, \lambda) = \sqrt{\frac{\sum_{i=1}^{N} w_p(\tau)\left(V(\tau_i, S; K_i) - V_i^*\right)^2}{N}}; \quad w_p(\tau) = \frac{1}{\tau^p}, \tag{4.94}$$

where p is some constant controlling the weight function $w_p(\tau)$. This means that when the value of p is high, the observed market prices with smaller maturity times contribute to the loss function more than the observed market prices with longer maturity times. Alternatively for the SABR model, we use the Hagan et al. formula in (3.4) and (3.6) to find optimal values of parameters which minimizes the difference between the corresponding BS implied volatility and the market volatility in the RMSE sense. Hence, the loss function $L(\theta, \lambda)$ for the SABR model calibration is:

$$L(\alpha, \beta, \sigma, \rho) = \sqrt{\frac{\sum_{i=1}^{N} w_p(\tau)\left(\sigma_{\text{hagan}}(\tau_i, S, \sigma; K_i) - \Sigma_i^*\right)^2}{N}}; \quad w_p(\tau) = \frac{1}{\tau^p}, \tag{4.95}$$

Variable Name	Description	Value
S	spot price	46.57
r	constant risk-free rate	0%
τ	maturity times (in years)	$0.008 \sim 1.792$
K	strike prices	$23 \sim 65$
TolX	termination tolerance on the current value	10^{-6}
TolFun	termination tolerance on the function value	10^{-6}

Table 4.1: Set of parameters and stopping criterion to be used for calibrating to the market data.

The summary of the market data used here can be found in Table 4.1. The set of optimal values of the parameters can be found in Tables 4.2 and 4.3, where we randomly chose $p = 0, 1, -1$ in our analysis. We found that the inverse gamma randomization performs better than the gamma randomization because the RMSE is smaller for fixed $p = 0, 1, -1$.[17] From Table 4.2, we can see that as p increases, the optimal value of θ decreases while the optimal value of λ increases under the gamma randomization, and the optimal values of θ

[17] Note that we can only compare the RMSE between randomized G and IG models for fixed p, but we cannot compare the RMSE across different values of p since the weight functions have different scaling. Also, we cannot compare between the G or IG randomization and the SABR since the loss functions are different.

and λ decrease under the inverse gamma randomization. For the SABR model parameters, we attempted to find optimal values for the parameters $(\alpha, \sigma, \rho) \equiv (\alpha(\beta), \sigma(\beta), \rho(\beta))$ across different values of $\beta \in [-1, 0]$, and find the optimal value by β comparing the associated RMSEs.[18] We found that $\beta = -1$ gave the lowest RMSE. From Table 4.3, we see that as p increases, the optimal value of α increases while the optimal value of σ decreases. The SABR model does not fit the market volatility for the time-invariant case (See Figure 4.7)[19]. We will see later that the model works substantially well for the time-variant case which gives consistency with a literature and will be stated in the next scenario. Since the market volatility at $\tau = 0.008$ exhibits a smile having a strong curvature (as we can see from Table 4.6 that it has a large value of α at the maturity time), the performance on the Hagan et al. implied BS volatility formula degrades and often gives out negative values. For the particular case, we instead use the Antonov et al. formula which takes up more time to compute. Overall, the inverse gamma randomization model is the best model to fit the Coca Cola market data set for the time-invariant case.

[18] In our data set, we saw that β was not a robust parameter since the optimal value for β varies with different initial values of β. So we used the calibration method in Hagan et al. [13] to find β in advance. There are different approaches for the SABR model calibration, see e.g., West [20].

[19] Detailed plots are shown in Figures D.1, D.2, D.3, D.4, D.5, D.6.

Model Parameters		θ	λ	RMSE	Time
Gamma	$p = 0$	1.214	0.021	0.168	28.746
	$p = 1$	0.358	0.092	0.396	75.737
	$p = -1$	2.481	0.010	0.124	25.132
Inverse Gamma	$p = 0$	1.356	0.013	0.159	37.845
	$p = 1$	0.931	0.005	0.356	31.712
	$p = -1$	2.187	0.031	0.121	34.557

Table 4.2: Optimal values of the model parameters for the time-invariant case under the gamma and the inverse gamma randomization with the weight function $w_p(\tau) = \frac{1}{\tau^p}$.

Model Parameters		α	β	σ	ρ	RMSE	Time
SABR	$p = 0$	5.314	-1	4.481	-0.924	0.166	149.149
	$p = 1$	18.861	-1	1.803	-0.826	1.025	493.847
	$p = -1$	0.562	-1	7.791	-0.706	0.053	12.307

Table 4.3: Optimal values of the model parameters for the time-invariant case under the SABR model with the weight function $w_p(\tau) = \frac{1}{\tau^p}$.

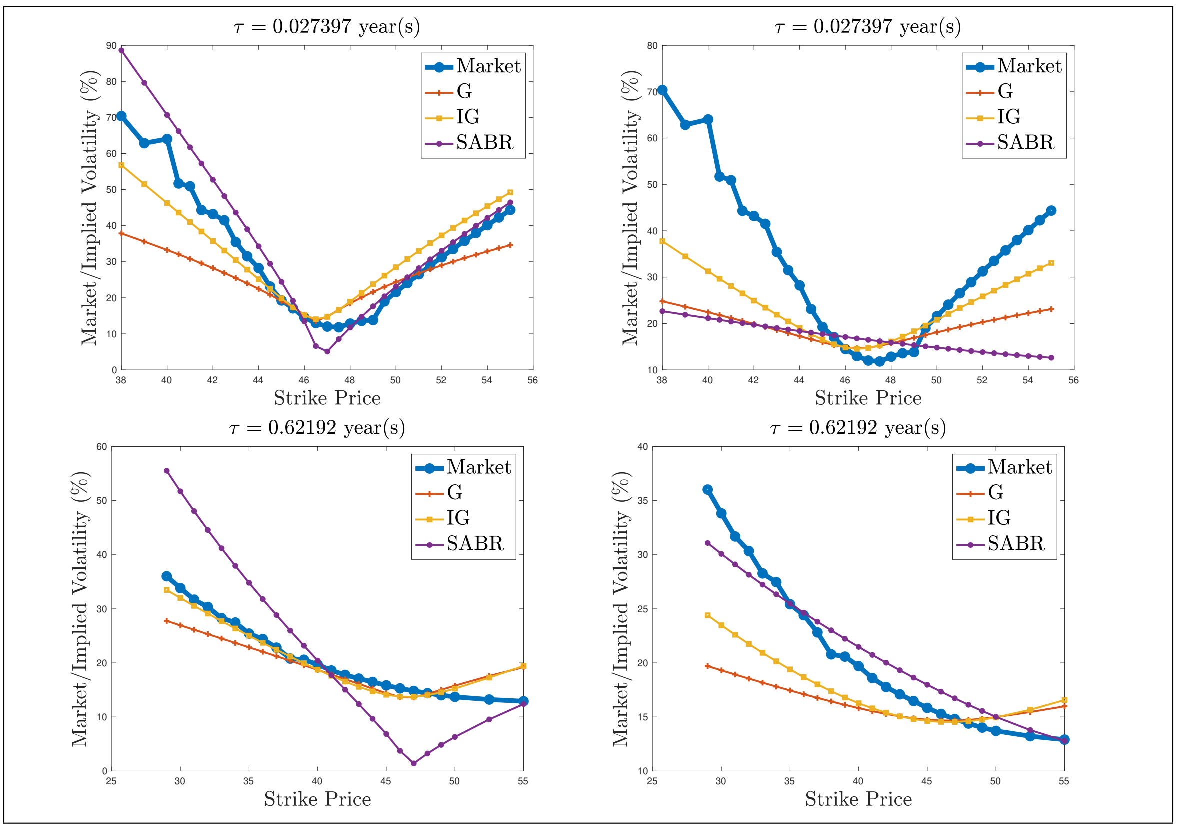

Figure 4.7: 2D Implied volatility plots for the time-invariant case for **SMALL** maturity times (top) and **LONG** maturity times (bottom) with $p = 1$ (left) $p = -1$ (right)

Now, we consider calibrating parameters among classes consisting of all observations with same maturity time. Define $\mathbb{T} = \{\tau_i : i = 1, \ldots, N\}$ as the collection of maturity times in the data set arranged in an increasing order. Let $\mathcal{S}_\tau = \{i | \tau_i = \tau \in \mathbb{T}\}$ be the collection of observations with maturity time $\tau \in \mathbb{T}$. For each τ, we use the usual RMSE ($w_p(\tau) = 1$) for the loss function under the gamma and the inverse gamma randomization:

$$L_\tau(\theta, \lambda) = \sqrt{\frac{\sum_{i \in \mathcal{S}_\tau} \left(V(\tau_i, S; K_i) - V_i^*\right)^2}{N_\tau}}; \quad \tau \in \mathbb{T}, \tag{4.96}$$

where $N_\tau = \#\mathcal{S}_\tau$ is the number of observations with maturity time τ. Similarly, the loss function for the SABR model calibration is:

$$L_\tau(\alpha, \beta, \sigma, \rho) = \sqrt{\frac{\sum_{i \in \mathcal{S}_\tau} \left(\sigma_{\text{hagan}}(\tau_i, S, \sigma; K_i) - \Sigma_i^*\right)^2}{N_\tau}}; \quad \tau \in \mathbb{T}, \tag{4.97}$$

Based on Tables 4.4, 4.5 and 4.6, we found that: The inverse gamma randomization performs[20] quite well for small maturity times. The SABR model fits almost perfectly for the time-variant case, although we saw in the first scenario that the model did not calibrate well for the time-invariant case. This result is consistent with the literature[21] that the time-invariant SABR model calibrates well at a single maturity, but does not calibrate well at multiple maturities.

Putting to the two scenarios together, we conclude that the inverse gamma randomization works the best for the time-invariant case and the SABR model works the best for the time-variant case.

[20]Note that we can only compare the RMSE across different models for fixed τ, but we cannot compare the RMSE across different values of τ.

[21]For example, see [21].

Maturity Times	Data Points	θ	λ	RMSE	Time
0.008	33	0.095	0.575	0.041	71.194
0.027	33	0.108	0.334	0.059	91.963
0.044	35	0.176	0.171	0.070	8.189
0.066	19	0.405	0.104	0.083	1.932
0.085	15	0.214	0.215	0.159	3.123
0.104	15	0.087	0.720	0.295	40.699
0.123	24	0.193	0.228	0.121	5.902
0.219	32	0.153	0.276	0.162	15.721
0.373	31	0.369	0.089	0.169	4.230
0.468	29	0.322	0.105	0.173	5.593
0.622	24	0.482	0.067	0.175	3.156
0.795	17	2.669	0.009	0.184	1.989
1.216	16	3.245	0.007	0.186	1.837
1.466	14	2.070	0.012	0.227	2.087
1.792	17	11.021	0.002	0.173	2.154

Table 4.4: Optimal values of θ and λ for the time-variant case under the gamma randomization

Maturity Times	Data Points	θ	λ	RMSE	Time
0.008	33	0.719	0.002	0.032	6.087
0.027	33	0.827	0.002	0.051	3.460
0.044	35	0.877	0.003	0.062	3.569
0.066	19	1.227	0.014	0.079	2.332
0.085	15	0.885	0.005	0.147	2.107
0.104	15	0.672	0.002	0.280	2.533
0.123	24	0.923	0.006	0.106	2.788
0.219	32	0.799	0.003	0.135	3.897
0.373	31	0.979	0.006	0.147	2.903
0.468	29	0.926	0.005	0.141	3.787
0.622	24	1.091	0.009	0.153	3.789
0.795	17	2.406	0.035	0.181	2.338
1.216	16	2.962	0.048	0.183	2.697
1.466	14	1.861	0.024	0.217	2.310
1.792	17	8.016	0.155	0.173	3.485

Table 4.5: Optimal values of θ and λ for the time-variant case under the inverse gamma randomization

τ	Data Points	α	β	σ	ρ	RMSE	Time
0.008	33	21.729	-1	2.994	-0.502	0.026	0.435
0.027	33	10.616	-1	3.643	-0.560	0.021	0.574
0.044	35	7.711	-1	4.204	-0.619	0.018	0.353
0.066	19	4.691	-1	6.793	-0.465	0.011	0.329
0.085	15	5.040	-1	6.239	-0.610	0.030	0.341
0.104	15	5.967	-1	5.473	-0.704	0.059	0.344
0.123	24	3.633	-1	6.119	-0.570	0.014	0.337
0.219	32	2.916	-1	5.424	-0.604	0.015	0.360
0.373	31	1.895	-1	5.701	-0.535	0.014	0.159
0.468	29	1.631	-1	5.680	-0.385	0.011	0.392
0.622	24	1.147	-1	6.256	-0.341	0.008	0.378
0.795	17	1.001	-1	6.032	-0.425	0.011	0.359
1.216	16	0.673	-1	6.272	-0.242	0.010	0.371
1.466	14	0.782	-1	5.940	-0.154	0.016	0.303
1.792	17	0.467	-1	6.371	-0.058	0.007	0.331

Table 4.6: Optimal values of θ and λ for the time-variant case under the SABR model

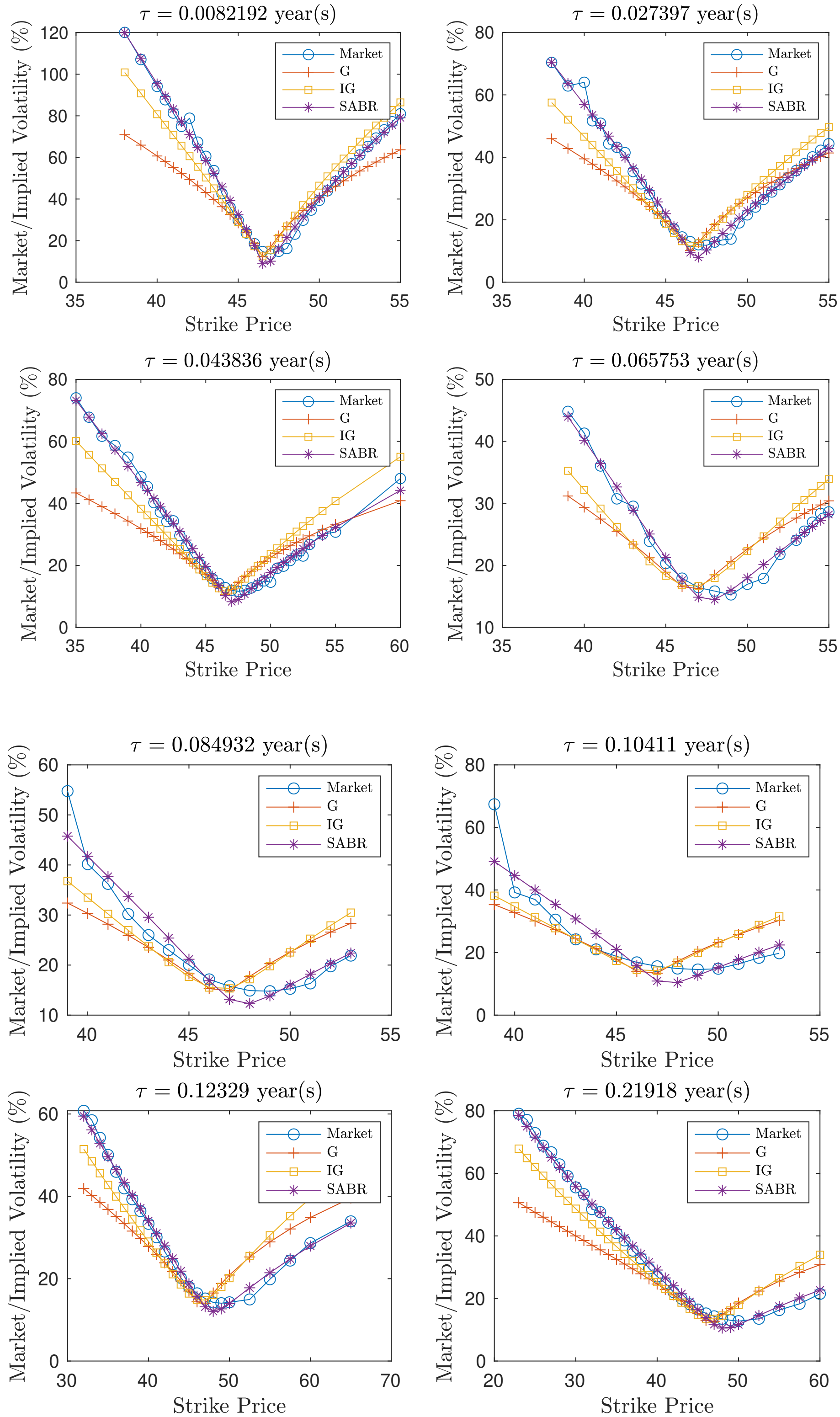

Figure 4.8: 2D Implied volatility plots for the time-variant case for small maturity times.

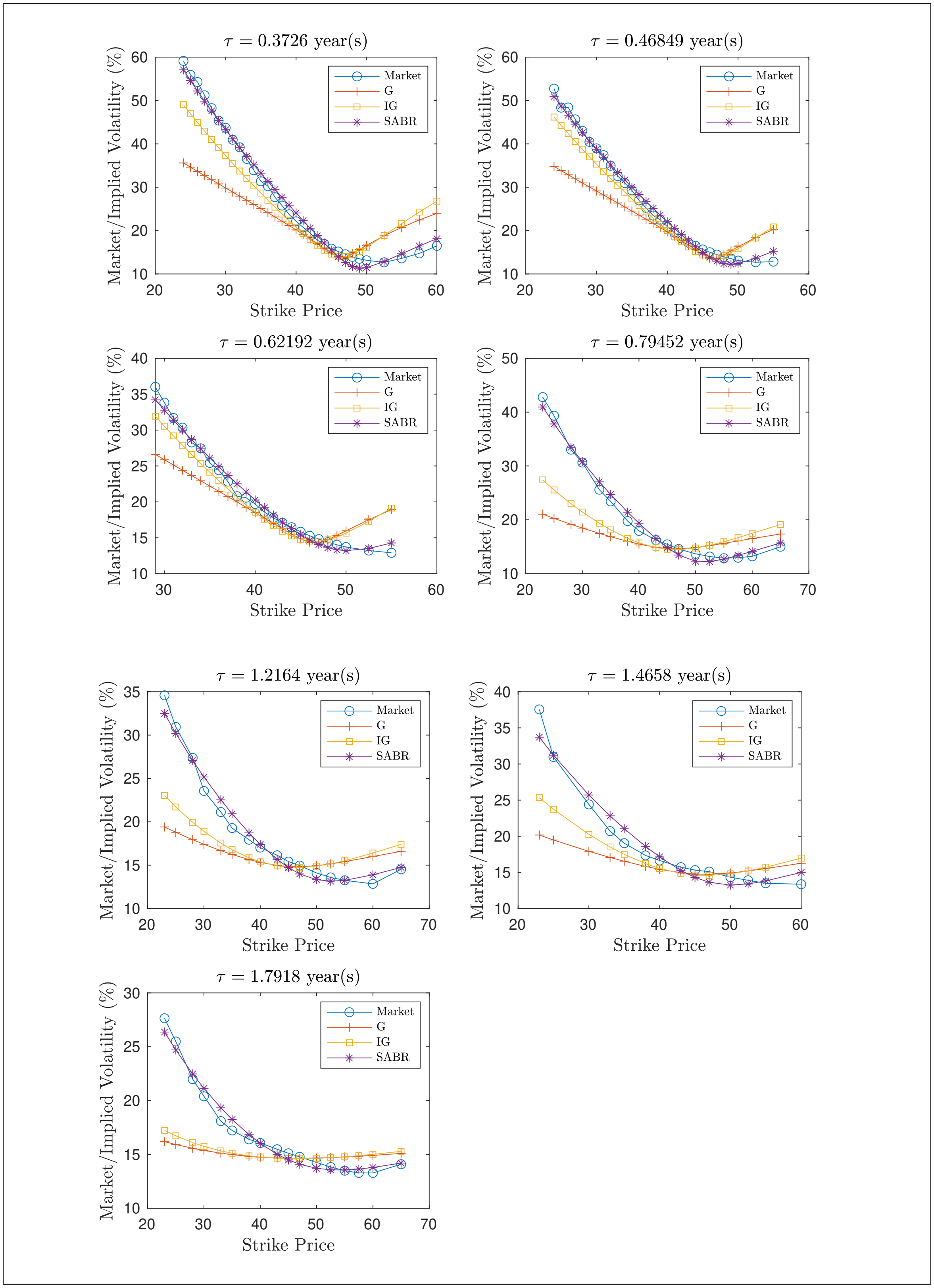

Figure 4.9: 2D Implied volatility plots for the time-variant case for long maturity times.

4.9 Stability of the Model Calibration Procedure

Suppose we can perfectly calibrate the market data in the sense that $L(\theta, \lambda) = 0$ for a given loss function L. In other words, we assume that the market prices can be generated from the chosen model parameters, i.e.,

$$V_{\tau,K}^{Mkt} = V_{\mathcal{V}}(\tau, S; K, r); \quad \mathcal{V} \sim G(\theta, \lambda) \text{ or } IG(\theta, \lambda). \tag{4.98}$$

In this section, we will calibrate to the market prices generated from the model itself with given parameters, and see whether the values for the calibrated parameters and the original model parameters coincide. Here is a sketch of the algorithm:

1. Generate two uniformly distributed random numbers between 0 and 20 for the model parameters, (i.e., $\theta^{Mod}, \lambda^{Mod} \overset{i.i.d.}{\sim} Unif(0, 20)$).

2. Generate two uniformly distributed random numbers between -5 and 5 (i.e., $u_\theta, u_\lambda \overset{i.i.d.}{\sim} Unif(-5, 5)$). Then add u_θ, u_λ to $\theta^{Mod}, \lambda^{Mod}$ respectively to determine the initial values of the model parameters (θ, λ must be positive):

$$\theta^{Init} = |\theta^{Mod} + u_\theta|, \quad \lambda^{Init} = |\lambda^{Mod} + u_\lambda|. \tag{4.99}$$

3. Calibrate to the market prices in the usual way.

4. Repeat $1 \sim 3$ multiple times.

We ran the test 10 times and the resulting tables under the gamma and the inverse gamma randomization can be found in Table 4.7 and 4.8 respectively. We can see that the values of the calibrated parameters and the original model parameters coincide most of the time except for one instance where the calibrated parameters $(43.482, 1.055)$ significantly differ from the model parameters $(16.424, 0.308)$.

model parameter		initial parameter		calibrated parameter		RMSE
θ	λ	θ	λ	θ	λ	
3.244	15.886	1.356	16.171	3.244	15.886	1.54×10^{-5}
3.313	12.040	0.943	13.580	3.313	12.040	4.79×10^{-5}
13.784	14.963	13.290	10.801	13.784	14.964	5.72×10^{-6}
4.580	18.267	1.103	21.525	4.580	18.267	8.10×10^{-5}
10.767	19.923	6.549	19.349	10.767	19.922	6.54×10^{-6}
2.133	19.238	2.821	21.987	2.133	19.238	6.48×10^{-5}
16.346	17.374	12.190	16.372	16.346	17.373	2.03×10^{-6}
5.197	16.001	4.512	20.108	5.197	16.001	2.26×10^{-5}
3.637	5.276	0.092	1.637	3.637	5.276	4.19×10^{-5}
17.386	11.594	17.884	8.044	17.386	11.594	4.26×10^{-6}

Table 4.7: A list of model, initial and calibrated parameters under the gamma randomization.

model parameter		initial parameter		calibrated parameter		RMSE
θ	λ	θ	λ	θ	λ	
17.061	12.441	15.570	12.574	17.060	12.441	1.54×10^{-6}
8.036	1.519	5.435	2.247	8.036	1.519	2.72×10^{-6}
3.678	4.799	2.851	0.296	3.678	4.799	2.60×10^{-5}
18.054	18.896	17.963	18.788	18.055	18.896	2.59×10^{-6}
6.754	18.001	5.447	14.113	6.754	18.001	1.89×10^{-5}
15.605	7.795	13.022	6.834	15.604	7.794	2.37×10^{-6}
1.929	2.639	6.350	7.201	1.929	2.639	2.81×10^{-5}
11.504	1.196	8.852	0.273	11.504	1.196	1.21×10^{-6}
16.424	0.308	11.854	3.002	43.482	1.055	0.52
12.982	14.634	14.460	14.144	12.983	14.635	3.81×10^{-6}

Table 4.8: A list of model, initial and calibrated parameters under the inverse gamma randomization.

Chapter 5

Alternative Randomization Models

5.1 Transition Density Functions with Imposed Killing

For the GBM model, the transition PDF for $\{S_t\}_{t\geqslant 0}$ killed at some threshold level $B > 0$ is:[1]

$$\begin{aligned}\widetilde{p}^{S_{(B)}}(t; S, y) = &\frac{1}{y\sqrt{2\pi v t}} \exp\left(-\frac{[\ln \frac{y}{S} - (r - \frac{1}{2}v)t]^2}{2vt}\right) \\ &- \left(\frac{B}{S}\right)^{\frac{2r}{v}-1} \frac{1}{y\sqrt{2\pi v t}} \exp\left(-\frac{[\ln \frac{yS}{B^2} - (r - \frac{1}{2}v)t]^2}{2vt}\right)\end{aligned} \tag{5.1}$$

defined on the respective domains $(0, B)$ and (B, ∞). Alternatively, let $\{X_t\}_{t\geqslant 0} = \{\ln \frac{S_t}{S}\}_{t\geqslant 0}$ be the log-return process and $b = \ln \frac{B}{S}$ be the corresponding threshold level. The transition

[1]See (12.133) from Campolieti and Makarov [10].

PDF for the drifted BM $\{X_t\}_{t\geqslant 0}$ killed at b is:[2]

$$
\begin{aligned}
\widetilde{p}^{X_{(b)}}(\tau;0,x) =& \frac{1}{\sqrt{2\pi v\tau}} \exp\left(-\frac{[x_r+\frac{1}{2}v\tau]^2}{2v\tau}\right) \\
&- \frac{1}{\sqrt{2\pi v\tau}} \exp\left(b\left(\frac{2r}{v}-1\right) - \frac{\left[x_r-2b+\frac{1}{2}v\tau\right]^2}{2v\tau}\right) \\
=& \frac{1}{\sqrt{2\pi v\tau}} \exp\left(-\frac{x_r}{2}-\frac{v\tau}{8}\right) \\
&\times \left[\exp\left(-\frac{x_r^2}{2v\tau}\right) - \exp\left(-\frac{x_b^2}{2v\tau}\right)\right],
\end{aligned}
\tag{5.2}
$$

where $x_r = x - r\tau$ and $x_b = \sqrt{(x-2b-r\tau)^2 - 4br\tau} \geqslant 0$. The transition PDF in (5.2) is defined on the respective domains $(-\infty, b)$ and (b, ∞). In this section, we derive the transition PDF of the stock price process with imposed killing under the randomized GBM model. If $\mathcal{V} \sim G(\theta, \lambda)$, by making use of (4.28) we have the transition PDF:

$$
\begin{aligned}
\widetilde{p}^{X_{(b)}}_{G(\theta,\lambda)}(\tau;0,x) =& \frac{2\mathrm{e}^{-\frac{x_r}{2}}}{\lambda^\theta \Gamma(\theta)\sqrt{2\pi\tau}} \left[\left(\frac{2|x_r|}{\sqrt{\tau}\sqrt{8+\lambda\tau}}\right)^{\theta-\frac{1}{2}} K_{\theta-\frac{1}{2}}\left(\frac{|x_r|\sqrt{8+\lambda\tau}}{\sqrt{4\lambda\tau}}\right)\right. \\
&\left. - \left(\frac{2x_b}{\sqrt{\tau}\sqrt{8+\lambda\tau}}\right)^{\theta-\frac{1}{2}} K_{\theta-\frac{1}{2}}\left(\frac{x_b\sqrt{8+\lambda\tau}}{\sqrt{4\lambda\tau}}\right)\right].
\end{aligned}
\tag{5.3}
$$

If $\mathcal{V} \sim IG(\theta, \lambda)$, the transition PDF is

$$
\begin{aligned}
\widetilde{p}^{X_{(b)}}_{IG(\theta,\lambda)}(\tau;0,x) =& \frac{2\lambda^\theta \mathrm{e}^{-\frac{x_r}{2}}}{\Gamma(\theta)\sqrt{2\pi\tau}} \left[\left(\frac{4[x_r^2+2\lambda\tau]}{\tau^2}\right)^{-\frac{\theta}{2}-\frac{1}{4}} K_{\theta+\frac{1}{2}}\left(\sqrt{\frac{x_r^2+2\lambda\tau}{4}}\right)\right. \\
&\left. - \left(\frac{4[x_b^2+2\lambda\tau]}{\tau^2}\right)^{-\frac{\theta}{2}-\frac{1}{4}} K_{\theta+\frac{1}{2}}\left(\sqrt{\frac{x_b^2+2\lambda\tau}{4}}\right)\right].
\end{aligned}
\tag{5.4}
$$

[2]See (10.80) from Campolieti and Makarov [10].

5.2 First hitting time in the driftless case

The first hitting time $\mathcal{T}_b^X \equiv \min\{t \geqslant 0 | X_t = b\}$ of standard driftless BM (i.e., $r = 0$) started at 0 up to level b has CDF:[3]

$$\begin{aligned}
F_{\mathcal{T}_b^X}(\tau) = 1 - \int_{-\infty}^{b} \widetilde{p}^{X_{(b)}}(\tau; 0, x)dx = \mathcal{N}\left(\frac{-b - \frac{1}{2}\upsilon\tau}{\sqrt{\upsilon\tau}}\right) + \mathrm{e}^{-b}\mathcal{N}\left(\frac{-b + \frac{1}{2}\upsilon\tau}{\sqrt{\upsilon\tau}}\right) \\
= \widetilde{\mathbb{P}}_{t,S}\left(X_T > b\right) + \mathrm{e}^{-b}\widetilde{\mathbb{P}}_{t,S}\left(X_T \leqslant -b\right); \quad b > 0, \\
F_{\mathcal{T}_b^X}(\tau) = 1 - \int_{b}^{\infty} \widetilde{p}^{X_{(b)}}(\tau; 0, x)dx = \mathcal{N}\left(\frac{b + \frac{1}{2}\upsilon\tau}{\sqrt{\upsilon\tau}}\right) + \mathrm{e}^{-b}\mathcal{N}\left(\frac{b - \frac{1}{2}\upsilon\tau}{\sqrt{\upsilon\tau}}\right) \\
= \widetilde{\mathbb{P}}_{t,S}\left(X_T \leqslant b\right) + \mathrm{e}^{-b}\widetilde{\mathbb{P}}_{t,S}\left(X_T > -b\right); \quad b < 0,
\end{aligned} \tag{5.5}$$

for $\tau > 0$, and 1 at $b = 0$. We can use (4.52) to obtain the first hitting time to level b with randomization. For example, if $\mathcal{V} \sim G(n, \lambda)$, $n \in \mathbb{N}$, then

$$F_{\mathcal{T}_b^X}^{G(n,\lambda)}(\tau) = \frac{\sqrt{|b|}}{\sqrt{\pi}}\left(\frac{8 + \lambda\tau}{\lambda\tau}\right)^{\frac{1}{4}} \mathrm{e}^{-\frac{b}{2}} \sum_{k=0}^{n-1}\left(\frac{2|b|}{\sqrt{\lambda\tau}\sqrt{8 + \lambda\tau}}\right)^k K_{k-\frac{1}{2}}\left(\frac{|b|}{2}\frac{\sqrt{8 + \lambda\tau}}{\sqrt{\lambda\tau}}\right). \tag{5.6}$$

if $\mathcal{V} \sim IG(n, \lambda)$, $n \in \mathbb{N}$, then

$$F_{\mathcal{T}_b^X}^{IG(n,\lambda)}(\tau) = \min\{1, \mathrm{e}^{-b}\} - \frac{|b|}{\sqrt{\pi}}(b^2 + 2\lambda\tau)^{-\frac{1}{4}}\mathrm{e}^{-\frac{b}{2}} \sum_{k=0}^{n-1}\left(\frac{\lambda\tau}{2\sqrt{b^2 + 2\lambda\tau}}\right)^k K_{k+\frac{1}{2}}\left(\frac{\sqrt{b^2 + 2\lambda\tau}}{2}\right). \tag{5.7}$$

5.3 First hitting time with a drift

The first hitting time (of drifted BM started at 0) up to level b has CDF:[4]

$$\begin{aligned}
F_{\mathcal{T}_b^X}(\tau) = \widetilde{\mathbb{P}}_{t,S}\left(X_T > b\right) + \mathrm{e}^{\frac{2\mu b}{\upsilon}}\widetilde{\mathbb{P}}_{t,S}\left(X_T \leqslant -b\right); \quad b > 0, \\
F_{\mathcal{T}_b^X}(\tau) = \widetilde{\mathbb{P}}_{t,S}\left(X_T \leqslant b\right) + \mathrm{e}^{\frac{2\mu b}{\upsilon}}\widetilde{\mathbb{P}}_{t,S}\left(X_T > -b\right); \quad b < 0,
\end{aligned} \tag{5.8}$$

for $\tau > 0$, and 1 at $b = 0$, where $\mu = r - \frac{1}{2}\upsilon$. We consider the first hitting time under the inverse gamma randomization[5]. We can use (4.52) to obtain the first hitting time under the

[3] See (10.83) and (10.88) from Campolieti and Makarov [10].

[4] See (10.83) and (10.88) from Campolieti and Makarov [10].

[5] The first hitting time under the gamma randomization cannot be obtained analytically for $r > 0$.

inverse gamma randomization:

$$
\begin{aligned}
F_{\mathcal{T}_b^X}^{IG(n,\lambda)}(\tau) =& A_1 - B_1 + \frac{\lambda^n}{(\lambda - 2br)^n}\mathrm{e}^{-b}; \qquad b > 0, \lambda \neq 2br, \\
F_{\mathcal{T}_b^X}^{IG(n,\lambda)}(\tau) =& 1 - A_1 + B_1; \qquad b < 0,
\end{aligned} \tag{5.9}
$$

where

$$
\begin{aligned}
A_1 =& \frac{1}{2}\frac{\sqrt{A}}{\sqrt{\pi}}\mathrm{e}^{-\frac{b-r\tau}{2}}\sum_{k=0}^{n-1}\frac{1}{k!}\left(\frac{\lambda\tau}{2A}\right)^k\left[K_{k-\frac{1}{2}}\left(\frac{A}{2}\right) - \frac{b-r\tau}{A}K_{k+\frac{1}{2}}\left(\frac{A}{2}\right)\right], \\
B_1 =& \frac{1}{2}\frac{\lambda^n}{(\lambda-2br)^n}\frac{\sqrt{A}}{\sqrt{\pi}}\mathrm{e}^{-\frac{b-r\tau}{2}}\sum_{k=0}^{n-1}\frac{1}{k!}\left(\frac{\lambda\tau - 2br\tau}{2A}\right)^k \\
& \times\left[K_{k-\frac{1}{2}}\left(\frac{A}{2}\right) + \frac{b+r\tau}{A}K_{k+\frac{1}{2}}\left(\frac{A}{2}\right)\right], \\
A =& \sqrt{(b-r\tau)^2 + 2\lambda\tau}.
\end{aligned} \tag{5.10}
$$

For $\lambda = 2br$, numerical tests showed (by applying the L'Hôspital's rule n times) that the limit exists. For example, if $n = 1, 2, 3$ we have

$$
\begin{aligned}
\lim_{\lambda\to 2br} F_{\mathcal{T}_b^X}^{IG(1,\lambda)}(\tau) =& A_1 + \mathrm{e}^{-b}\frac{br\tau}{(b+r\tau)^2}(b+r\tau+1), \\
\lim_{\lambda\to 2br} F_{\mathcal{T}_b^X}^{IG(2,\lambda)}(\tau) =& A_1 + \frac{\mathrm{e}^{-b}}{2}\left(\frac{br\tau}{(b+r\tau)^2}\right)^2((b+r\tau)^2 + 4(b+r\tau) + 6), \\
\lim_{\lambda\to 2br} F_{\mathcal{T}_b^X}^{IG(3,\lambda)}(\tau) =& A_1 + \frac{\mathrm{e}^{-b}}{3!}\left(\frac{br\tau}{(b+r\tau)^2}\right)^3 \\
& \times((b+r\tau)^3 + 9(b+r\tau)^2 + 36(b+r\tau) + 60).
\end{aligned} \tag{5.11}
$$

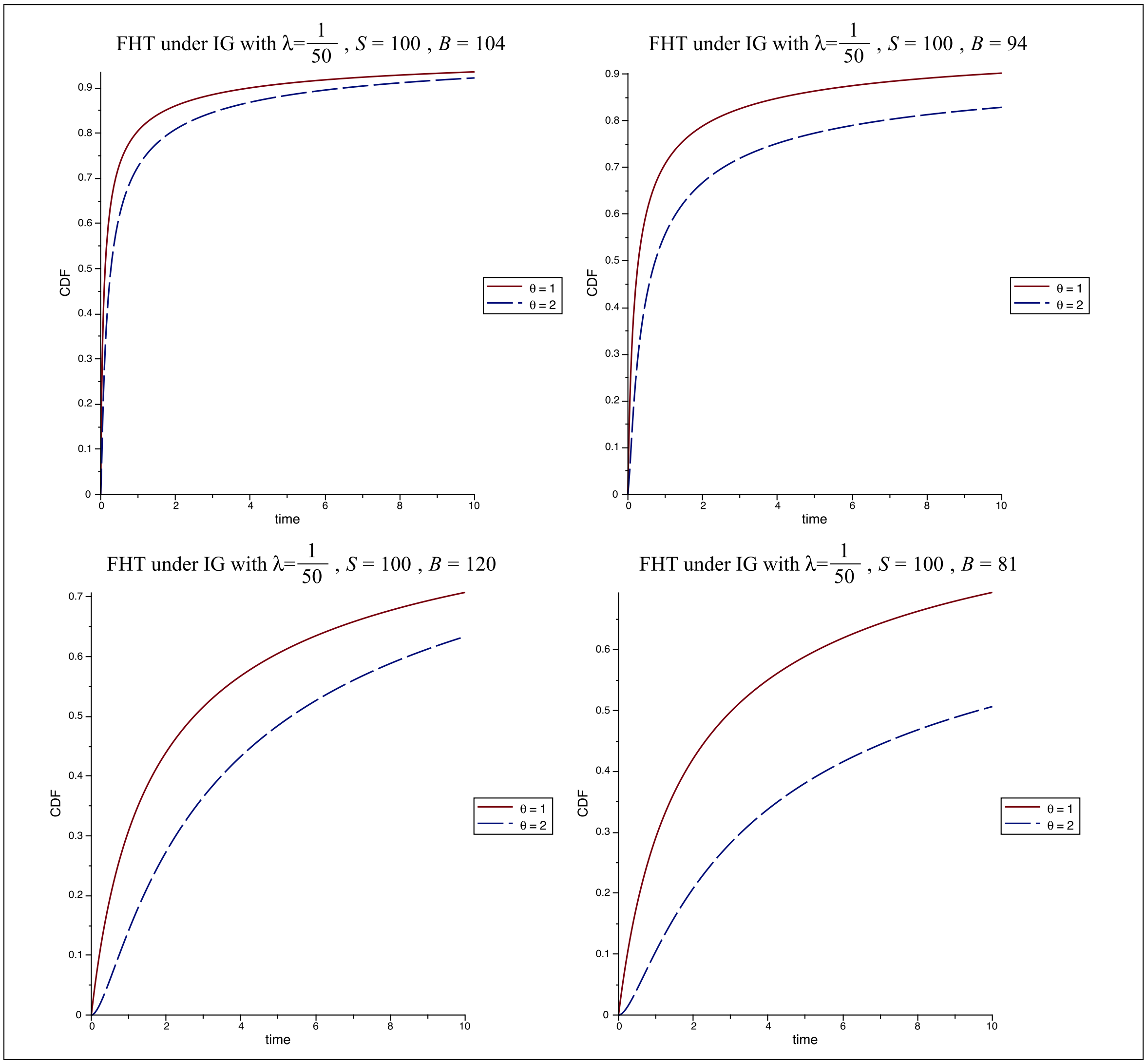

Figure 5.1: Plots of the first hitting times (with a drift $r = 0.01$) under the inverse gamma randomization.

5.4 Two-Asset Economy with perfectly correlated volatility

In this section we consider extending the randomized GBM model to a two-asset economy whose driven asset price processes are necessarily correlated. We denote $\{S_t^{(j)}\}_{t\geqslant 0}$ as the j^{th} asset price (diffusion) process with constant volatility $\sqrt{\lambda_j v}$, given parameters $\lambda_j > 0, v > 0$. For simplicity we assume the volatility of the two risky assets are perfectly correlated [6]. The two-dimensional process $\{\vec{S}_t\}_{t\geqslant 0} = \{(S_t^{(1)}, S_t^{(2)})\}_{t\geqslant 0}$ (with constant variances v_1, v_2 respectively) obeys the following SDEs:

$$\begin{cases} \dfrac{dS_t^{(1)}}{S_t^{(1)}} = (r - q_1)dt + \sqrt{\lambda_1 v} d\widetilde{W}_t^{(1)}; \quad S_0^{(1)} > 0, \\ \dfrac{dS_t^{(2)}}{S_t^{(2)}} = (r - q_2)dt + \sqrt{\lambda_2 v} d\widetilde{W}_t^{(2)}; \quad S_0^{(2)} > 0, \\ d\widetilde{W}_t^{(1)} d\widetilde{W}_t^{(2)} = \rho dt, \end{cases} \tag{5.12}$$

where q_j is the continuous dividend rate for the j^{th} asset price process. Define

$$X_t^{(1)} = \ln\left(\frac{S_t^{(1)}}{S_0^{(1)}}\right) - rt, \qquad X_t^{(2)} = \ln\left(\frac{S_t^{(2)}}{S_0^{(2)}}\right) - rt; \quad t \geqslant 0. \tag{5.13}$$

Recall that the pair $\vec{X}_t = (X_t^{(1)}, X_t^{(2)})$ follows the bivariate normal distribution whose joint PDF is:[7]

$$\begin{aligned} \widetilde{p}(\tau; x_1, x_2) =& \frac{1}{2\pi v\tau\sqrt{\lambda_1\lambda_2(1-\rho^2)}} \exp\Bigg(-\frac{1}{2(1-\rho^2)} \\ & \left[\frac{(x_1 + \frac{1}{2}\lambda_1 v\tau)^2}{\lambda_1 v\tau} + \frac{(x_2 + \frac{1}{2}\lambda_2 v\tau)^2}{\lambda_2 v\tau} - \frac{2\rho(x_1 + \frac{1}{2}\lambda_1 v\tau)(x_2 + \frac{1}{2}\lambda_2 v\tau)}{\sqrt{\lambda_1\lambda_2} v\tau} \right] \Bigg) \\ =& \left(\frac{D}{v}\right) \exp\left(-\frac{A}{v} - B - Cv \right) \end{aligned} \tag{5.14}$$

[6] Asset pricing in the imperfect correlation case may introduce the multivariate gamma/inverse gamma distributions which can be difficult to employ.

[7] For example, see (9.82) from Campolieti and Makarov [10].

where

$$
\begin{aligned}
A =& \frac{1}{2(1-\rho^2)\lambda_1\lambda_2\tau^2}[\lambda_1\tau x_1^2 + \lambda_2\tau x_2^2 - 2\rho\sqrt{\lambda_1\lambda_2}\tau x_1 x_2],\\
B =& \frac{1}{2(1-\rho^2)\sqrt{\lambda_1\lambda_2}\tau}[\sqrt{\lambda_1\lambda_2}\tau(x_1+x_2) - \rho(\lambda_1\tau x_2 + \lambda_2\tau x_1)],\\
C =& \frac{1}{8(1-\rho^2)}[\lambda_1\tau + \lambda_2\tau - 2\rho\sqrt{\lambda_1\lambda_2}\tau],\\
D =& \frac{1}{2\pi\tau\sqrt{\lambda_1\lambda_2(1-\rho^2)}}.
\end{aligned}
\tag{5.15}
$$

We will consider a static randomization in the variance parameter v. In particular, we consider $\mathcal{V} \sim G(\theta, 1)$ and $\mathcal{V} \sim IG(\theta, 1)$. We set $\lambda = 1$ here so that we can specify the randomized variance $\mathcal{V}_j$ of the j^{th} asset price process $\{S_t^{\mathcal{V}_j}\}_{t\geqslant 0}$ to be either $G(\theta, \lambda_j)$ or $IG(\theta, \lambda_j)$. We can use the integral identity in Prudnikov et al within (4.28) to extend our analytical expressions for the one-dimensional transition PDFs in (4.30) and (4.40) to the two-dimensional case. First we will look at the randomized process under the gamma randomization. The (joint) transition PDF for $\{\overrightarrow{X}_t^{G(\theta,\lambda_1,\lambda_2)}\}_{t\geqslant 0} \equiv \{(X_t^{G(\theta,\lambda_1)}, X_t^{G(\theta,\lambda_2)})\}_{t\geqslant 0}$ is:

$$
\begin{aligned}
\widetilde{p}_{G(\theta,\lambda_1,\lambda_2)}(\tau; x_1, x_2) &= \int_0^\infty \frac{1}{\Gamma(\theta)} v^{\theta-1} \mathrm{e}^{-v} \widetilde{p}(\tau; x_1, x_2) dv\\
&= \int_0^\infty \frac{1}{\Gamma(\theta)} v^{\theta-2} \mathrm{e}^{-v} D \exp\left(-\frac{A}{v} - B - Cv\right) dv\\
&= \frac{D\mathrm{e}^{-B}}{\Gamma(\theta)} \left(\frac{A}{C+1}\right)^{\frac{\theta}{2}-\frac{1}{2}} K_{\theta-1}\left(2\sqrt{A(C+1)}\right).
\end{aligned}
\tag{5.16}
$$

Similarly, the transition PDF for $\{\overrightarrow{X}_t^{IG(\theta,\lambda_1,\lambda_2)}\}_{t\geqslant 0}$ is:

$$
\begin{aligned}
\widetilde{p}_{IG(\theta,\lambda_1,\lambda_2)}(\tau; x_1, x_2) &= \int_0^\infty \frac{1}{\Gamma(\theta)} \left(\frac{1}{v}\right)^{\theta+1} \mathrm{e}^{-\frac{1}{v}} \widetilde{p}(\tau; x_1, x_2) dv\\
&= \int_0^\infty \frac{1}{\Gamma(\theta)} w^{\theta} \mathrm{e}^{-w} D \exp\left(-Aw - B - \frac{C}{w}\right) dw\\
&= \frac{D\mathrm{e}^{-B}}{\Gamma(\theta)} \left(\frac{C}{A+1}\right)^{\frac{\theta}{2}+\frac{1}{2}} K_{\theta+1}\left(2\sqrt{C(A+1)}\right),
\end{aligned}
\tag{5.17}
$$

where A, B, C, D are given in (5.15).

Consider any standard European options with payoff function $\Lambda(S_1, S_2)$, where S_1, S_2 are the spot variables (at time $t < T$), at maturity time $T > 0$. The no-arbitrage pricing function, $V(\tau, S_1, S_2)$, in the time-to-maturity $\tau > 0$ satisfies the two-dimensional BSPDE:

$$\frac{\partial V}{\partial \tau} = \mathcal{G}_{S_1,S_2} V - rV, \tag{5.18}$$

where

$$\mathcal{G}_{S_1,S_2} := \frac{1}{2}\sum_{j=1}^{2}\left(\lambda_j v S_j^2 \frac{\partial^2}{\partial S_j^2} + (r - q_j) S_j \frac{\partial}{\partial S_j}\right) + \rho v \sqrt{\lambda_1 \lambda_2} S_1 S_2 \frac{\partial}{\partial S_1 \partial S_2}. \tag{5.19}$$

We now define

$$Y_t := \frac{S_t^{(1)}}{S_t^{(2)}}; \qquad t \geqslant 0. \tag{5.20}$$

By Feymann-Kac Theorem, the process $\{Y_t\}_{t\geqslant 0}$ has generator:[8]

$$\mathcal{G}_y^{(Y)} \equiv \frac{1}{2}\lambda_y v y^2 \frac{\partial}{\partial y^2} + (q_2 - q_1) y \frac{\partial}{\partial y}, \tag{5.21}$$

where

$$y = \frac{S_1}{S_2}, \quad \lambda_y = \lambda_1 + \lambda_2 - 2\rho\sqrt{\lambda_1 \lambda_2}. \tag{5.22}$$

We wish to consider payoffs having a symmetry. In particular, consider a payoff of the form (e.g., an exchange option):

$$\Lambda(S_1, S_2) = (aS_1 - bS_2)^+ = aS_2\,(y - c)^+; \qquad a, b > 0, c = \frac{b}{a}, \tag{5.23}$$

where $y = \frac{S_1}{S_2}$ is an effective spot price variable. The no-arbitrage price of the exchange option can be obtained by setting $V(\tau; S_1, S_2) = S_2 f(\tau, y)$, where $f(\tau, y)$ satisfies an effective one-dimensional BSPDE in (5.21) with effective discount rate q_2 and effective dividend rate q_1, i.e.,

$$\frac{\partial f}{\partial \tau} = \mathcal{G}_y^{(Y)} f - q_2 f, \tag{5.24}$$

[8] See (13.78) in Campolieti and Makarov [10].

subject to $\lim_{\tau \searrow 0} f(\tau, y) = \phi(y) = a(y-c)^+$. By Feymann-Kac Theorem, we have

$$\begin{aligned} f(\tau, y) =& \mathrm{e}^{-q_2 \tau} \widetilde{\mathbb{E}}_{t,y} \left[a \left(Y_T - c \right)^+ \right] \\ =& a C_{BS} \left(\tau, y; c, q_2, q_1 \right) \\ =& a \mathrm{e}^{-q_1 \tau} C_{BS} \left(\tau, y; c, q_2 - q_1 \right), \end{aligned} \tag{5.25}$$

where we used the symmetry:

$$V_{BS}(\tau, S; r, q) = \mathrm{e}^{-q\tau} V_{BS}(\tau, s; r-q, 0). \tag{5.26}$$

Then, by randomization in (5.25) we get

$$V_{\mathcal{V}}(\tau, S_1, S_2) = a S_2 \mathrm{e}^{-q_1 \tau} C_{\mathcal{V}}(\tau, y; c, q_2 - q_1) = a S_1 \mathrm{e}^{-q_1 \tau} \frac{C_{\mathcal{V}}(\tau, y; c, q_2 - q_1)}{y}. \tag{5.27}$$

Since we have expressions for $\frac{C_{\mathcal{V}}(\tau, y; c, q_2 - q_1)}{y}$ in analytically closed forms in Section 4.5, we can obtain the following explicit formulas for $V_{\mathcal{V}}(\tau, S_1, S_2)$ under $G(n, \lambda_1, \lambda_2)$ and $IG(n, \lambda_1, \lambda_2)$, $n \in \mathbb{N}$:

$$\begin{aligned} \frac{V_{G(n,\lambda_1,\lambda_2)}(\tau, S_1, S_2)}{a \mathrm{e}^{-q_1 \tau} S_1} =& (1 - \mathrm{e}^{-m})^+ + \frac{\sqrt{|m|}}{\sqrt{\pi}} \left(\frac{\lambda_y \tau}{8 + \lambda \tau} \right)^{\frac{1}{4}} \mathrm{e}^{-\frac{m}{2}} \\ & \sum_{k=0}^{n-1} \frac{1}{k!} \left(\frac{2|m|}{\sqrt{\lambda_y \tau} \sqrt{8 + \lambda_y \tau}} \right)^k K_{k+\frac{1}{2}} \left(\frac{|m|}{2} \frac{\sqrt{8 + \lambda_y \tau}}{\sqrt{\lambda_y \tau}} \right), \\ \frac{V_{IG(n,\lambda_1,\lambda_2)}(\tau, S_1, S_2)}{a \mathrm{e}^{-q_1 \tau} S_1} =& 1 - \frac{(m^2 + 2\lambda_y \tau)^{\frac{1}{4}}}{\sqrt{\pi}} \mathrm{e}^{-\frac{m}{2}} \\ & \sum_{k=0}^{n-1} \frac{1}{k!} \left(\frac{\lambda_y \tau}{2\sqrt{m^2 + 2\lambda_y \tau}} \right)^k K_{k-\frac{1}{2}} \left(\frac{\sqrt{m^2 + 2\lambda_y \tau}}{2} \right), \end{aligned} \tag{5.28}$$

where

$$m = \ln \frac{a S_1}{b S_2} + (q_2 - q_1)\tau \tag{5.29}$$

is an effective log-forward moneyness.

5.5 Randomized CEV Models

Recall that the standard CEV (diffusion) process (with variance parameter v and a drift parameter r) $\{S_t\}_{t\geqslant 0}$ obeys the SDE:

$$\frac{dS_t}{S_t} = rdt + \sqrt{v} S_t^{\beta} d\widetilde{W}_t. \tag{5.30}$$

Assume $\beta < 0$ and 0 is a killing boundary. We consider static randomization in $\mathcal{V} \equiv \frac{\Upsilon_{t,T}}{\tau}$. By sending $\Upsilon(t,T) \mapsto v\tau$ in (2.13) the transition PDF for the drifted CEV process is

$$\begin{aligned} \widetilde{p}_{\text{cev}}(\tau; S, y) =& \mathrm{e}^{-r\tau} \frac{(\mathrm{e}^{-r\tau} y)^{-2\beta - \frac{3}{2}} S^{\frac{1}{2}}}{v|\beta|\tau} \exp\left(- \frac{(\mathrm{e}^{-r\tau} y)^{-2\beta} + S^{-2\beta}}{2v\beta^2\tau} \right) \\ & \times I_{\frac{1}{2|\beta|}} \left(\frac{(\mathrm{e}^{-r\tau} y)^{-\beta} S^{-\beta}}{v\beta^2\tau} \right). \end{aligned} \tag{5.31}$$

We will consider randomization in the parameter v. Note that we have the following integral formula in terms of the Gaussian hypergeometric function:

$$\int_0^\infty \frac{1}{v^a} \mathrm{e}^{-\frac{b}{v}} I_r\left(\frac{c}{v}\right) dv = \left(\frac{c}{2}\right)^r \frac{\Gamma(a+r-1)}{\Gamma(1+r)} \frac{{}_2F_1\left(\frac{a+r}{2}, \frac{a+r-1}{2}; 1+r; \frac{c^2}{b^2}\right)}{b^{a+r-1}}. \tag{5.32}$$

We consider $\mathcal{V} \sim IG(\theta, \lambda)$. Then the transition PDF of $\{S_t^{IG}\}_{t\geqslant 0}$ is

$$\widetilde{p}^{\text{cev}}_{IG(\theta,\lambda)}(\tau; S, y) = \frac{\lambda^\theta}{\Gamma(\theta)} \mathrm{e}^{-r\tau} \frac{(\mathrm{e}^{-r\tau} S)^{-2\beta - \frac{3}{2}} S_0^{\frac{1}{2}}}{|\beta|\tau} \int_0^\infty \frac{1}{v^a} \mathrm{e}^{-\frac{b}{v}} I_r\left(\frac{c}{v}\right) dv, \tag{5.33}$$

where

$$\begin{aligned} a &= \theta + 2, & b &= \lambda + \frac{(\mathrm{e}^{-r\tau} y)^{-2\beta} + S^{-2\beta}}{2\beta^2\tau}, \\ c &= \frac{(\mathrm{e}^{-r\tau} y)^{-\beta} S^{-\beta}}{\beta^2\tau}, & r &= \frac{1}{2|\beta|} = |\nu|. \end{aligned} \tag{5.34}$$

Thus,

$$
\begin{aligned}
\widetilde{p}^{\mathrm{cev}}_{IG(\theta,\lambda)}(\tau;S,y) = & \frac{\lambda^\theta}{\Gamma(\theta)} \mathrm{e}^{-r\tau} \frac{(\mathrm{e}^{-r\tau}y)^{-2\beta-\frac{3}{2}} S^{\frac{1}{2}}}{|\beta|\tau} \left(\frac{(\mathrm{e}^{-r\tau}y)^{-\beta} S^{-\beta}}{2\beta^2\tau} \right)^{|\nu|} \\
& \times \left(\frac{2\beta^2\tau}{2\beta^2\lambda\tau + (\mathrm{e}^{-r\tau}y)^{-2\beta} + S^{-2\beta}} \right)^{\theta+|\nu|+1} \frac{\Gamma(\theta+|\nu|+1)}{\Gamma(1+|\nu|)} \\
& \times \ {}_2F_1 \left(\frac{\theta+|\nu|+2}{2}, \frac{\theta+|\nu|+1}{2}; 1+|\nu|; \left(\frac{2(\mathrm{e}^{-r\tau}y)^{-\beta} S^{-\beta}}{2\beta^2\lambda\tau + (\mathrm{e}^{-r\tau}y)^{-2\beta} + S^{-2\beta}} \right)^2 \right) \\
= & \lambda^\theta \mathrm{e}^{-r\tau} \frac{(\mathrm{e}^{-r\tau}y)^{-2\beta-1} S}{|\beta|\tau} \frac{(2\beta^2\tau)^{\theta+1}}{(2\beta^2\lambda\tau + (\mathrm{e}^{-r\tau}y)^{-2\beta} + S^{-2\beta})^{\theta+|\nu|+1}} \frac{\Gamma(\theta+|\nu|+1)}{\Gamma(\theta)\Gamma(1+|\nu|)} \\
& \times \ {}_2F_1 \left(\frac{\theta+|\nu|+2}{2}, \frac{\theta+|\nu|+1}{2}; 1+|\nu|; \left(\frac{2(\mathrm{e}^{-r\tau}y)^{-\beta} S^{-\beta}}{2\beta^2\lambda\tau + (\mathrm{e}^{-r\tau}y)^{-2\beta} + S^{-2\beta}} \right)^2 \right),
\end{aligned}
\tag{5.35}
$$

where $|\nu| = \frac{1}{2|\beta|}$. When $\beta = -1$, (i.e., the asset price process follows an Ornstein–Uhlenbeck process) we have the special elementary case of the Gaussian hypergeometric function:[9]

$$
{}_2F_1 \left(\frac{1}{2} + a, a; \frac{3}{2}; z^2 \right) = \frac{(1+z)^{1-2a} - (1-z)^{1-2a}}{2z(1-2a)}. \tag{5.36}
$$

So the transition PDF in (5.35) becomes

$$
\begin{aligned}
\widetilde{p}^{\mathrm{cev}}_{IG(\theta,\lambda)}(\tau;S,y) = & (2\lambda\tau)^\theta \left(\frac{\Gamma(\theta+\frac{3}{2})}{2\Gamma(\theta)\Gamma(\frac{3}{2})} \right) \\
& \times \left([2\lambda\tau + (\mathrm{e}^{-r\tau}y+S)^2]^{-\theta-\frac{1}{2}} - [2\lambda\tau + (\mathrm{e}^{-r\tau}y-S)^2]^{-\theta-\frac{1}{2}} \right).
\end{aligned}
\tag{5.37}
$$

We can see from Figures 5.2 and 5.3 that the randomized CEV processes exhibits non-symmetric smiles as opposed to symmetric smiles observed from the randomized GBM processes. The CEV process under the gamma randomization have sharp kinks at-the-money, whereas the CEV process under the inverse gamma randomization have smooth BS implied volatility against the strikes. Hence, the randomized CEV model with inverse randomization may be useful for model calibrations as each BS implied volatility exhibits an asymmetric and U-shaped smile.

[9] See 15.1.10 in Abramowitz and Stegun [1].

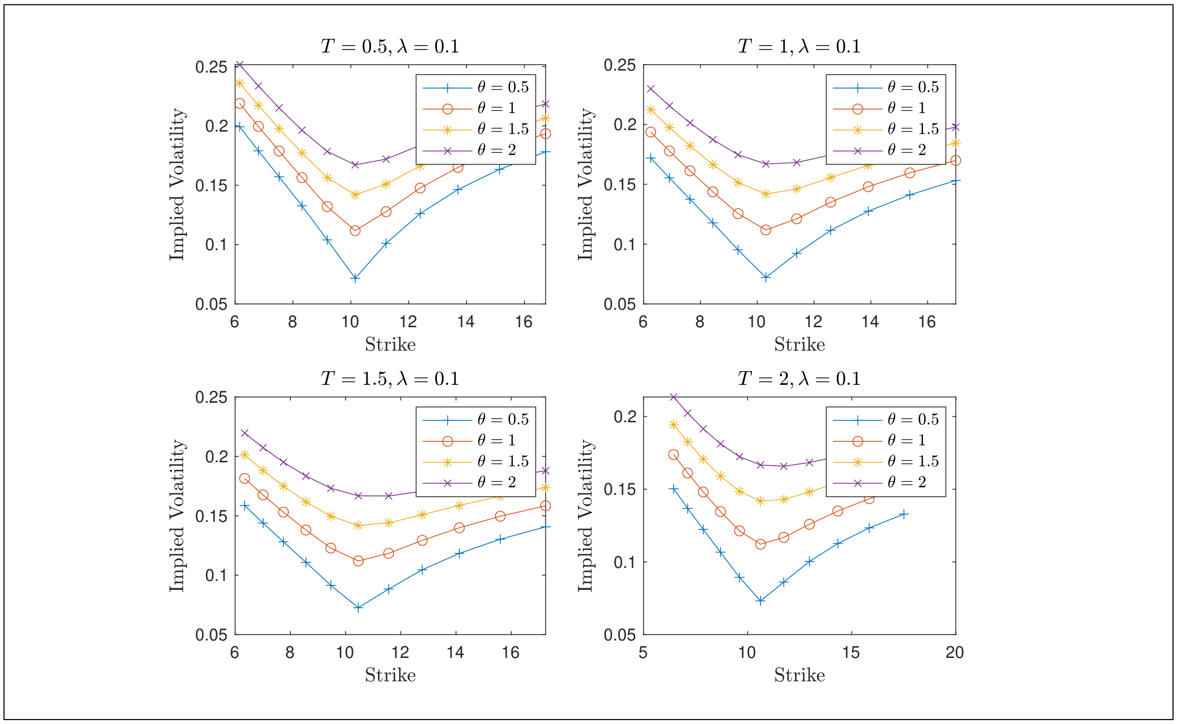

Figure 5.2: BS implied volatility of a European vanilla call option under the gamma randomization.

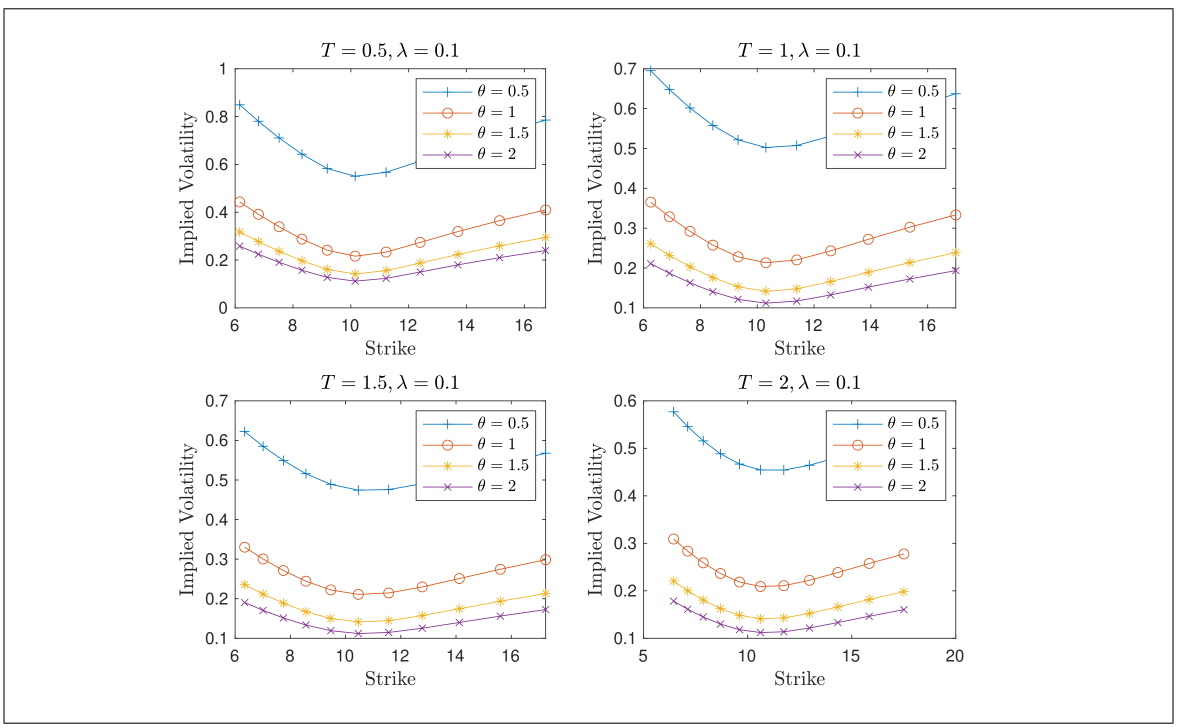

Figure 5.3: BS implied volatility of a European vanilla call option under the inverse gamma randomization.

Chapter 6

Summary and Future Work

6.1 Summary

In this thesis, we constructed the randomized GBM processes under the gamma and the inverse gamma randomization, namely the randomized G and IG processes. The European-style option prices under the new processes exhibit symmetric smiles in the log-forward moneyness and admit simple closed-form analytical expressions for European-style option prices. Surprisingly, the pricing formulas presented in this thesis are even simpler than the classical GBM model as they are expressed as elementary analytical functions. The option prices were also obtained numerically in an efficient manner since they only involve one-dimensional integrals of complementary error functions w.r.t. the variable of integration.

In Chapter 2, we briefly introduced the CEV model. In Section 2.1 we provided the pricing formula for a European vanilla call option. In Section 2.2, we stated the alternative pricing formula which can be extended to the SABR model.

In Chapter 3, we stated some main facts about the SABR model. In Section 3.1, we stated the well-known Hagan et al. formula for the approximate implied BS volatility, and we showed that it works well for European options with small times to maturity. In Section 3.2 we considered pricing European vanilla call options in the zero correlation case, with derivations given in Appendix A. It also provides the Antonov et al. formula by mappping the parameters in the general correlation case to the zero correlation one. In Section 3.3, we performed a numerical experiment which showed that both formulas work well for small times to maturity. For large times to maturity, the accuracy of the Hagan et al. formula worsens, but the Antonov et al. formula retains good accuracy.

In Chapter 4, we presented our main work in the proposed randomization models. In Section 4.3, we derived the transition (marginal) PDF for the randomized G and IG processes. We observed that both processes had thicker tails than the GBM process, and the randomized IG process had heaviest tails among the three. In Section 4.4, we investigated the risk-neutral probability which was later used in pricing European-style options under the new models. In Section 4.5, we obtained explicit pricing formulas for European vanilla call options with integer-valued shape parameter, as well as ATMF option prices with real-valued shape parameter. In Section 4.6, we derived analytical expressions for the greeks of European vanilla call options under volatility randomization, and plotted the greeks as a function of strike and time to maturity. We also made comparisons to the greeks for the classical GBM model. In Section 4.7, we showed that the BS implied volatility under the gamma and the inverse gamma randomization exhibit symmetric smiles in the log-forward moneyness. In Section 4.8 we calibrated the randomized GBM models and the SABR model to the actual market data set from Coca Cola. We found that the inverse gamma randomization fitted well especially for small maturity times, and fitted quite decently when calibrated across all maturity times. The SABR model fitted to the market data almost perfectly when calibrated at a single maturity time, but the the model fails miserably when calibrated across all maturity times. In Section 4.9, we tested the robustness of the parameters, and observed that they were robust.

In Chapter 5, we provided extensions to (1) the transition PDFs with killing, (2) the multi-asset pricing models with perfectly correlated volatility randomization, and (3) the randomized CEV models. In Section 5.1, we observed that the transition PDFs with killing admit analytically closed-form expressions under the gamma and the inverse gamma randomization. The CDFs of the first hitting times were derived in Section 5.2 and 5.3. In Section 5.4, We built the randomization framework in a two-asset economy, and derived closed-form expressions for a European-style exchange option. In Section 5.5, we briefly introduced the randomized CEV models, which exhibit skew smiles and admit closed-form solutions for European vanilla call option prices under the inverse gamma randomization which were expressed in terms of the Gaussian hypergeometric functions.

6.2 Future Work

An obvious disadvantage of our new models is that the models assume zero correlation between the asset price and its volatility as empirical work suggests that they must be negatively correlated. One feasible solution might be to employ copula methods in the models which can introduce dependencies between the asset price process and its volatility.

We also make use of the use of the transition PDFs with killing and FHT to exotic option pricing of barrier and lookback options under the randomized models.

We would like to further extend the multi-asset pricing model with perfectly correlated volatility randomization in Section 5.4 to the general correlated volatility randomization. We might employ copula methods in the model to price options such as exchange options.

We may extend to more general solvable diffusion models such as hypergeometric diffusion models. Once we have constructed the randomized models, we may also consider efficient algorithms for numerical integrations. This includes the randomized CEV process under the inverse gamma randomization whose integrand involves the Gaussian hypergeometric functions.

Bibliography

[1] M. Abramowitz and I. A. Stegun, *Handbook of mathematical functions with formulas, graphs, and mathematical tables*. US Government printing office, 1948, vol. 55.

[2] C. Albanese, G. Campolieti, P. Carr, and A. Lipton, "Black-scholes goes hypergeometric," *RISK-LONDON-RISK MAGAZINE LIMITED-*, vol. 14, no. 12, pp. 99–103, 2001.

[3] A. Antonov, M. Konikov, and M. Spector, "Sabr spreads its wings," *Risk*, vol. 26, no. 8, p. 58, 2013.

[4] A. Antonov, M. Konikov, D. Rufino, and M. Spector, "Exact solution to cev model with uncorrelated stochastic volatility," *Available at SSRN 2386731*, 2014.

[5] A. Antonov, M. Konikov, and M. Spector, *Modern SABR analytics: formulas and insights for quants, former physicists and mathematicians*. Springer, 2019.

[6] A. Antonov and M. Spector, "Advanced analytics for the sabr model," *Available at SSRN 2026350*, 2012.

[7] F. Black and M. Scholes, "The pricing of options and corporate liabilities," *Journal of political economy*, vol. 81, no. 3, pp. 637–654, 1973.

[8] A. N. Borodin and P. Salminen, *Handbook of Brownian motion-facts and formulae*. Birkhäuser, 2012.

[9] G. Campolieti and R. N. Makarov, "On properties of analytically solvable families of local volatility diffusion models," *Mathematical Finance: An International Journal of Mathematics, Statistics and Financial Economics*, vol. 22, no. 3, pp. 488–518, 2012.

[10] ——, *Financial mathematics: a comprehensive treatment*. CRC Press, 2016.

[11] P. P. Carr and R. A. Jarrow, "The stop-loss start-gain paradox and option valuation: A new decomposition into intrinsic and time value," *The review of financial studies*, vol. 3, no. 3, pp. 469–492, 1990.

[12] T. Darsinos and S. Satchell, "Bayesian analysis of the black-scholes option price," in *Forecasting expected returns in the financial markets*, Elsevier, 2007, pp. 117–150.

[13] P. S. Hagan, D. Kumar, A. S. Lesniewski, and D. E. Woodward, "Managing smile risk," *The Best of Wilmott*, vol. 1, pp. 249–296, 2002.

[14] S. L. Heston, "A closed-form solution for options with stochastic volatility with applications to bond and currency options," *The review of financial studies*, vol. 6, no. 2, pp. 327–343, 1993.

[15] J. D. MacBeth and L. J. Merville, "An empirical examination of the black-scholes call option pricing model," *The journal of finance*, vol. 34, no. 5, pp. 1173–1186, 1979.

[16] H. Matsumoto, M. Yor, *et al.*, "Exponential functionals of brownian motion, i: Probability laws at fixed time," *Probability surveys*, vol. 2, pp. 312–347, 2005.

[17] A. P. Prudnikov, I. A. Brychkov, and O. I. Marichev, *Integrals and series: special functions*. CRC Press, 1986, vol. 2.

[18] E. Renault and N. Touzi, "Option hedging and implied volatilities in a stochastic volatility model 1," *Mathematical Finance*, vol. 6, no. 3, pp. 279–302, 1996.

[19] M. Rubinstein, "Nonparametric tests of alternative option pricing models using all reported trades and quotes on the 30 most active cboe option classes from august 23, 1976 through august 31, 1978," *The Journal of Finance*, vol. 40, no. 2, pp. 455–480, 1985.

[20] G. West, "Calibration of the sabr model in illiquid markets," *Applied Mathematical Finance*, vol. 12, no. 4, pp. 371–385, 2005.

[21] Q. Wu, "Analytical solutions of the sabr stochastic volatility model," PhD thesis, Columbia University, 2012.

[22] ——, "Series expansion of the sabr joint density," *Mathematical Finance: An International Journal of Mathematics, Statistics and Financial Economics*, vol. 22, no. 2, pp. 310–345, 2012.

Part III

Appendix

Appendix A

Derivation of the Pricing Formula under the SABR Model in the Zero correlation Case

Recall that the drifted SABR model is a two-factor model governed by two SDEs (assuming the risk-neutral probability measure $\widetilde{\mathbb{P}}$ exists):

$$\begin{cases} \dfrac{dS_t}{S_t} = rdt + \sigma_t S_t^{\beta} dW_t^{(1)}; \quad S_0 > 0, \\ \dfrac{d\sigma_t}{\sigma_t} = \alpha dW_t^{(2)}; \qquad\qquad\quad \sigma_0 > 0, \\ dW_t^{(1)} dW_t^{(2)} = 0, \end{cases} \tag{A.1}$$

Note that the stochastic time change is the integrated squared GBM process given $\sigma_t = \sigma$ which was defined by:

$$\Upsilon_\tau(\sigma) \equiv \int_0^\tau \mathrm{e}^{\beta r s} \sigma_{t+s}^2 ds. \tag{A.2}$$

Then, the joint distribution of $(\Upsilon_\tau(\sigma), \sigma_T)$ given $\sigma_t = \sigma$ is:

$$
\begin{aligned}
(\Upsilon_\tau(\sigma), \sigma_T) &\overset{d}{=} \left(\sigma^2 \int_0^\tau \mathrm{e}^{(2\beta r - \alpha^2)t + 2Z_{\alpha^2 t}} dt, \quad \sigma \mathrm{e}^{(\beta r - \frac{1}{2}\alpha^2)\tau + Z_{\alpha^2\tau}} \right). \\
&= \left(\frac{\sigma^2}{\alpha^2} \int_0^{\alpha^2\tau} \mathrm{e}^{(2\beta r/\alpha^2 - 1)t + 2Z_t} dt, \quad \sigma \mathrm{e}^{(\beta r - \frac{1}{2}\alpha^2)\tau + Z_{\alpha^2\tau}} \right) \\
&= \left(\frac{\sigma^2}{\alpha^2} A_{\alpha^2\tau}^{(\beta r/\alpha^2 - \frac{1}{2})}, \quad \sigma \exp\left(B_{\alpha^2\tau}^{(\beta r/\alpha^2 - \frac{1}{2})} \right) \right),
\end{aligned}
\tag{A.3}
$$

where

$$
A_t^{(\mu)} = \int_0^t \exp\left(2B_s^{(\mu)}\right) ds, \quad B_t^{(\mu)} = B_t + \mu t. \tag{A.4}
$$

From Matsumoto and Yor [16], we have

$$
\mathbb{E}\left[\exp\left(-\frac{\lambda}{A_t^{(\mu)}} \right) | B_t^{(\mu)} = x \right] = \exp\left(-\frac{\phi_x(\lambda)^2 - x^2}{2t} \right), \tag{A.5}
$$

where

$$
\phi_x(\lambda) = \cosh^{-1}\left(\lambda \mathrm{e}^{-x} + \cosh x \right). \tag{A.6}
$$

Integrating over the density of $B_t^{(\mu)}$, we have

$$
\mathbb{E}\left[\exp\left(-\frac{\lambda}{A_t^{(\mu)}} \right) \right] = \frac{\mathrm{e}^{-\frac{\mu^2 t}{2}}}{\sqrt{2\pi t}} \int_{-\infty}^{\infty} \exp\left(-\frac{\phi_x(\lambda)^2 - 2\mu t x}{2t} \right) dx, \tag{A.7}
$$

where $\mu = \frac{\beta r}{\alpha^2} - \frac{1}{2}$ and $t = \alpha^2 \tau$. So

$$
\mathbb{E}\left[\exp\left(-\frac{\lambda}{\Upsilon_\tau(\sigma)} \right) \right] = \frac{\mathrm{e}^{-\frac{\mu^2\alpha^2\tau}{2}}}{\sqrt{2\pi\alpha^2\tau}} \int_{-\infty}^{\infty} \exp\left(-\frac{\phi_x\left(\alpha^2\lambda/\sigma^2\right)^2 - 2\mu\alpha^2\tau x}{2\alpha^2\tau} \right) dx. \tag{A.8}
$$

Observe that

$$
u = \phi_x\left(\frac{\alpha^2\lambda}{\sigma^2} \right) = \cosh^{-1}\left(\frac{\alpha^2\lambda}{\sigma^2} \mathrm{e}^{-x} + \cosh(x) \right) \tag{A.9}
$$

satisfies

$$
\begin{aligned}
\cosh(u) &= \frac{\alpha^2\lambda}{\sigma^2}\mathrm{e}^{-x} + \cosh(x) \\
&= \frac{\alpha^2\lambda}{\sigma^2}\mathrm{e}^{-x} + \frac{\mathrm{e}^x + \mathrm{e}^{-x}}{2} = \frac{\mathrm{e}^x}{2} + \left(\frac{1}{2} + \frac{\alpha^2\lambda}{\sigma^2} \right)\mathrm{e}^{-x} \\
&= \frac{\mathrm{e}^x}{2} + \frac{1}{2}\left(1 + \frac{\alpha^2\lambda}{\sigma^2} \right)\mathrm{e}^{-x} \\
&= \frac{1}{2}\mathrm{e}^x + \frac{1}{2}\left(1 + \frac{2\alpha^2\lambda}{\sigma^2} \right)\mathrm{e}^{-x}
\end{aligned}
\tag{A.10}
$$

Let $x = v + \frac{1}{2}\ln\left(1+\frac{2\alpha^2\lambda}{\sigma^2}\right)$, then

$$\begin{aligned}
\cosh(u) &= \frac{1}{2}\mathrm{e}^{v+\frac{1}{2}\ln\left(1+\frac{2\alpha^2\lambda}{\sigma^2}\right)} + \frac{1}{2}\left(1+\frac{2\alpha^2\lambda}{\sigma^2}\right)\mathrm{e}^{-v-\frac{1}{2}\ln\left(1+\frac{2\alpha^2\lambda}{\sigma^2}\right)} \\
&= \frac{1}{2}\mathrm{e}^{v}\left(1+\frac{2\alpha^2\lambda}{\sigma^2}\right)^{\frac{1}{2}} + \frac{1}{2}\left(1+\frac{2\alpha^2\lambda}{\sigma^2}\right)\mathrm{e}^{-v}\left(1+\frac{2\alpha^2\lambda}{\sigma^2}\right)^{-\frac{1}{2}} \qquad \text{(A.11)} \\
&= \left(1+\frac{2\alpha^2\lambda}{\sigma^2}\right)^{\frac{1}{2}}\left(\frac{1}{2}\mathrm{e}^{v}+\frac{1}{2}\mathrm{e}^{-v}\right) = \left(1+\frac{2\alpha^2\lambda}{\sigma^2}\right)^{\frac{1}{2}}\cosh(v).
\end{aligned}$$

Thus, $u \equiv u(v)$ and

$$\begin{aligned}
&\mathbb{E}\left[\exp\left(-\frac{\lambda}{\Upsilon_\tau(\sigma)}\right)\right] = \frac{\mathrm{e}^{-\frac{\mu^2\alpha^2\tau}{2}}}{\sqrt{2\pi\alpha^2\tau}}\int_{-\infty}^{\infty}\exp\left(-\frac{\phi_x\left(\alpha^2\lambda/\sigma^2\right)^2 - 2\mu\alpha^2\tau x}{2\alpha^2\tau}\right)dx \\
&= \frac{\mathrm{e}^{-\frac{\mu^2\alpha^2\tau}{2}}}{\sqrt{2\pi\alpha^2\tau}}\int_{-\infty}^{\infty}\exp\left(-\frac{u(v)^2 - 2\mu\alpha^2\tau x}{2\alpha^2\tau}\right)dv \\
&= \frac{\mathrm{e}^{-\frac{\mu^2\alpha^2\tau}{2}}}{\sqrt{2\pi\alpha^2\tau}}\int_{-\infty}^{\infty}\exp\left(-\frac{u(v)^2}{2\alpha^2\tau}\right)\exp\left(\frac{2\mu\alpha^2\tau v}{2\alpha^2\tau}\right)\exp\left(\frac{\mu\alpha^2\tau\ln\left(1+\frac{2\alpha^2\lambda}{\sigma^2}\right)}{2\alpha^2\tau}\right)dv \qquad \text{(A.12)} \\
&= \frac{\mathrm{e}^{-\frac{\mu^2\alpha^2\tau}{2}}}{\sqrt{2\pi\alpha^2\tau}}\int_{-\infty}^{\infty}\exp\left(-\frac{u(v)^2}{2\alpha^2\tau}\right)\mathrm{e}^{\mu v}\exp\left(\frac{\mu}{2}\ln\left(1+\frac{2\alpha^2\lambda}{\sigma^2}\right)\right)dv \\
&= \frac{\mathrm{e}^{-\frac{\mu^2\alpha^2\tau}{2}}}{\sqrt{2\pi\alpha^2\tau}}\int_{-\infty}^{\infty}\exp\left(-\frac{u(v)^2}{2\alpha^2\tau}\right)\mathrm{e}^{\mu v}\sqrt{\left(1+\frac{2\alpha^2\lambda}{\sigma^2}\right)^{\mu}}dv.
\end{aligned}$$

By applying the symmetry about the $v-$axis and $u(v)$ is an even function, we have

$$\mathbb{E}\left[\exp\left(-\frac{\lambda}{\Upsilon_\tau(\sigma)}\right)\right] = \frac{2\mathrm{e}^{-\frac{\mu^2\alpha^2\tau}{2}}}{\sqrt{2\pi\alpha^2\tau}}\sqrt{\left(1+\frac{2\alpha^2\lambda}{\sigma^2}\right)^{\mu}}\int_{0}^{\infty}\exp\left(-\frac{u(v)^2}{2\alpha^2\tau}\right)\cosh(|\mu|v)dv. \qquad \text{(A.13)}$$

By substituting (A.11) into (A.13), we have

$$\cosh(|\mu|v)dv = \frac{1}{|\mu|}d(\sinh(|\mu|v)) = \frac{1}{|\mu|}d\left(\sinh\left(|\mu|\cosh^{-1}\left(\frac{\cosh(u)}{\sqrt{1+\frac{2\alpha^2\lambda}{\sigma^2}}}\right)\right)\right). \qquad \text{(A.14)}$$

By plugging (A.14) into (A.12), we obtain

$$
\begin{aligned}
\mathbb{E}\left[\exp\left(-\frac{\lambda}{\Upsilon_\tau(\sigma)}\right)\right] &= \frac{2\mathrm{e}^{-\frac{\mu^2\alpha^2\tau}{2}}}{\sqrt{2\pi\alpha^2\tau}}\sqrt{\left(1+\frac{2\alpha^2\lambda}{\sigma^2}\right)^{\mu}} \\
&\times\int_s^\infty \exp\left(-\frac{u^2}{2\alpha^2\tau}\right)\frac{1}{|\mu|}d\left(\sinh\left(|\mu|\cosh^{-1}\left(\frac{\cosh(u)}{\sqrt{1+\frac{2\alpha^2\lambda}{\sigma^2}}}\right)\right)\right) \\
&= \frac{2\mathrm{e}^{-\frac{\mu^2\alpha^2\tau}{2}}}{|\mu|\sqrt{2\pi\alpha^2\tau}}(1+\frac{2\alpha^2\lambda}{\sigma^2})^{\frac{\mu}{2}} \qquad\qquad (A.15) \\
&\times\int_s^\infty \frac{u}{\alpha^2\tau}\exp\left(-\frac{u^2}{2\alpha^2\tau}\right)\frac{1}{|\mu|}\left(\sinh\left(|\mu|\cosh^{-1}\left(\frac{\cosh(u)}{\sqrt{1+\frac{2\alpha^2\lambda}{\sigma^2}}}\right)\right)\right)du \\
&= \frac{G(\tau,s)}{\sqrt{1+\frac{2\alpha^2\lambda}{\sigma^2}}} = \frac{G(\tau,s)}{\cosh(s)},
\end{aligned}
$$

where

$$
\begin{aligned}
G(\tau,s) =& \frac{2e^{-\frac{\mu^2\alpha^2\tau}{2}}}{\mu^2\sqrt{2\pi\alpha^2\tau}}\left(1+\frac{2\alpha^2\lambda}{\sigma^2}\right)^{\frac{1+\mu}{2}} \\
&\times\int_s^\infty \frac{u}{\alpha^2\tau}\exp\left(-\frac{u^2}{2\alpha^2\tau}\right)\sinh\left[|\mu|\cosh^{-1}\left(\frac{\cosh u}{\cosh s}\right)\right]du, \\
\mu =& \frac{\beta r}{\alpha^2}-\frac{1}{2}, \qquad\qquad (A.16) \\
s =& \cosh^{-1}\left(\sqrt{1+\frac{2\alpha^2\lambda}{\sigma^2}}\right) = \sinh^{-1}\left(\sqrt{\frac{2\alpha^2\lambda}{\sigma^2}}\right).
\end{aligned}
$$

For a special case when $r = 0$, then the kernel function G in (A.16) simplifies to:

$$
G(\tau,s) = \frac{2\mathrm{e}^{-\frac{\alpha^2\tau}{8}}}{\sqrt{\pi(\alpha^2\tau)^3}}\int_s^\infty u\mathrm{e}^{-\frac{u^2}{2\alpha^2\tau}}\sqrt{\cosh(u)-\cosh(s)}du. \qquad (A.17)
$$

The reader can consult Antonov et al. [4] for more details.

Appendix B

Exact Pricing Formulas for ATMF Options under the Randomized GBM Models

Recall that the price of a European vanilla call option under the GBM model, with variance randomized according to the PDF $f_{\mathcal{V}}$, can be expressed as:

$$\begin{aligned}\widehat{C}_{\mathcal{V}}(\tau, m) \equiv \frac{C_{\mathcal{V}}(\tau, S; K, r)}{S} &= \int_0^\infty \frac{C_{BS}(\tau, S; K, r, v)}{S} f_{\mathcal{V}}(v) dv \\ &= \int_0^\infty \mathcal{N}\left(\frac{m + \frac{1}{2}v\tau}{\sqrt{v\tau}}\right) f_{\mathcal{V}}(v) dv - \mathrm{e}^{-m} \int_0^\infty \mathcal{N}\left(\frac{m - \frac{1}{2}v\tau}{\sqrt{v\tau}}\right) f_{\mathcal{V}}(v) dv,\end{aligned} \tag{B.1}$$

where $\mathcal{N}(\cdot)$ is the standard normal CDF. We state the following identity that

$$\mathcal{N}(x) - \mathcal{N}(-x) = \operatorname{erf}\left(\frac{x}{\sqrt{2}}\right) \tag{B.2}$$

where erf$(\cdot)$ is the error function. For ATMF call options (i.e., $m = \ln \frac{S}{K} + rt = 0$), we can reformulate (B.1) as:

$$\begin{aligned}\widehat{C}_{\mathcal{V}}(\tau, 0) &= \int_0^\infty \mathcal{N}\left(\frac{\sqrt{v\tau}}{2}\right) f_{\mathcal{V}}(v)dv - \int_0^\infty \mathcal{N}\left(-\frac{\sqrt{v\tau}}{2}\right) f_{\mathcal{V}}(v)dv \\ &= \int_0^\infty \operatorname{erf}\left(\frac{\sqrt{v\tau}}{2\sqrt{2}}\right) f_{\mathcal{V}}(v)dv\end{aligned} \tag{B.3}$$

We can use (B.3) to derive the pricing formulas for ATMF options explicitly under the gamma and inverse gamma randomization for shape parameter $\theta \in \mathbb{R}_+$.

Proposition B.1. *Assume $\mathcal{V}$ is the gamma r.v. with pdf:*

$$f_{\mathcal{V}}(v) \equiv f_{G(\theta,\lambda)}(v) = \frac{1}{\lambda^\theta \Gamma(\theta)} v^{\theta-1} e^{-\frac{v}{\lambda}}; \quad \theta, \lambda > 0, \tag{B.4}$$

then the price of an ATMF European vanilla call option under the gamma randomization is:

$$\widehat{C}_{G(\theta,\lambda)}(\tau, 0) = \left[1 - \frac{\Gamma(\theta + \frac{1}{2})}{\sqrt{\pi}\Gamma(\theta+1)} \left(\frac{8}{\lambda\tau}\right)^\theta {}_2F_1(\theta, \theta + \frac{1}{2}; \theta + 1, -\frac{8}{\lambda\tau})\right] \tag{B.5}$$

where ${}_pF_q(\mathbf{a}; \mathbf{b}; z)$ is the generalized hypergeometric function.

Proof. We first make a note that the incomplete gamma function can be expressed in terms of generalized hypergeometric functions. i.e.,

$$\begin{aligned}\gamma(\theta, x) =& \theta^{-1} x^\theta M(\theta, \theta+1, -x), \\ M(a, b, c) =& {}_1F_1(a; b; c).\end{aligned} \tag{B.6}$$

And an integral representation of a generalized hyperbolic function is

$${}_{p+1}F_q\begin{pmatrix} a_0, \dots, a_p & \\ & ; z \\ b_1, \dots, b_q & \end{pmatrix} = \frac{1}{\Gamma(a_0)} \int_0^\infty s^{a_0-1} \mathrm{e}^{-s} {}_pF_q\begin{pmatrix} a_1, \dots, a_p & \\ & ; zs \\ b_1, \dots, b_q & \end{pmatrix} ds. \tag{B.7}$$

From (B.6) and (B.7), we have

$$\begin{aligned}
&\int_0^\infty f_{G(\theta,\lambda)}(v)\,\mathrm{erf}\left(\frac{\sqrt{vt}}{2\sqrt{2}}\right)dv = \int_0^\infty f_{G(\theta,\lambda)}(v)\left[\int_0^{\frac{\sqrt{v\tau}}{2\sqrt{2}}}\frac{2}{\sqrt{\pi}}\mathrm{e}^{-x^2}dx\right]dv\\
=&\int_0^\infty \frac{2}{\sqrt{\pi}}\mathrm{e}^{-x^2}\left[\int_{\frac{8x^2}{\tau}}^\infty f_{G(\theta,\lambda)}(v)dv\right]dx = \frac{2}{\sqrt{\pi}}\int_0^\infty \mathrm{e}^{-x^2}\left[1-\frac{\gamma(\theta,\frac{8x^2}{\lambda\tau})}{\Gamma(\theta)}\right]dx\\
=&1-\frac{2}{\sqrt{\pi}\Gamma(\theta)}\int_0^\infty \gamma\left(\theta,\frac{8x^2}{\lambda\tau}\right)\mathrm{e}^{-x^2}dx\\
=&1-\frac{2}{\sqrt{\pi}\Gamma(\theta)}\left(\frac{8}{\lambda\tau}\right)^\theta\theta^{-1}\int_0^\infty M\left(\theta,\theta+1,-\frac{8x^2}{\lambda\tau}\right)x^{2\theta}\mathrm{e}^{-x^2}dx\\
=&1-\frac{1}{\sqrt{\pi}\Gamma(\theta+1)}\left(\frac{8}{\lambda\tau}\right)^\theta\int_0^\infty {}_1F_1\left(\theta;\theta+1;-\frac{8y}{\lambda\tau}\right)y^{\theta-\frac{1}{2}}\mathrm{e}^{-y}dy\\
=&1-\frac{\Gamma\left(\theta+\frac{1}{2}\right)}{\sqrt{\pi}\Gamma(\theta+1)}\left(\frac{8}{\lambda\tau}\right)^\theta {}_2F_1\left(\theta,\theta+\frac{1}{2};\theta+1;-\frac{8}{\lambda\tau}\right).
\end{aligned} \tag{B.8}$$

Proposition B.2. *Assume $\mathcal{V}$ is the inverse gamma r.v. with pdf:*

$$f_{\mathcal{V}}(v) \equiv f_{IG(\theta,\lambda)}(v) = \frac{\lambda^\theta}{\Gamma(\theta)}\left(\frac{1}{v}\right)^{\theta+1}e^{-\frac{\lambda}{v}};\quad \theta,\lambda>0, \tag{B.9}$$

then the price of an ATMF European vanilla call option under the inverse gamma randomization is:

$$\begin{aligned}
\widehat{C}_{IG(\theta,\lambda)}(\tau,0) =&\frac{\sqrt{\lambda\tau}}{2\sqrt{2\pi}\left(\theta-\frac{1}{2}\right)\Gamma(\theta+1)}\left[2\theta\Gamma\left(\theta+\frac{1}{2}\right){}_1F_2\left(\frac{1}{2};\frac{3}{2},\frac{3}{2}-\theta;\frac{\lambda\tau}{8}\right)\right.\\
&\left.-\left(\frac{\lambda\tau}{8}\right)^{\theta-\frac{1}{2}}\Gamma\left(\frac{3}{2}-\theta\right){}_1F_2\left(\theta;\theta+1,\theta+\frac{1}{2};\frac{\lambda\tau}{8}\right)\right]
\end{aligned} \tag{B.10}$$

Proof. We first make a note of an integral representation of the Kummer function of the first kind

$$M(a,b,c) = \frac{\Gamma(b)}{\Gamma(a)\Gamma(b-a)}\int_0^1 \mathrm{e}^{cu}u^{a-1}(1-u)^{b-a-1}du. \tag{B.11}$$

Then,

$$
\begin{aligned}
&\int_0^\infty f_{IG(\theta,\lambda)}(v)\,\mathrm{erf}\left(\frac{\sqrt{vt}}{2\sqrt{2}}\right)dv = \int_0^\infty f_{IG(\theta,\lambda)}(v)\left[\int_0^{\frac{\sqrt{v\tau}}{2\sqrt{2}}}\frac{2}{\sqrt{\pi}}\mathrm{e}^{-x^2}dx\right]dv\\
=&\int_0^\infty \frac{2}{\sqrt{\pi}}\mathrm{e}^{-x^2}\left[\int_{\frac{8x^2}{\tau}}^\infty f_{IG(\theta,\lambda)}(v)dv\right]dx = \frac{2}{\sqrt{\pi}}\int_0^\infty \mathrm{e}^{-x^2}\left[1-\frac{\Gamma(\theta,\frac{\lambda\tau}{8x^2})}{\Gamma(\theta)}\right]dx\\
=&\frac{2}{\sqrt{\pi}\Gamma(\theta)}\int_0^\infty \gamma\left(\theta,\frac{\lambda\tau}{8x^2}\right)\mathrm{e}^{-x^2}dx\\
=&\frac{2}{\sqrt{\pi}\Gamma(\theta+1)}\left(\frac{\lambda\tau}{8}\right)^\theta\int_0^\infty M\left(\theta,\theta+1,-\frac{\lambda\tau}{8x^2}\right)x^{-2\theta}\mathrm{e}^{-x^2}dx\\
=&\frac{1}{\sqrt{\pi}\Gamma(\theta+1)}\left(\frac{\lambda\tau}{8}\right)^\theta\int_0^\infty {}_1F_1\left(\theta;\theta+1;-\frac{\lambda\tau}{8y}\right)y^{-\theta-\frac{1}{2}}\mathrm{e}^{-y}dy\\
=&\frac{1}{\sqrt{\pi}\Gamma(\theta)}\left(\frac{\lambda\tau}{8}\right)^\theta\int_0^\infty\left[\int_0^1 u^{\theta-1}\exp\left(-\frac{\lambda\tau}{8y}u\right)du\right]y^{-\theta-\frac{1}{2}}\mathrm{e}^{-y}dy\\
=&\frac{1}{\sqrt{\pi}\Gamma(\theta)}\left(\frac{\lambda\tau}{8}\right)^\theta\int_0^1 u^{\theta-1}\left[\int_0^\infty y^{-\theta-\frac{1}{2}}\exp\left(-\frac{\lambda\tau u}{8y}-y\right)dy\right]du\\
=&\frac{1}{\sqrt{\pi}\Gamma(\theta)}\left(\frac{\lambda\tau}{8}\right)^\theta\int_0^1 u^{\theta-1}\left[2\left(\frac{\lambda\tau u}{8}\right)^{\frac{1}{4}-\frac{\theta}{2}}K_{\frac{1}{2}-\theta}\left(2\sqrt{\frac{\lambda\tau u}{8}}\right)\right]du\\
=&\frac{2}{\sqrt{\pi}\Gamma(\theta)}\left(\frac{\lambda\tau}{8}\right)^{\frac{1}{4}+\frac{\theta}{2}}\int_0^1 u^{\frac{\theta}{2}-\frac{3}{4}}K_{\frac{1}{2}-\theta}\left(\sqrt{\frac{\lambda\tau u}{2}}\right)du\\
=&\frac{\sqrt{\pi}}{\cos(\theta\pi)\Gamma(\theta)}\left(\frac{\lambda\tau}{8}\right)^{\frac{1}{4}+\frac{\theta}{2}}\cdot\left[\int_0^1 u^{\frac{\theta}{2}-\frac{3}{4}}\frac{\left(\frac{\lambda\tau u}{2}\right)^{\frac{\theta}{2}-\frac{1}{4}}{}_0F_1(;\theta+\frac{1}{2};\frac{\lambda\tau u}{8})}{2^{\theta-\frac{1}{2}}\Gamma(\theta+\frac{1}{2})}du\right.\\
&\left.-\int_0^1 u^{\frac{\theta}{2}-\frac{3}{4}}\frac{\left(\frac{\lambda\tau u}{2}\right)^{\frac{1}{4}-\frac{\theta}{2}}{}_0F_1(;\frac{3}{2}-\theta;\frac{\lambda\tau u}{8})}{2^{\frac{1}{2}-\theta}\Gamma(\frac{3}{2}-\theta)}du\right]
\end{aligned} \tag{B.12}
$$

The last line in (B.12) came from the fact that modified Bessel functions of the first and second kind can be expressed in terms of generalized hypergeometric functions. i.e.,

$$
\begin{aligned}
I_\theta(x) =&\frac{\left(\frac{x}{2}\right)^\theta}{\Gamma(\theta+1)}{}_0F_1(;\theta+1;\frac{x^2}{4})\\
K_\theta(x) =&\frac{\pi}{2}\frac{I_{-\theta}(x)-I_\theta(x)}{\sin(\theta\pi)}
\end{aligned} \tag{B.13}
$$

Another integral representation of a generalized hyperbolic function is

$$
{}_{p+1}F_{q+1}\begin{pmatrix} a_0,\dots,a_p & \\ & ;z \\ b_0,\dots,b_q & \end{pmatrix} = \frac{\Gamma(b_0)}{\Gamma(a_0)\Gamma(b_0-a_0)}\int_0^\infty s^{a_0-1}(1-s)^{b_0-a_0-1}{}_pF_q\begin{pmatrix} a_1,\dots,a_p & \\ & ;zs \\ b_1,\dots,b_q & \end{pmatrix}ds. \tag{B.14}
$$

From the integral representation in (B.14), we obtain the final expression in (B.10).

Part IV

Numerical Plots

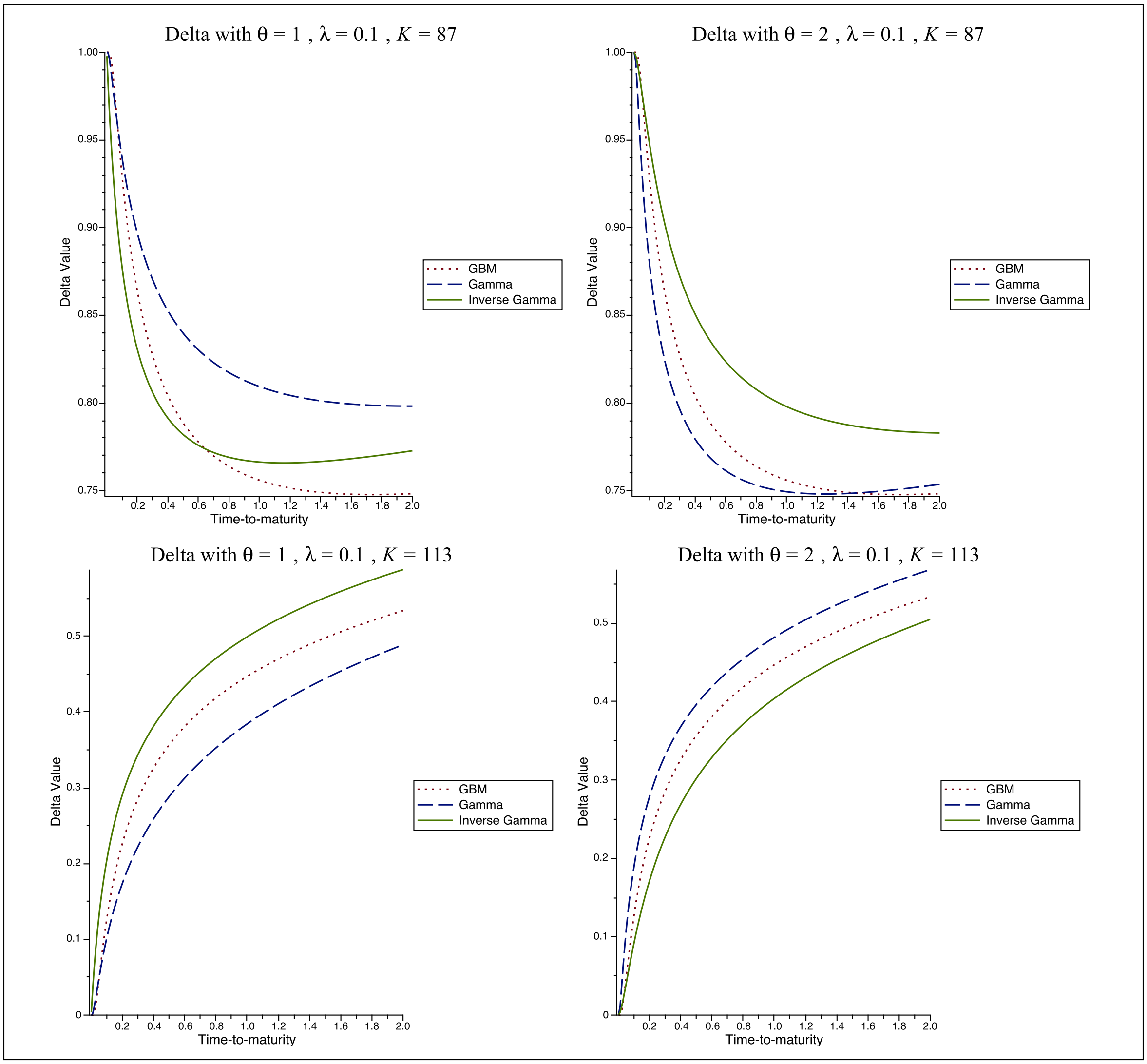

Figure C.1: Plots of the in-the-money call option deltas (top row) and out-of-the-money call option deltas (bottom row), where $S = 100$, $r = 0.03$ and $v = 0.1$ is the variane parameter in the GBM model.

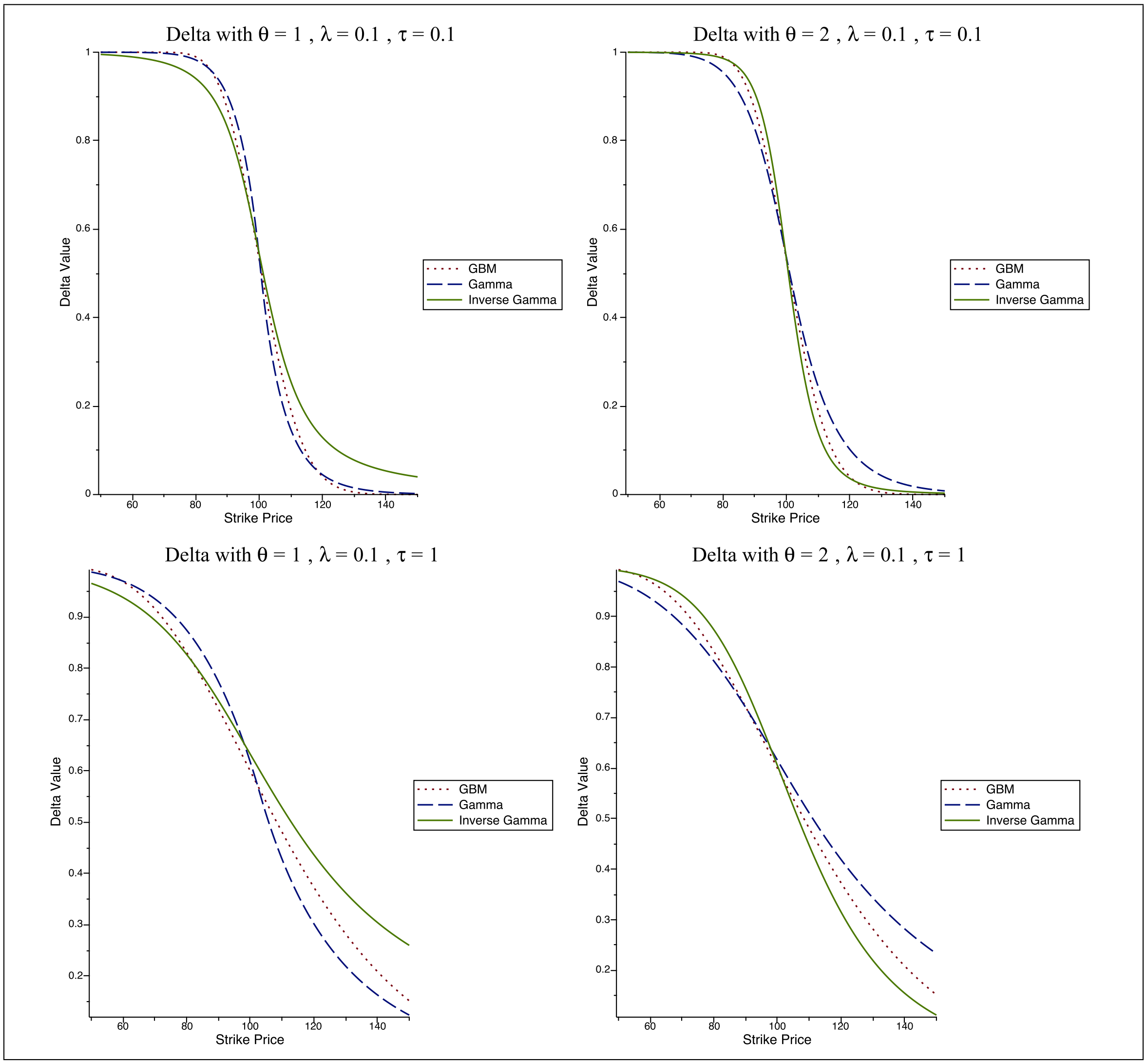

Figure C.2: Plots of the call option deltas for short time-to-maturity (top row) and for long time-to-maturity (bottom row), where $S = 100$, $r = 0.03$ and $v = 0.1$ is the variane parameter in the GBM model.

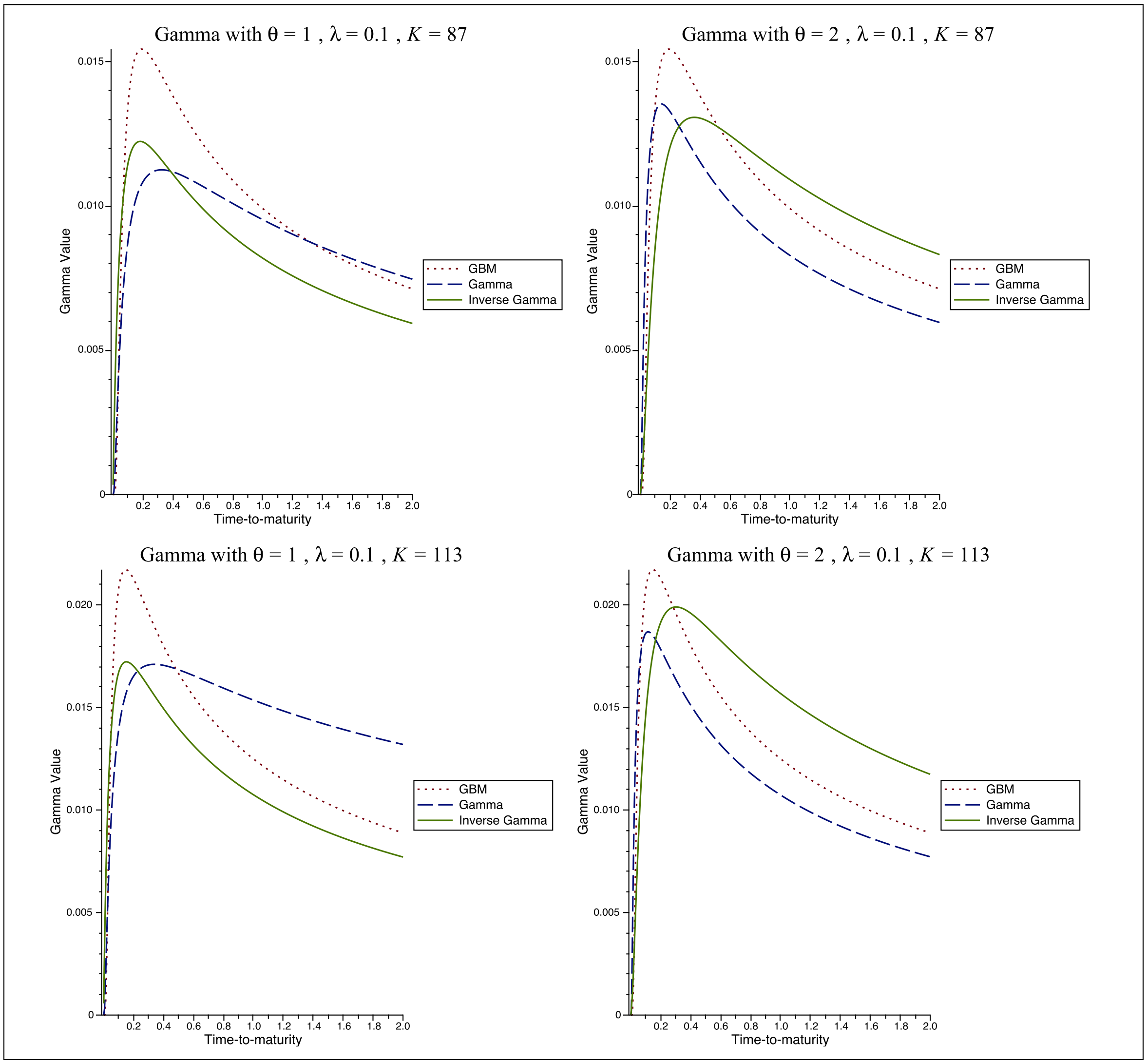

Figure C.3: Plots of the in-the-money call option gammas (top row) and out-of-the-money call option gammas (bottom row), where $S = 100$, $r = 0.03$, $r = 0.03$ and $v = 0.1$ is the variane parameter in the GBM model.

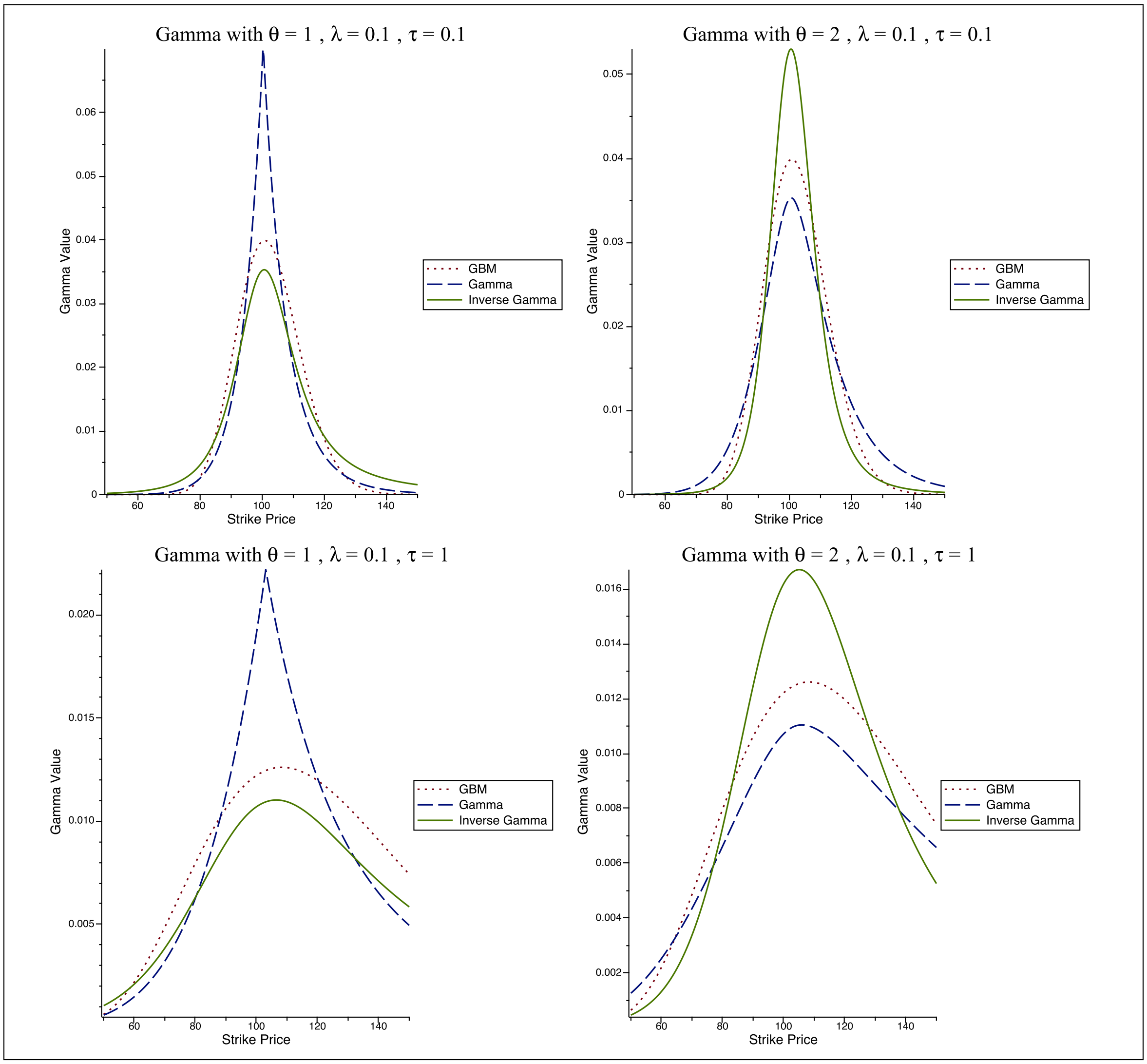

Figure C.4: Plots of the call option gammas for short time-to-maturity (top row) and for long time-to-maturity (bottom row), where $S = 100$, $r = 0.03$ and $v = 0.1$ is the variane parameter in the GBM model.

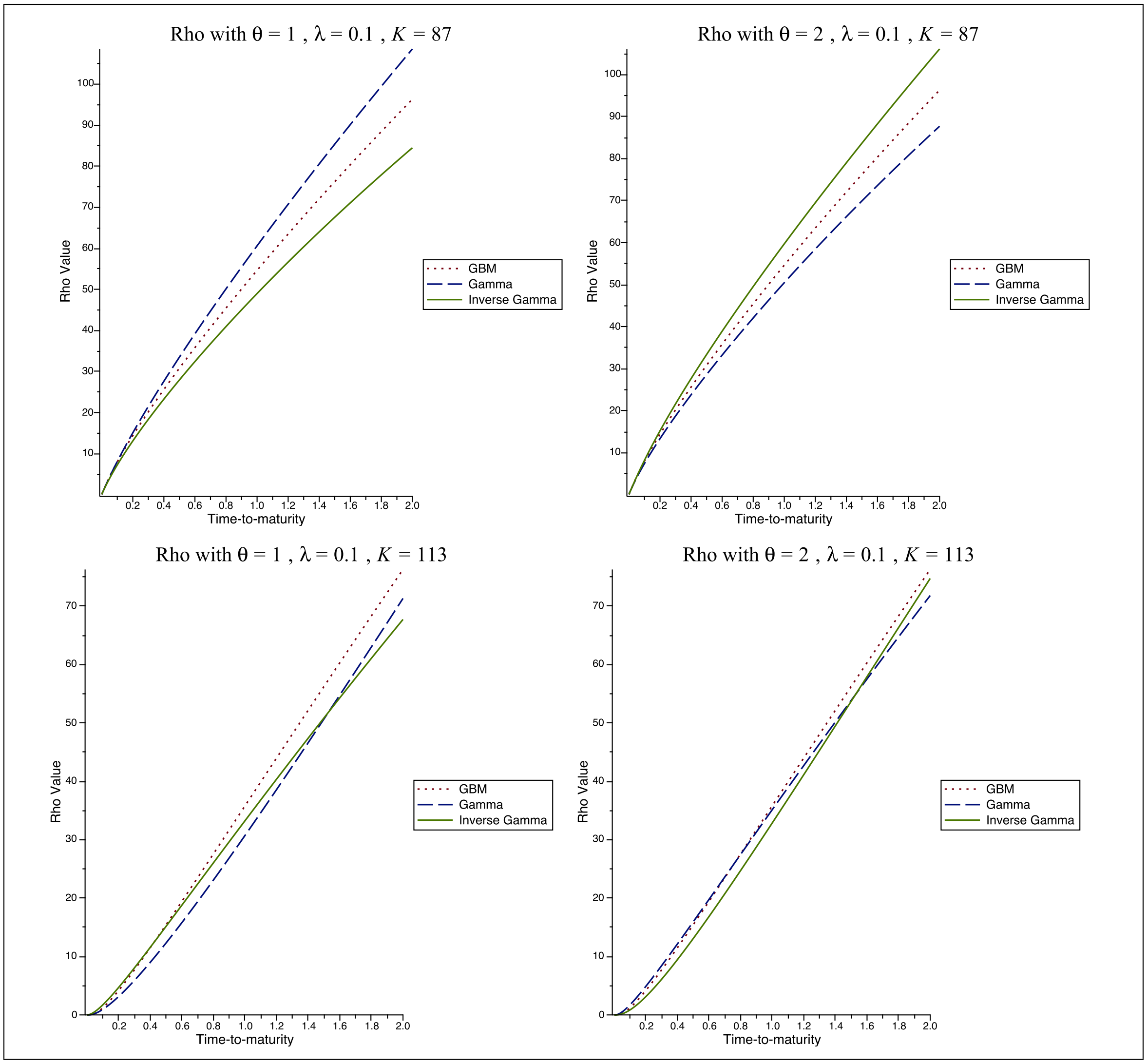

Figure C.5: Plots of the in-the-money call option rhos (top row) and out-of-the-money call option rhos (bottom row), where $S = 100$, $r = 0.03$ and $v = 0.1$ is the variane parameter in the GBM model.

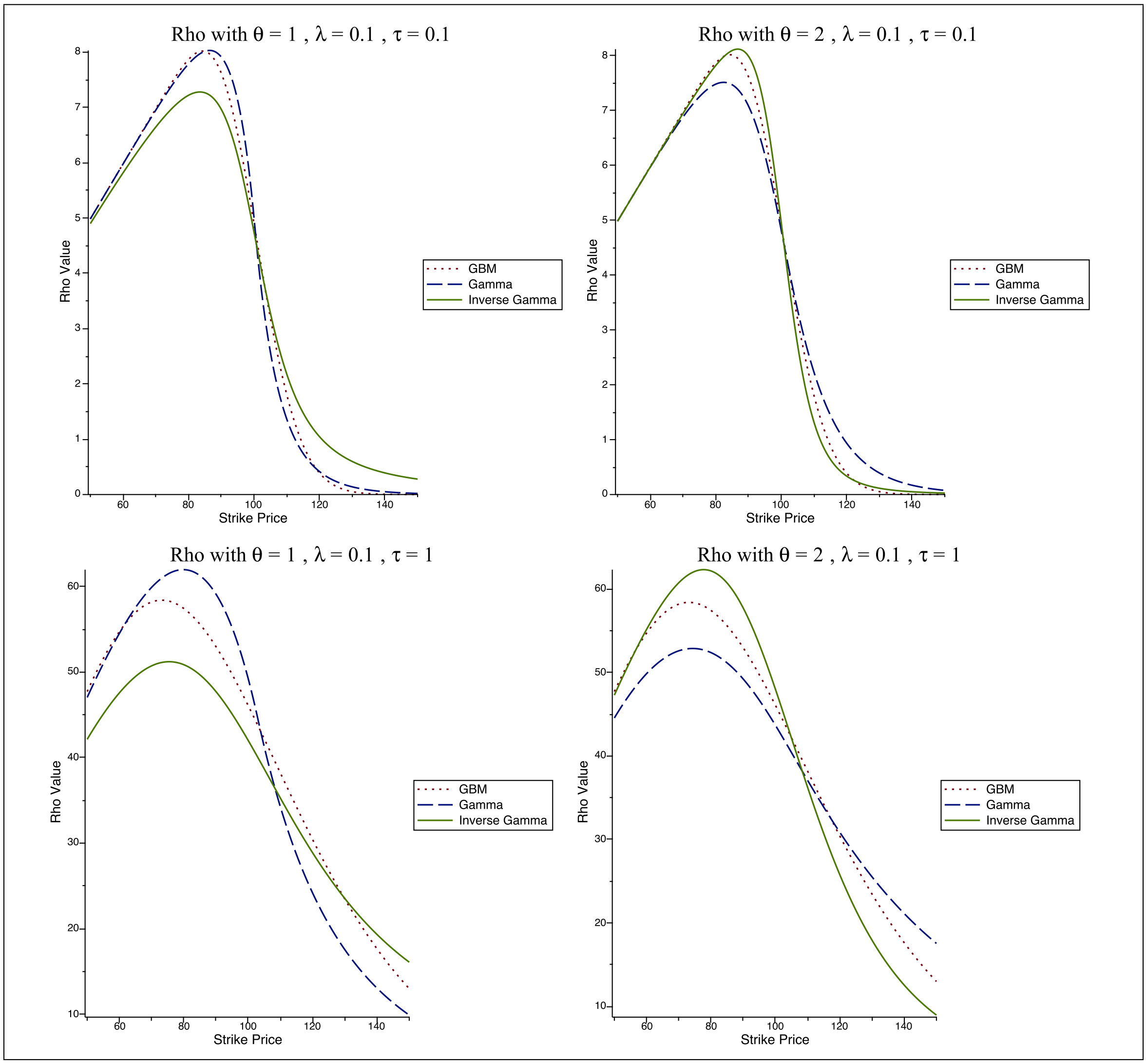

Figure C.6: Plots of the call option rhos for short time-to-maturity (top row) and for long time-to-maturity (bottom row), where $S = 100$, $r = 0.03$ and $v = 0.1$ is the variane parameter in the GBM model.

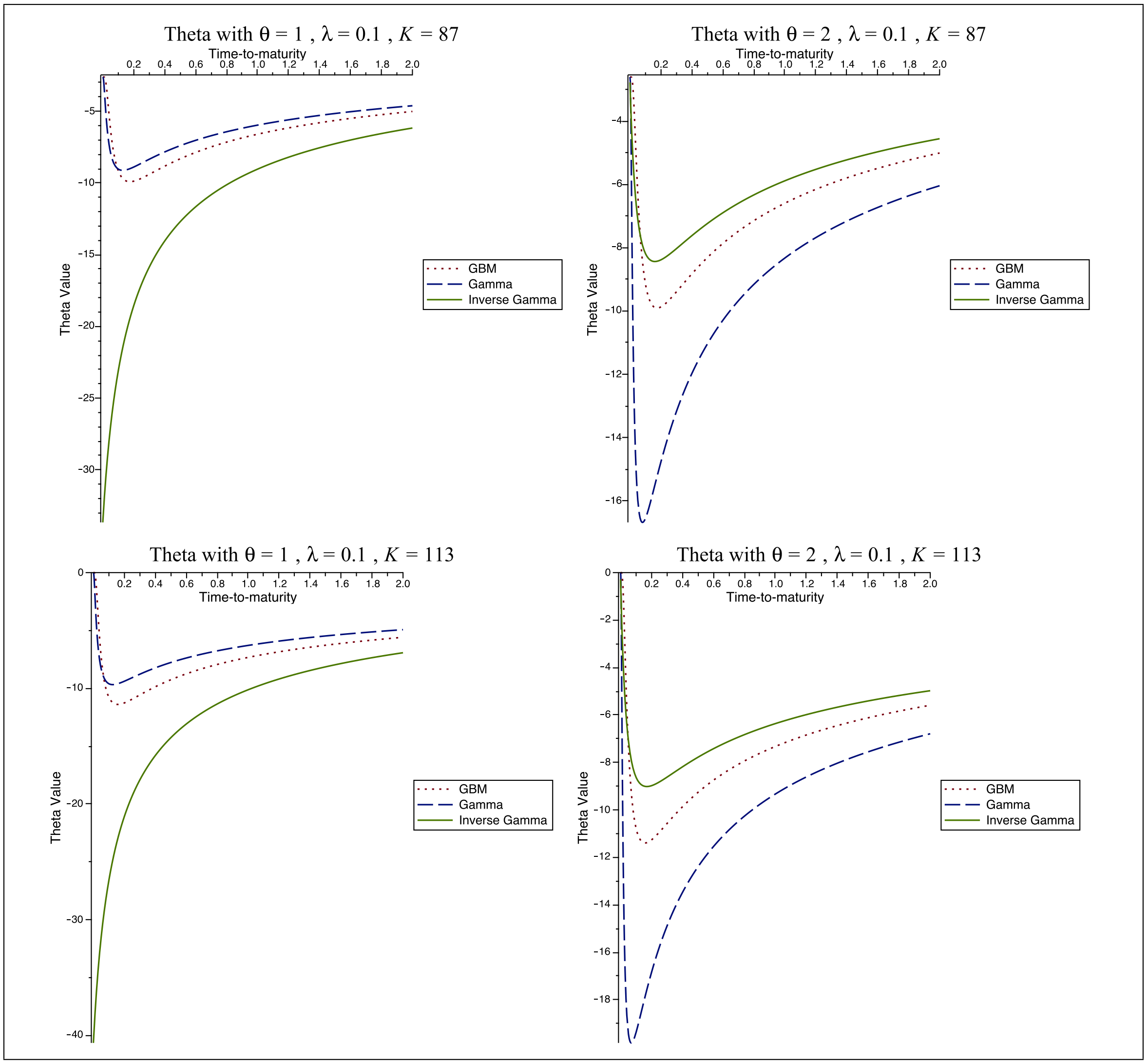

Figure C.7: Plots of the in-the-money call option thetas (top row) and out-of-the-money call option thetas (bottom row), where $S = 100$, $r = 0.03$ and $v = 0.1$ is the variane parameter in the GBM model. It is interesting that the theta value for the call option embedded by the inverse gamma process with $\theta = 1$ diverges as τ goes to zero.

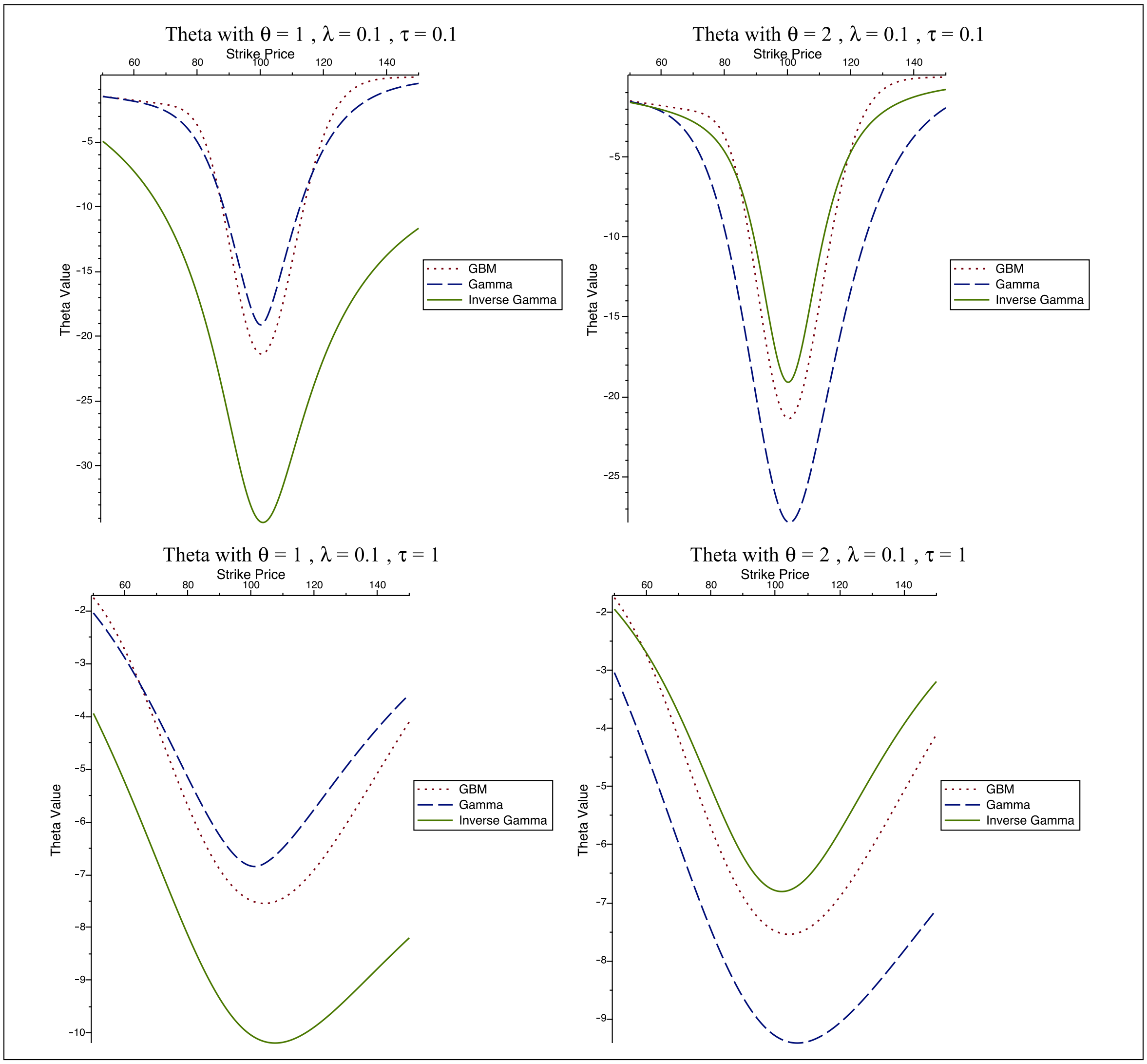

Figure C.8: Plots of the call option thetas for short time-to-maturity (top row) and for long time-to-maturity (bottom row), where $S = 100$, $r = 0.03$ and $v = 0.1$ is the variane parameter in the GBM model.

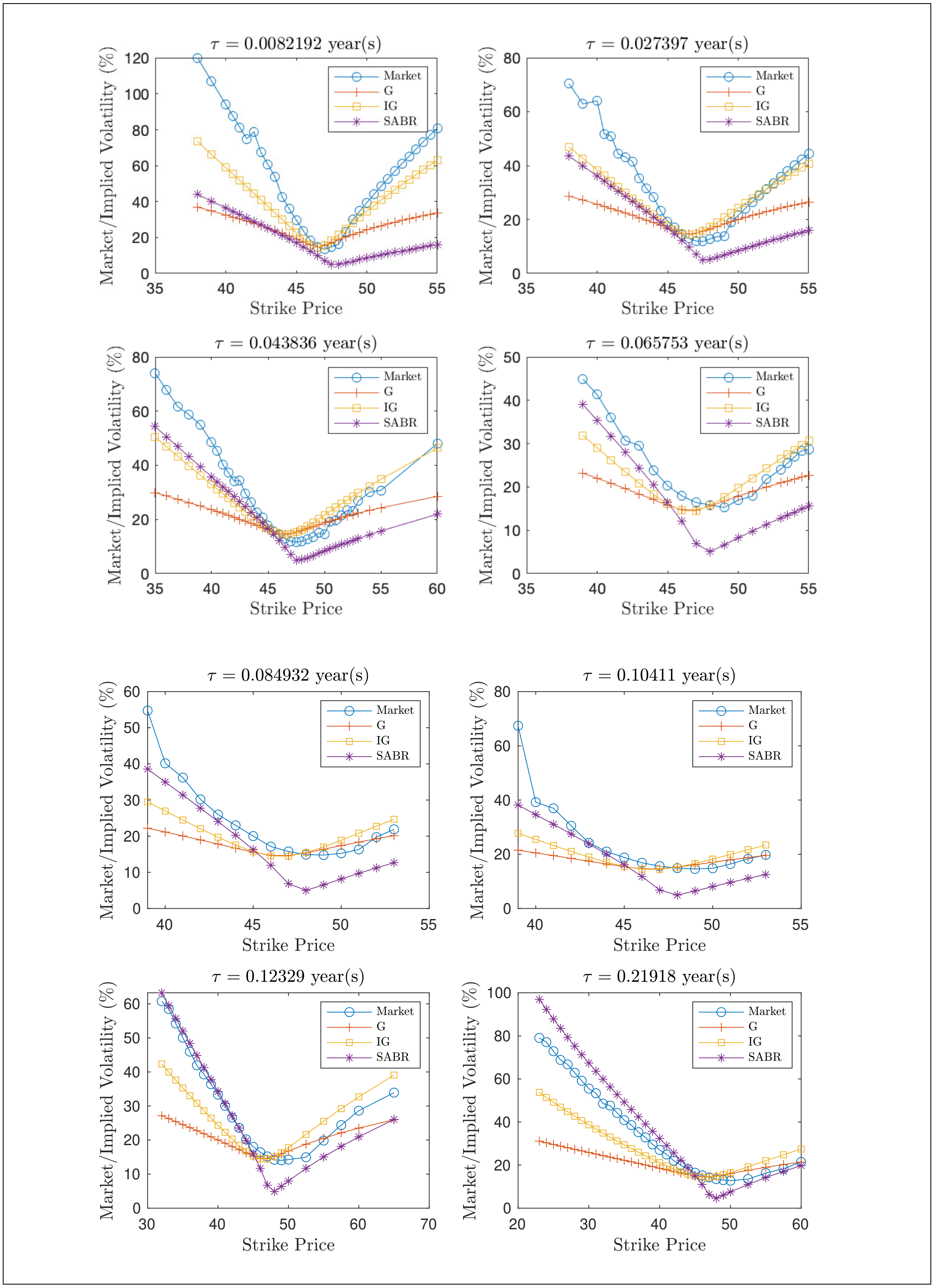

Figure D.1: 2D Implied volatility plots for the time-invariant case for small maturity times with $p = 0$.

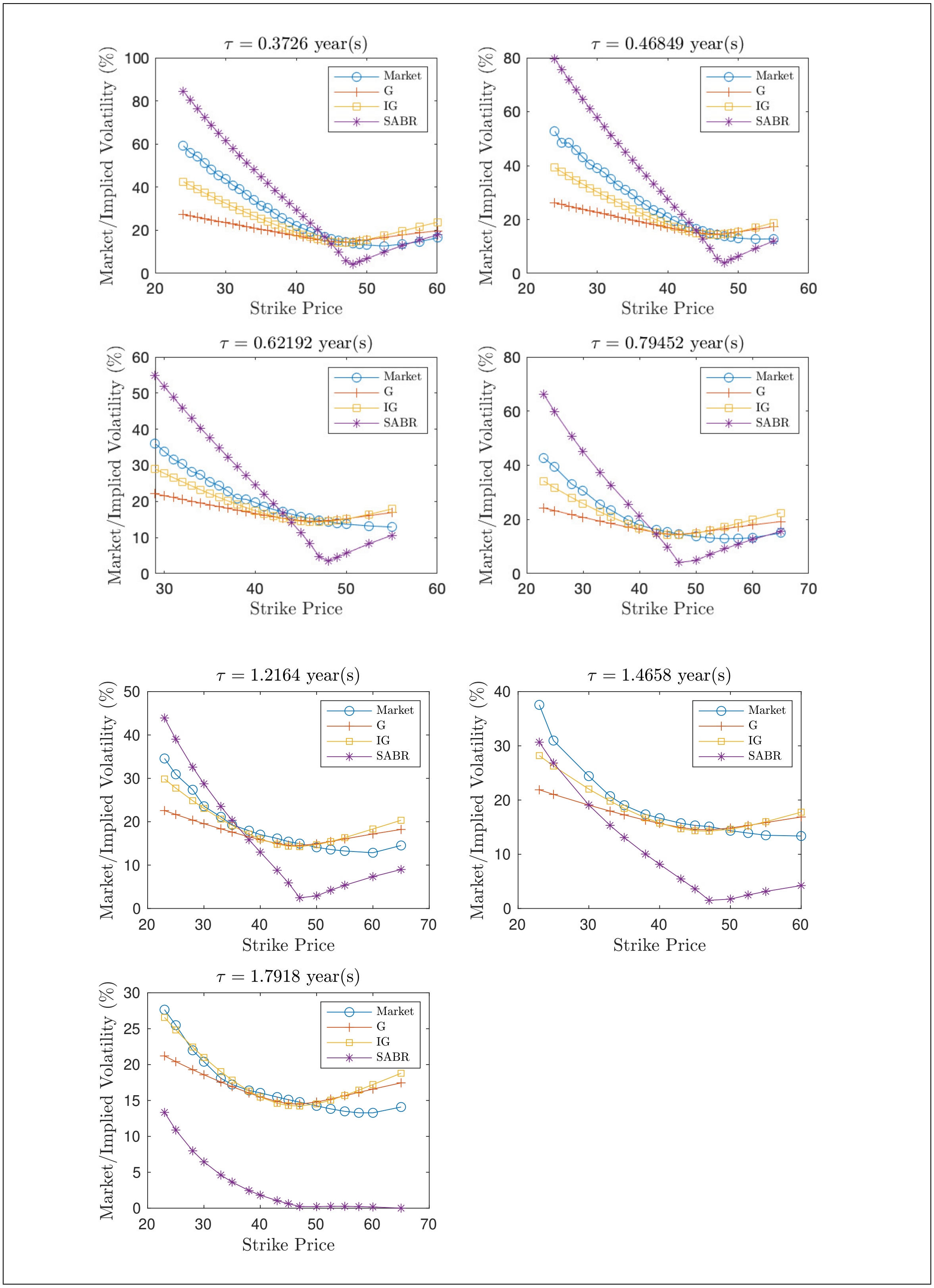

Figure D.2: 2D Implied volatility plots for the time-invariant case for long maturity times with $p = 0$.

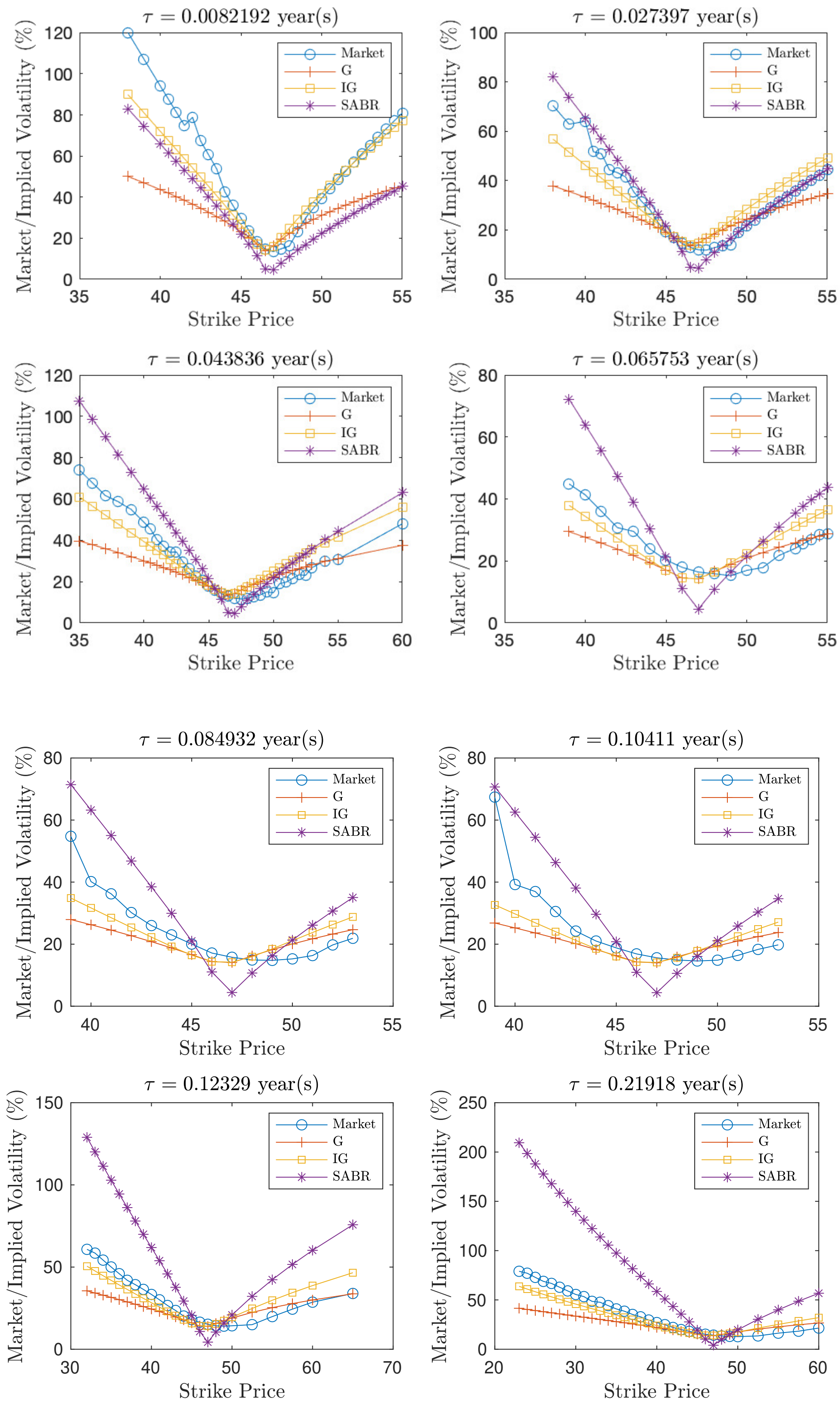

Figure D.3: 2D Implied volatility plots for the time-invariant case for small maturity times with $p = 1$.

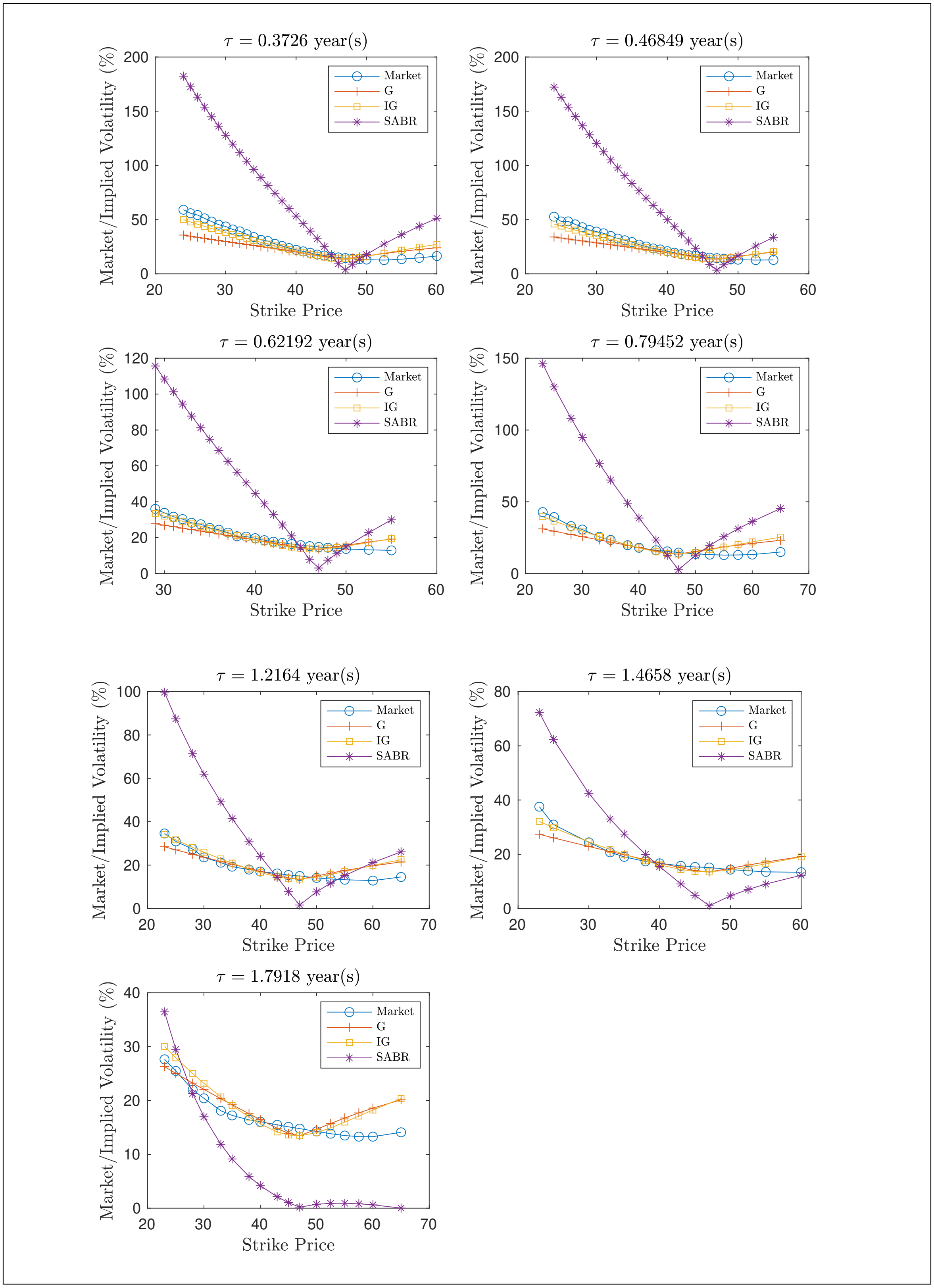

Figure D.4: 2D Implied volatility plots for the time-invariant case for long maturity times with $p = 1$.

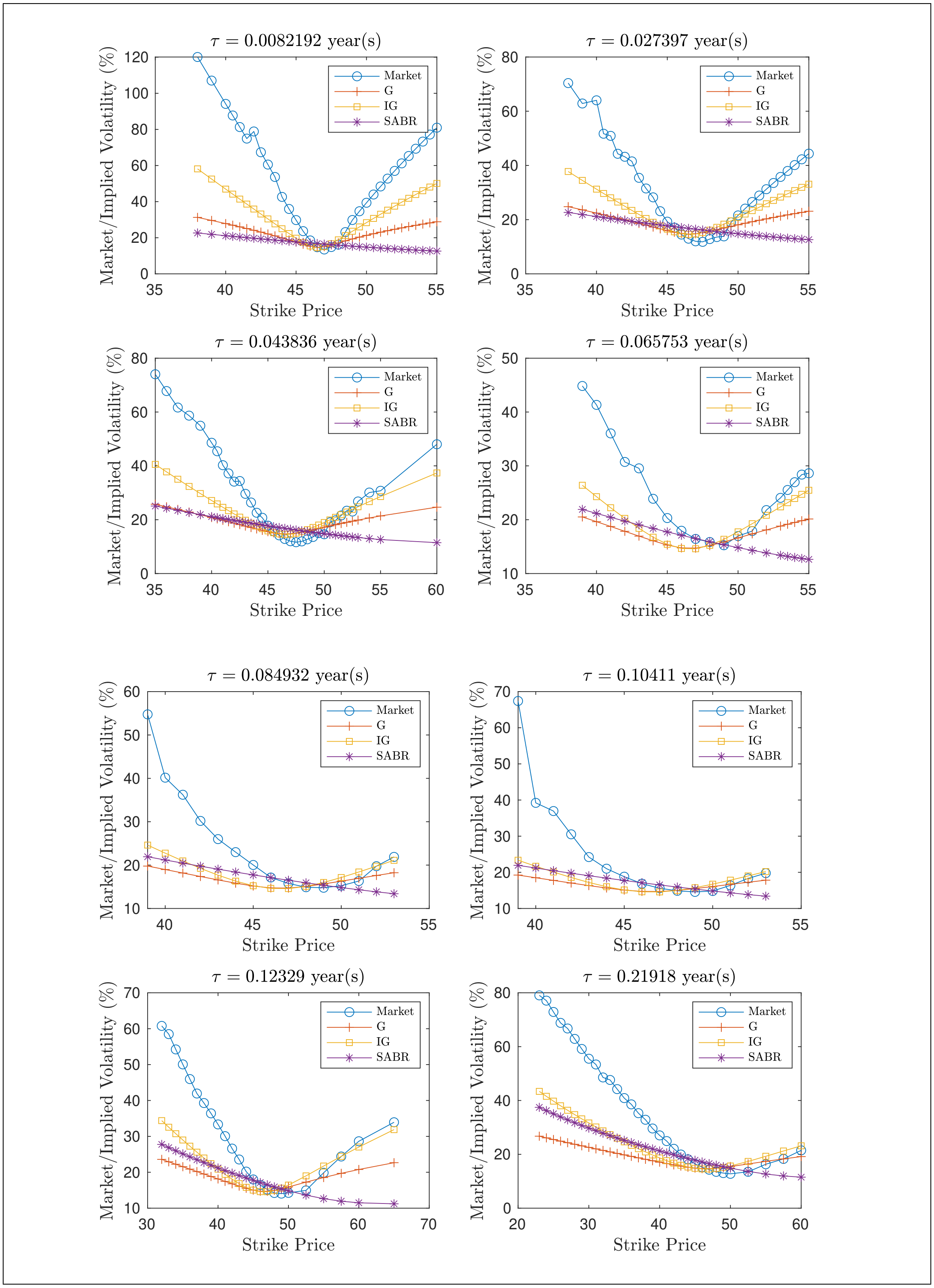

Figure D.5: 2D Implied volatility plots for the time-invariant case for small maturity times with $p = -1$.

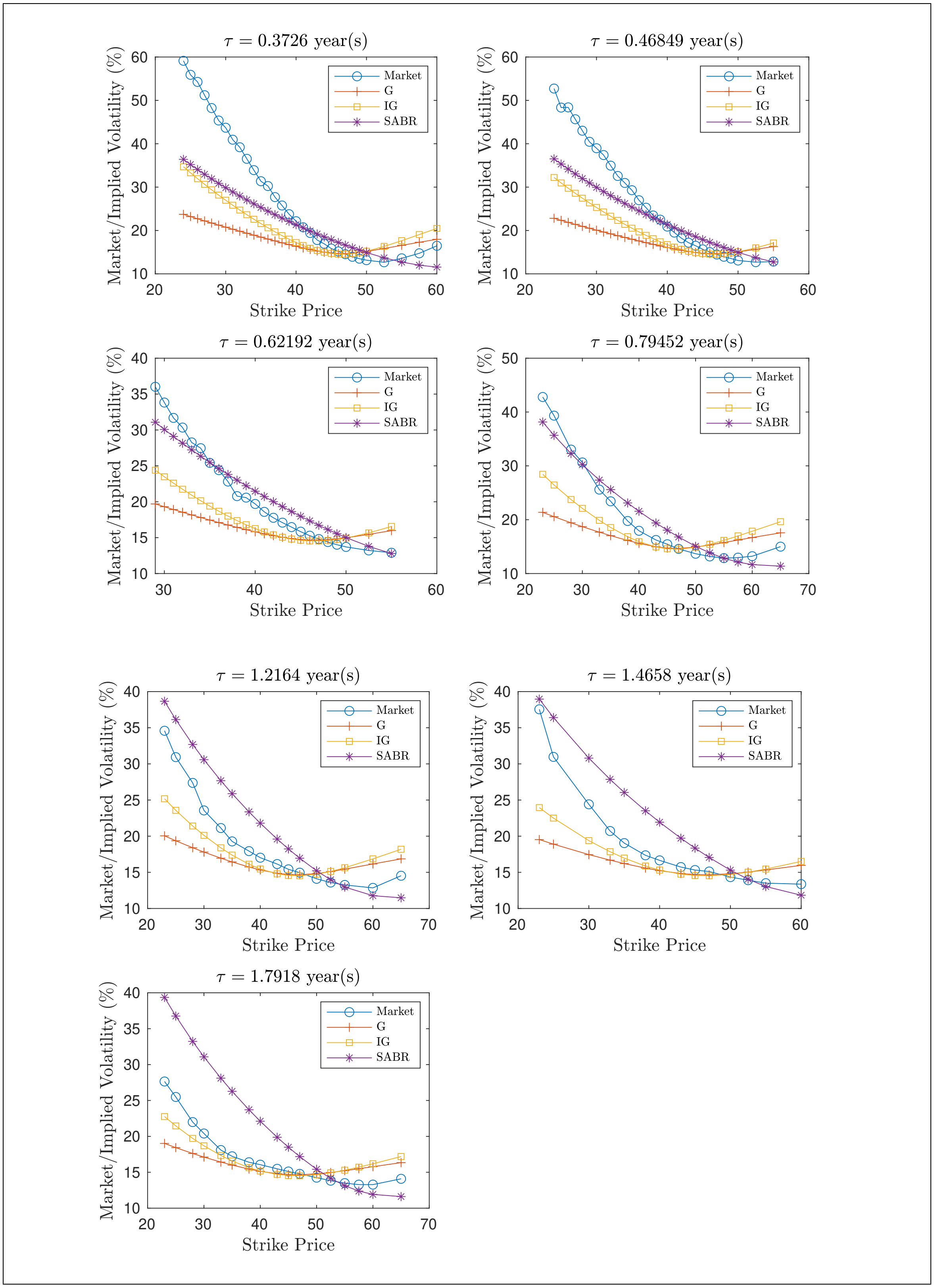

Figure D.6: 2D Implied volatility plots for the time-invariant case for long maturity times with $p = -1$.